
# Production of polymeric carbon solids (PCS) and their application as adsorbents for potentially toxic elements in water and wastewater

By

**Dance Mabu** (218051670)

Dissertation submitted to the Faculty of Science in fulfilment of the requirements for the degree of

Master of Science in Chemistry

at the

UNIVERSITY OF JOHANNESBURG

Supervisor: Prof C.M. Zvinowanda

Co-supervisor: Dr A.A. Ambushe

November 2020

# DEDICATION

This dissertation is sincerely dedicated to my mother Mohubedu Dorcus Mabu for her encouragement and support towards my studies.

ACKNOWLEDGEMENTS

This work was financial supported by the National Research Fund (NRF) and the Water Research Commission (WRC). The University of Johannesburg (UJ), in particular the Department of Chemical Sciences is acknowledged for providing a platform for the opportunity to sustain my academic journey to the end of this dissertation.

I will continuously be indebted to my supervisor Prof C.M. Zvinowanda and co-supervisor Dr A.A. Ambushe for their guidance, encouragement, and support throughout this work. They've managed to find time within their tight schedule and provided healthy supervision and discussion in my studies.

I would like to acknowledge my mother, family members, and friends for the support they have provided to me during the difficult times while I was working on this dissertation. My labmate, Ms. Dipuo Precious Kgabi for the endless support she has shown me when I felt tired. Remarkable thanks to the analytical chemistry research group, University of Johannesburg (UJ), Department of Chemical Sciences, for their valuable discussions.

The characterization of the polymeric carbon solids (PCS) could not have been possible without the unconditional willingness of many: TGA by Mr. Hulisani Meshack Thivhani from the Department of Chemical Sciences, University of Johannesburg, Zeta analysis by Mr.Solomon Pole from the Department of Chemical Sciences, University of Johannesburg, SEM, TEM and EDX by Mr. Siyasanga Mpelane from the Analytical facility, University of Johannesburg. I truly appreciate.

Lastly, I would like to thank God for giving me life and the great opportunity He has given me to keep on with my studies. Truly, He is the Beginning and the End.

"Be strong and take heart, all you who hope in the LORD"

Psalm 31:24 *(NIV)*

## DECLARATION

I Dance Mabu hereby declare that this dissertation titled '**Production of polymeric carbon solids (PCS) and their application as adsorbents for potentially toxic elements in water and wastewater**' is my own work carried out as a Master's student at the University of Johannesburg. All the sources that I have used or quoted have been indicated and acknowledged by means of references and this work has not been submitted before for any other degree to any other institution.



……..... ……

Mabu D, (Mr) Date

## ABSTRACT

Heavy metals are considered as some of the toxic substances that pollute water globally, as such, they tend to have negative effects on living organisms. Manganese and chromium metals exist in different oxidation states which some are dangerous at their low concentrations and they can cause dementia, anxiety, and ataxia, and nervous system problems. The main aim of this study was to produce PCS, hydrochar, and AC from wood chips and evaluate their potential as adsorbents for toxic inorganic ions from aqueous systems. The hydrochar was successfully produced by hydrothermal carbonization (HTC) of eucalyptus wood chips in the presence of a catalyst, water as a solvent, under the temperature of 240 °C and pressure of 4 bars. The activated carbon (AC) was generated by heating the hydrochar in a tube furnace, this process is called annealing. The hydrochar and AC were used as adsorbents for the removal of Mn(II) and Cr(VI) from aqueous solutions. The hydrochar and AC were characterized by sophisticated analytical instruments such as scanning electron microscopy (SEM), transmission electron microscopy (TEM), x-ray powder diffraction (XRD), thermogravimetric analyzer (TGA), energy dispersive x-ray (EDX), Dynamic Light Scattering (DLS), Fourier transform infrared spectroscopy (FTIR), and Brunauer–Emmett–Teller (BET). The parameters explored on the adsorption of Mn(II) and Cr(VI) include initial metal ion concentration, temperature, solution pH, contact time, and adsorbent dose. The filtrates of Mn(II) and Cr(VI) were analyzed by using the flame atomic absorption spectrometer (FAAS). Based on the results obtained from the characterization techniques, the surface area, average diameter, and pore volume of the hydrochar were found to be 29.16 $m^2/g$, 305.7 Å, and 0.223 $cm^3/g$ while the surface area, average diameter, and pore volume of the AC were revealed to be 63.35 $m^2/g$, 515.00 Å and 0.767 $cm^3/g$. The surface parameters had increased after the hydrochar was activated by heating it in a tube furnace generating AC. Therefore, the surface parameters of the AC had been improved. The achieved average particle size values of hydrochar and AC were discovered to be 2084 and 3543 d.nm, respectively. When hydrochar was used as an adsorbent, the adsorption of Mn(II) resulted in the adsorption capacity of Mn(II) being 44.03 mg/g at pH 8, adsorbent dose=0.25 g/L, contact

time=180 mins, and temperature= 25°C. When AC was used as an adsorbent, the adsorption capacity of Mn(II) increased to 56.31 mg/g at pH 7, adsorbent dose=0.25 g/L, contact time=210 mins, and temperature=25°C. The results of the adsorption of Cr(VI) showed the maximum adsorption capacity of 43.81 mg/g at pH 5, adsorbent dose=0.25 g/L, contact time=150 mins, and temperature= 25°C when hydrochar was applied. The results obtained when AC was used as an adsorbent in the adsorption of Cr(VI) were: adsorption capacity=38.26 mg/g at pH 7, adsorbent dose=0.25 g/L, contact time=120 mins, and temperature=25°C. Adsorption kinetics were studied and the experimental data was modelled with Langmuir and Freundlich isotherms. The coefficient of determination of the Langmuir model for Mn(II) and Cr(VI) metal ions were higher than that of Freundlich model. The Langmuir coefficient of determination obtained were $R^2$ =0.9915 for hydrochar and $R^2$ =0.9924 for AC for Mn(II); $R^2$ =0.5326 for hydrochar and $R^2$ =0.5082 for AC for Cr(VI). Therefore, Langmuir isotherm model best fitted the experimental data. The produced Hydrochar and AC were applied in aqueous solutions as adsorbents, and they were efficient enough to obviate Mn(II) and Cr(VI) ions from aqueous solution. Hydrochar and AC could be applied in real samples for the removal of heavy metals.

## LIST OF PUBLICATIONS AND CONFERENCES

Publications

- A paper titled 'The application of mesoporous hydrochars in the removal of Mn(II) in wastewater' has been submitted to the Journal of Physics and Chemistry of the Earth.

Presentations

- Dance Mabu, Caliphs Zvinowanda and Abayane Ambushe, The application of mesoporous hydrochars in the removal of Mn(II) in wastewater, 21st WaterNet/WARFSA/GWP-SA Symposium, October 2020, Victoria Falls, Zimbabwe.

TABLE OF CONTENTS

LIST OF FIGURES

**Chapter two:**



**Chapter three:**



**Chapter four:**

LIST OF TABLES

**Chapter two:**



**Chapter three:**



**Chapter four:**

## ABBREVIATIONS AND ACRONYMS

| | |
|---|---|
| AC | Activated carbon |
| ACNPs | Activated carbon nanoparticles |
| AMD | Acid mine drainage |
| BET | Brunauer– Emmett–Teller |
| CBC | Carbonization bacterial cellulose |
| CCD | Charge-coupled device |
| DAF | Dissolved air flotation |
| DLS | Dynamic Light Scattering |
| EDLC | Electrical double layer capacitance |
| EDS | Energy dispersive spectrometer |
| EDTA | Ethylenediaminetetraacetic acid |
| EDX | Energy dispersive x-ray |
| FAAS | Flame atomic absorption spectroscopy |
| FTIR | Fourier transform infrared spectroscopy |
| GA | Glutaric acid |
| HTC | Hydrothermal carbonization |
| IAF | Induced air flotation |
| KOH | Potassium hydroxide |
| PCS | Polymeric carbon solids |
| SANS | South African national standards |

| | |
|---|---|
| SEM | Scanning electron microscopy |
| SSA | Sulfosuccinic acid |
| TEM | Transmission electron microscopy |
| TGA | Thermogravimetric analyzer |
| UF | Ultrafiltration |
| WHO | World health organization |
| WWTPs | Wastewater treatment plants |
| XRD | X-ray powder diffraction |

# CHAPTER ONE: INTRODUCTION

## 1.1. BACKGROUND

Water pollution has raised a serious concern worldwide as clean water is essential for human activities such as agriculture, industrial, and domestic purposes [1, 2]. Water is polluted by pernicious substances like heavy metals, pathogens, and dyes which tend to have a calamitous effect on human and animal lives [3]. When heavy metals enter water bodies they bioaccumulate. Long time exposure to heavy metal ions can cause serious diseases. The health effects associated with chromium include asthma, perforated eardrums, respiratory irritation, kidney damage, liver damage, pulmonary congestion and edema, upper abdominal pain, nose irritation and damage, respiratory cancer, skin and eye irritation [4–6]. Chromium occurs in two oxidation states that are trivalent Cr(III) and hexavalent Cr(VI) [7, 8]. The solubility of Cr(VI) is higher and consequently, it is more toxic at lower concentrations than Cr(III) [9]. The Cr(VI) is carcinogenic, genotoxic, and hemotoxic [10]. When Cr(VI) enters the bloodstream, it harms blood cells because it causes oxidation reactions. The damage that may result from these oxidation reactions can lead to hemolysis and the patients might be treated with dialysis [11, 12]. Manganese is another heavy metal that negatively affects human biochemical processes too. The inhalation of manganese is perilous, the body normally transports the minerals straight into the brain without first being processed for their actual use. The exposure to manganese by inhalation for a long period can lead to a consequential condition called manganism [13]. Manganism is a disease that is similar to Parkinson's disease [14]. Manganese can also damage the central nervous system and this may result in permanent disability [15, 16]. Manganese displays oxidation states from +2 to +7, but the common oxidation states are +2, +4, and +7 [17]. The removal of heavy metal from water, wastewater, and acid mine drainage (AMD) has been reported [18]. Various conventional methods such as chemical precipitation, adsorption, coagulation and flocculation, flotation, ion exchange, membrane filtration, electrochemical treatment, and bioremediation have been employed in the removal of heavy metals from wastewater [19–22]. Urbanization and industrialization are the major sources of heavy metals for the contamination of water.

## 1.2. PROBLEM STATEMENT

Manganese and chromium metals affect the living organisms in a pessimistic way. These heavy metals exist in different oxidation states which some are hazardous at their low concentrations and extremely toxic at high concentrations. The Cr(VI) is toxic even at its lowest concentrations [23]. Industries are generally the common sources of different heavy metals, for instance, Cr(VI) is used in wood preservation, metal finishing, leather tanning, and steel fabrication [24]. South Africa's economic growth is attributed to the mining industry. In mining industries, the ore contains very high levels of chromium, and the wastes that come from the industries are deposited into the rivers via runoff [25]. Moreover, the sources of drinking water like boreholes in Mpumalanga province, South Africa, were indicated to be having chromium [26]. This is ascribed to the high concentration of chromium in shallow levels of groundwater and it results in chromium contamination of groundwater [27]. The wastewater is always having high concentrations of heavy metals [28], Mn(II) is one of the rich metal ions [29, 30]. Although manganese has a variety of applications in dry battery cells, ceramics, and electrical coils [31]; Mn(II) has neurotoxic consequences on the nervous system by giving rise to the following conditions: dementia, anxiety, and ataxia [32]. A solid waste from the production of electrolytic manganese contains a lot of soluble Mn(II) [33]. Leachate that contains Mn(II) would be released when it rains. Heavy metals need to be removed from industrial wastewater before the wastewater could be released into the streams and rivers.



## 1.3. RATIONALE OF THE STUDY

Heavy metals are among many other pollutants that pollute water in the world. The main source of heavy metals is the industrial activities that are taking place. The reports showed that there is an escalation of potentially toxic elements through fertilizers, treated woods, and aging water supply infrastructures that rise a worry of water and environmental pollution [34, 35]. Various researches have been conducted on the removal of heavy metals from water and wastewater. The adsorption is a developed method preferred in removing heavy metals from water and wastewater due to its operational simplicity, cheap to use, and the materials used as adsorbents are easily

obtainable [36]. The adsorbents such as agricultural wastes, sludges from wastewater treatment plants, and plant materials are used in the adsorption methods. Some of the plant materials that have been triumphantly utilized for this purpose are as follows: sea-buckthorn stones [37], wooden precursors [38], rice husk [39], coffee grounds [40], tomato processing solid waste [41], corncob [42], oil palm shell [43], hazelnut husks [44], apricot stones [45], cherry/sweet cherry kernels [46], pistachio nut shells [47], Brazilian pine-fruit shell [48], grape processing wastes [49], blue jacaranda and plum stones [50], pine cone [51], and forest biowaste [52]. Adsorption technique also reuses waste products to benefit humans. In this study, hydrochar produced from eucalyptus wood chips would be exploited for its efficacy to remove Mn(II) and Cr(VI) from aqueous solutions.

## 1.4. PURPOSE OF THE STUDY

### 1.4.1. Aim

The main aim of this study is to produce polymeric carbon solids (PCS), hydrochar and (AC, from wood chips and evaluate their potential as adsorbents for toxic inorganic ions from aqueous systems.

### 1.4.2. Objectives

The objectives of this study are to:

- investigate conditions for the production of PCS suitable for inorganic ion adsorption:
    - reactor pressure
    - reactor temperature
    - reaction time
- characterize PCS by using DLS, BET, XRD, EDX, FTIR, TGA, SEM, and TEM techniques
- investigate adsorption capacities of PCS from eucalyptus wood chips for the removal of Mn(II) and Cr(VI) using aqueous solutions.

- investigate the effect of initial metal ions concentration, pH, solution temperature, contact time and adsorbent dose on metal ion adsorption.
- study the kinetics and thermodynamic properties of the adsorbent to these ions.

## 1.5. REFERENCES


[1] Hossain, N., Bhuiyan, M. A., Pramanik, B. K., Nizamuddin, S., & Griffin, G. (2020). Waste Materials for Wastewater Treatment and Waste Adsorbents for Biofuel and Cement Supplement Applications: A Critical Review. *Journal of Cleaner Production*, 120261.

[2] Hossain, N., & Mahmud, L. (2019). Experimental investigation of water quality and inorganic solids in Malaysian urban lake, Taman Tasik Medan Idaman. *Lakes & Reservoirs: Research & Management*, *24*(2), 107-114.

[3] Jawed, A., Saxena, V., & Pandey, L. M. (2020). Engineered nanomaterials and their surface functionalization for the removal of heavy metals: A review. *Journal of Water Process Engineering*, *33*, 101009.

[4] Li, B., Zhang, T., & Yang, Z. (2019). Immobilizing unicellular microalga on pellet-forming filamentous fungus: Can this provide new insights into the remediation of arsenic from contaminated water?. *Bioresource technology*, *284*, 231-239.

[5] Li, J., Ding, Y., Wang, K., Li, N., Qian, G., Xu, Y., & Zhang, J. (2020). Comparison of humic and fulvic acid on remediation of arsenic contaminated soil by electrokinetic technology. *Chemosphere*, *241*, 125038.

[6] Ma, J., Lei, E., Lei, M., Liu, Y., & Chen, T. (2018). Remediation of Arsenic contaminated soil using malposed intercropping of Pteris vittata L. and maize. *Chemosphere*, *194*, 737-744.

[7] Penke, Y. K., Anantharaman, G., Ramkumar, J., & Kar, K. K. (2019). Redox synergistic Mn-Al-Fe and Cu-Al-Fe ternary metal oxide nano adsorbents for arsenic remediation with environmentally sTable As (0) formation. *Journal of hazardous materials*, *364*, 519-530.

[8] Alam, R., & McPhedran, K. (2019). Applications of biological sulfate reduction for remediation of arsenic–A review. *Chemosphere*.

[9] Lopez-Luna, J., Gonzalez-Chavez, M. C., Esparza-Garcia, F. J., & Rodriguez-Vazquez, R. (2009). Toxicity assessment of soil amended with tannery sludge, trivalent chromium and hexavalent chromium, using wheat, oat and sorghum plants. *Journal of Hazardous Materials*, *163*(2-3), 829-834.

[10] Donald, G., & Donald, B. (1999). Chromium. *Clinical Toxicology*, *37*(2), 173-194.

[11] Dayan, A. D., & Paine, A. J. (2001). Mechanisms of chromium toxicity, carcinogenicity and allergenicity: review of the literature from 1985 to 2000. *Human & experimental toxicology*, *20*(9), 439-451.

[12] Katz, S. A., & Salem, H. (1993). The toxicology of chromium with respect to its chemical speciation: a review. *Journal of Applied Toxicology*, *13*(3), 217-224.

[13] Almomani, F., Bhosale, R., Khraisheh, M., & Almomani, T. (2020). Heavy metal ions removal from industrial wastewater using magnetic nanoparticles (MNP). *Applied Surface Science*, *506*, 144924.

[14] Sharma, Y. C., Singh, S. N., & Gode, F. (2007). Fly ash for the removal of Mn (II) from aqueous solutions and wastewaters. *Chemical Engineering Journal*, *132*(1-3), 319-323.

[15] Moreno-Piraján, J. C., Garcia-Cuello, V. S., & Giraldo, L. (2011). The removal and kinetic study of Mn, Fe, Ni and Cu ions from wastewater onto activated carbon from coconut shells. *Adsorption*, *17*(3), 505-514.

[16] Egila, J. N., Dauda, B. E. N., Iyaka, Y. A., & Jimoh, T. (2011). Agricultural waste as a low cost adsorbent for heavy metal removal from wastewater. *Int J Phys Sci*, *6*(8), 2152-2157.

[17] Omri, A., & Benzina, M. (2012). Removal of manganese (II) ions from aqueous solutions by adsorption on activated carbon derived a new precursor: Ziziphus spina-christi seeds. *Alexandria Engineering Journal*, *51*(4), 343-350.

[18] Aragaw, T. A. (2020). Recovery of Iron Hydroxides from Electro-coagulated Sludge for Adsorption Removals of Dye Wastewater: Adsorption Capacity and Adsorbent Characteristics. *Surfaces and Interfaces*, 100439.

[19] Padmavathy, K. S., Madhu, G., & Haseena, P. V. (2016). A study on effects of pH, adsorbent dosage, time, initial concentration and adsorption isotherm study for the removal of hexavalent chromium (Cr (VI)) from wastewater by magnetite nanoparticles. *Procedia Technology*, *24*, 585-594.

[20] Jiang, W., Pelaez, M., Dionysiou, D. D., Entezari, M. H., Tsoutsou, D., & O'Shea, K. (2013). Chromium (VI) removal by maghemite nanoparticles. *Chemical Engineering Journal*, *222*, 527-533.

[21] Mbelengwa, N. S. (2016). *Community participation in the Integrated Development Plan of the City of Johannesburg municipality* (Doctoral dissertation, University of Pretoria).

[22] Jaishankar, M., Tseten, T., Anbalagan, N., Mathew, B. B., & Beeregowda, K. N. (2014). Toxicity, mechanism and health effects of some heavy metals. *Interdisciplinary toxicology*, *7*(2), 60-72.

[23] Yoon, Y., Kim, S., Chae, Y., Jeong, S. W., & An, Y. J. (2016). Evaluation of bioavailable arsenic and remediation performance using a whole-cell bioreporter. *Science of the Total Environment*, *547*, 125-131.

[24] Roy, A., van Genuchten, C. M., Mookherjee, I., Debsarkar, A., & Dutta, A. (2019). Concrete stabilization of arsenic-bearing iron sludge generated from an electrochemical arsenic remediation plant. *Journal of environmental management*, *233*, 141-150.

[25] Musvoto, C., & de Lange, W. J. (2019). A framework for selecting crops for irrigation using mining contaminated water: An example from the Olifants basin of South Africa. *Journal of environmental management*, *231*, 49-58.

[26] Nthunya, L. N., Masheane, M. L., Malinga, S. P., Nxumalo, E. N., Mamba, B. B., & Mhlanga, S. D. (2017). Determination of toxic metals in drinking water sources in the Chief Albert Luthuli Local Municipality in Mpumalanga, South Africa. *Physics and Chemistry of the Earth, Parts A/B/C*, *100*, 94-100.

[27] Rahman, S. H., Khanam, D., Adyel, T. M., Islam, M. S., Ahsan, M. A., & Akbor, M. A. (2012). Assessment of heavy metal contamination of agricultural soil around Dhaka Export Processing Zone (DEPZ), Bangladesh: implication of seasonal variation and indices. *Applied sciences*, *2*(3), 584-601.

[28] Tatani, A., Imai, T., & Fujima, Y. (2004). Effect of Mn2+ on sulfite oxidation in limestone scrubbing. *Energy & fuels*, *18*(1), 54-62.

[29] R. Yan, D. Gauthier, G. Flamant, J.M. Badie, Thermodynamic study of the behavior of minor coal elements and their affinities to sulphur during coal combustion, Fuel 78 (1999) 1817–1829.

[30] W.L.Weisnicht, J. Overman, C.C.Wang, H.J.Wang, J. Frwin, J.L. Hudaon, Calcium sulfite oxidation in a slurry reactor, Chem. Eng. Sci. 35 (1980) 463–468.

[31] Sharma, Y. C., Singh, S. N., & Gode, F. (2007). Fly ash for the removal of Mn (II) from aqueous solutions and wastewaters. *Chemical Engineering Journal*, *132*(1-3), 319-323.

[32] Selikhova, M., Tripoliti, E., Fedoryshyn, L., Matvienko, Y., Stanetska, H., Boychuk, M., ... & Sanotsky, Y. (2016). Analysis of a distinct speech disorder seen in chronic manganese toxicity following Ephedrone abuse. *Clinical Neurology and Neurosurgery*, *147*, 71-77.

[33] Harris, K. (1977). The production of electrolytic manganese in South Africa. *Journal of the Southern African Institute of Mining and Metallurgy*, *77*(7), 137-142.

[34] Bolan, S., Kunhikrishnan, A., Seshadri, B., Choppala, G., Naidu, R., Bolan, N. S., & Noller, B. (2017). Sources, distribution, bioavailability, toxicity, and risk assessment of heavy metal (loid) s in complementary medicines. *Environment international*, *108*, 103-118.

[35] Zhang, M., He, P., Qiao, G., Huang, J., Yuan, X., & Li, Q. (2019). Heavy metal contamination assessment of surface sediments of the Subei Shoal, China: Spatial distribution, source apportionment and ecological risk. *Chemosphere*, *223*, 211-222.

[36] Kadirvelu, K., Senthilkumar, P., Thamaraiselvi, K., & Subburam, V. (2002). Activated carbon prepared from biomass as adsorbent: elimination of Ni (II) from aqueous solution. *Bioresource technology*, *81*(1), 87-90.

[37] Mohammadi, S.Z.M., Karimi, A., Afzali, D., Mansouri, F., 2010. Removal of Pb(II) from aqueous solutions using activated carbon from Sea-buckthorn stones by chemical activation. Desalination 262, 86e93.

[38] Largitte, L., Brudey, T., Tant, T., Couespel Dumesnil, P., Lodewyckx, P., 2016. Comparison of the adsorption of lead by activated carbons from three lignocellulosic precursors. Microporous. Mesoporous. Mater. 219, 265e275.

[39] Huzir, N. M., Aziz, M. M. A., Ismail, S. B., Mahmood, N. A. N., Umor, N. A., & Muhammad, S. A. F. A. S. (2019). Optimization of coagulation-flocculation process for the palm oil mill effluent treatment by using rice husk ash. *Industrial Crops and Products*, *139*, 111482.

[40] Reffas, A., Bernardet, V., David, B., Reinert, L., Lehocine, M.B., Dubois, M., Batisse, N., Duclaux, L., 2010. Carbons prepared from coffee grounds by H3PO4 activation: characterization and adsorption of methylene blue and Nylosan Red N-2RBL. J. Hazard. Mater. 175, 779e788.

[41] Saygılı, H., Güzel, F., 2016. High surface area mesoporous activated carbon from tomato processing solid waste by zinc chloride activation: process optimization, characterization and dyes adsorption. J. Clean. Prod. 113, 995e1004.

[42] Sych, N., Trofymenko, S., Poddubnaya, O., Tsyba, M., Sapsay, V., Klymchuk, D., Puziy, A., 2012. Porous structure and surface chemistry of phosphoric acid activated carbon from corncob. Appl. Surf. Sci. 261, 75e82.

[43] Tan, I., Ahmad, A., Hameed, B., 2008. Adsorption of basic dye using activated carbon prepared from oil palm shell: batch and fixed bed studies. Desalination 225, 13e28.

[44] Imamoglu, M., Tekir, O., 2008. Removal of copper (II) and lead (II) ions from aqueous solutions by adsorption on activated carbon from a new precursor hazelnut husks. Desalination 228, 108e113.

[45] Soleimani, M., Kaghazchi, T., 2008. Adsorption of gold ions from industrial wastewater using activated carbon derived from hard shell of apricot stones-an agricultural waste. Biores. Technol. 99, 5374e5383.

[46] Pap, S., Radonic, J., Trifunovic, S., Adamovic, D., Mihajlovic, I., Vojinovic Miloradov, M., Turk Sekulic, M., 2016. Evaluation of the adsorption potential

[47] Nowicki, P., Bazan, A., Kazmierczak-Razna, J., Pietrzak, R., 2015. Sorption properties of carbonaceous adsorbents obtained by pyrolysis and activation of pistachio nut shells. Adsorpt. Sci. Technol. 33, 581e586.

[48] Royer, B., Cardoso, N.F., Lima, E.C., Vaghetti, J.C., Simon, N.M., Calvete, T., Veses, R.C., 2009. Applications of Brazilian pine-fruit shell in natural and carbonized forms as adsorbents to removal of methylene blue from aqueous solutions: kinetic and equilibrium study. J. Hazard. Mater. 164, 1213e1222.

[49] Saygılı, H., Güzel, F., Onal, Y., 2015. Conversion of grape industrial processing waste to activated carbon sorbent and its performance in cationic and anionic dyes adsorption. J. Clean. Prod. 93, 84e93.

[50] Trevino-Cordero, H., Juarez-Aguilar, L.G., Mendoza-Castillo, D.I., Hernandez Montoya, V., Bonilla-Petriciolet, A., Montes-Moran, M.A., 2013. Synthesis and adsorption properties of activated carbons from biomass of Prunus domestica and Jacaranda mimosifolia for the removal of heavy metals and dyes fromwater. Ind. Crop. Prod. 42, 315e323.

[51] Ozer, A., Dursun, G., 2007. Removal of methylene blue from aqueous solution by dehydrated wheat bran carbon. J. Hazard. Mater. 146, 262e269.

[52] Kim, N., Park, M., Park, D., 2015. A new efficient forest biowaste as biosorbent for removal of cationic heavy metals. Bioresour. Technol. 175, 629e632.

# CHAPTER TWO: LITERATURE REVIEW

## 2.1. INTRODUCTION

Water is a principal natural resource, the life of humans and animals revolve around it. Studies show that water envelops about 71% of the earth's surface, solely 2.5% of this water is freshwater, with at most 98.8% of this being groundwater and then merely 0.3% being available for utilization from streams or rivers, atmosphere, and the lakes [1]. There is a lesser percentage of water obtainable for consumption; therefore, there has been a focus on how to sustain water resources, assuring that water of good quality is available [2, 3]. The little percentage of water available for consumption gets polluted which then results in water scarcity and leaves people with less amount of pure water for utilization [4]. There is chemical pollution that occurs when chemicals/metals get into rivers directly by effluent outfalls from industries, refineries, and waste treatment plants and also indirectly by the contaminants that enter the water sources from soils/groundwater systems and the atmosphere via rainwater [5].

The reactivity of elements differs, for example, chromium is a highly reactive element and exists in two oxidation states, Cr(III) and Cr(VI) [6]. Heavy metals affect the environment negatively, other heavy metals tend to kill the plants when their concentrations are extremely high. Some heavy metals are needed by a human body in small amounts, for instance, zinc is an essential element needed in the body of infants to grow and develop properly and it also heals wounds [7–9]. The high concentration of various heavy metals found in industrial wastewater could cause brain damage, kidney failure, and many other diseases [10]. Cadmium is another heavy metal that is very toxic at low exposure that can cause serious damage to the kidneys and bones [11]. Consequently, heavy metals need to be prevented from entering the environment and water bodies. Thus, the treatment of wastewater from industries should take place so that water quality is achieved. Numerous methods have been employed for the removal of heavy metals from wastewater. In the adsorption method, different adsorbents have been reported in the removal of heavy metals from wastewater [12].

## 2.2. WATER POLLUTION

Water pollution is the presence of chemical, physical, biological components or factors producing a condition or impairment of a given water body for some beneficial use [13]. Naturally, there are different types of waters which include groundwater that is found beneath the earth and surface water, the water on the earth, for instance, rivers, lakes, oceans, etc. There are a lot of things like constructions that tend to pollute surface water and it is known that water pollution in construction sites influences the environment of the affected community and its natural surroundings [14]. The pollutants involved in water pollution depend on different sources. The pollutants that come from wastewater and agriculture are mainly chemicals, sediments, and nitrates [15]. The chemical salts like nitrates that are found in the surface water can also be found in underground water due to farming resulting from manures or human excrement or urine. Fertilizers are the major sources of nitrate in surface and underground water [16]. Water is polluted daily, more especially the surface water since the pollutants have to first travel all the way down the Earth's surface to reach the underground water. The other sources of water pollution may either be natural or artificial, that is human activities [17, 18]. One example of natural water pollution includes deforestation [19].

Figure 2.1: Photograph depicting the effluent discharged from metal industry source [20].

## 2.3. POLLUTION OF WATER BY POTENTIALLY TOXIC ELEMENTS

Industries release a variety of chemicals as wastes that are the source of potentially toxic elements into water bodies. A list of potentially toxic metals that are likely to be found in polluted water is as follows Hg, As, Pb, Sb, Ni, Sr, and Cd. These potentially toxic metals mostly occur at their lower concentrations in water [21, 22]. During the rainfall and other natural processes, these metals sink deep into the ground then in the later stages they enter rivers, lakes, and dam systems. The potentially toxic metals are absorbed by sediments and their residuals act as an organic and inorganic nutrients reservoir [23]. There is a large number of mineral resources distributed in which some toxic elements could leach [24]. It was reported that most of the potentially toxic metals cause problems to aquatic organisms [25]. The potentially toxic metals also occur naturally in the soil, but they occur at a low concentration and keep on increasing due to different human activities performed daily [26, 27].

### 2.3.1. Manganese

Mn(II) is one of the most abundant elements in the Earth's crust and it is a major pollutant in drinking water [28]. Manganese is a vital element for humans and other animals and occurs naturally in various food sources. In drinking water, the consumption of a maximum concentration of 0.3 mg/L does not have any harmful effects on human health [ 29]. The World Health Organization (WHO) guideline value for manganese in drinking water is from 400 to 500 µg/L [30, 31] and the legal limit for manganese according to South African national standards (SANS) is ≤ 400 (chronic health), ≤100 (aesthetic) [32, 33], but above 500 µg/L it is undesirable and had caused health problems and also deteriorates the water quality [34]. The most essential manganese's oxidative states for the environment and biology are as follows: Mn(II), Mn(IV), and Mn(VII). When water is exposed to air, Mn(II) combines chemically with oxygen to form manganese(IV) oxide, $MnO_2$. Mn(IV) precipitate can discolor household utensils and clothes [35]. Some of the physical and chemical properties of manganese are given in Table 2.1.

Table 2.1: Physical and chemical properties of manganese [36, 37]

| Property | Manganese | Mn(II) chloride | Manganese sulfate |
|---|---|---|---|
| Molecular weight | 54.94 | 125.85 | 151.00 |
| Color | Steel-gray | Pink | Pale rose-red |
| Physical state | Solid | Solid | Solid |
| Melting point | 1244 °C | 650 °C | 700 °C |
| Boiling point | 2095 °C | 1412 °C | 850 °C (decomposes) |
| Odor | No data | No data | Odorless |
| Density at 20 °C | 7.26 g/cm$^3$ at 20 °C | 2.325 g/cm$^3$ at 25 °C | 3.25 g/cm$^3$ |

Manganese is useful in agriculture when it is combined with urea, nitrates, potassium, and phosphates [38]. Manganese is produced from mining, organic chemicals, pesticides, rubber and plastics, lumber and wood products, metal processing, pharmaceuticals, and tanneries and it is not corrosive in the presence of glass [39, 40]. Manganese is also used as an effective adsorbent, manganese oxide coated zeolite, for Mn removal in wastewater [41]. Manganese is soluble in both cold and hot water. In an aqueous solution, manganese is present mostly as Mn(II) ion depending on other parameters such as pH and temperature [42].



### 2.3.2. Chromium

Very small quantities of chromium are needed by the human body. Chromium exists in two oxidative states which are hexavalent chromium, Cr(VI), and trivalent chromium, Cr(III). Chromium is a common contaminant in the environment and aquatic systems. It has gained global attention, (Cr(VI) is known to be more mobile, a strong oxidizing agent, and more toxic than Cr(III) [43, 44]. Chromium causes health problems in humans when exceeding the permissible level [45]. It comes from natural sources such as rocks and also from effluents of industries such as metallurgy, electroplating, leather tanning, paints and pigments, textile, and steel fabrication [46]. Some of the physical and chemical properties of chromium are given in Table 2.2.

Table 2.2: Physical and chemical properties of chromium

| Properties | Value |
|---|---|
| Atomic Number | 24 |
| Atomic Weight | 52.00 |
| Charge | $3^+$ and $6^+$ |
| Electron configuration | [Ar] $3d^5 4s^1$ |
| Electronegativity of atom | 1.66 |
| Ionic radius (Å) | 2 |

## 2.4. TECHNIQUES USED FOR THE REMOVAL OF HEAVY METALS FROM CONTAMINATED WATER

For the security of humans, the environment, and other living organisms from the significant negative effect of toxic heavy metals including manganese and chromium, different methods have been advanced and used for the removal of heavy metals from water and wastewater. The following are the employed techniques: chemical precipitation, adsorption, coagulation and flocculation, flotation, ion exchange, membrane filtration, electrochemical treatment, and bioremediation [47–52]. These techniques have their advantages and disadvantages. Table 2.3 below shows some of the advantages and disadvantages of these techniques.

Table 2.3: Advantages and disadvantages of different techniques

| Techniques | Advantage | Disadvantage | References |
|---|---|---|---|
| Chemical precipitation | •Permanent<br>•Immediate results<br>•Efficient<br>•Easily implemented<br>•Easy to monitor | •High cost<br>•Not applicable for all cases<br>•Requires operation and maintenance (O&M)<br>•Requires power<br>•May generate a waste product | [53, 54] |
| Adsorption | •Low energy and maintenance costs<br>•Simple to operate<br>• Reliable<br>• Effectiveness(also at low contaminant concentrations)<br>• Selectivity (tailored adsorbents)<br>• Regenerability of used adsorbents<br>•Cost-efficiency (low-cost adsorbents) | •Waste product<br>•Rapid saturation and clogging of the reactors | [55–57] |
| Coagulation and flocculation | •Reduction of the time required to settle out suspended solids<br>•Very effective in removing fine particles that are otherwise very difficult to remove<br>•Effective in removing many protozoa, bacteria and viruses | •Costly and the need for accurate dosing and frequent monitoring<br>•Need accurate dosing equipment to function efficiently and the dose required depends on raw water quality that can vary rapidly | [58–61] |

| | | | |
|---|---|---|---|
| Flotation | •Almost all minerals can be separated by this technique<br>•Highly appreciate for the separation of sulfide minerals<br>•Low cost | •The method is quite complex and expensive<br>•Long production cycle | [62, 63] |
| Ion exchange | •Simple equipment<br>•Easy operation<br>•No or little use of organic solvents | •Sometimes poor product quality<br>•Large pH changes in the process | [64–68] |
| Membrane filtration | •Flexible; can be used in the separation, concentration, and purification of a huge variety of materials across a wide range in industries.<br>•Microfiltration and ultrafiltration processes can operate as highly efficient "sieves", capable of fractionating particle species according to size<br>•The processes can function effectively at low temperatures<br>•Energy requirements are low.<br>•Processes are relatively simple to scale up.<br>•Membranes can be manufactured in a uniform and highly precise manner | •The processes are prone to membrane fouling effects which lead to a decrease in permeate flux<br>•Expensive cleaning and regeneration schemes may be necessary<br>•The high flow rates used in cross-flow feed can damage shear sensitive materials.<br>•Equipment costs can be high | [69–72] |
| Electrochemical treatment | •Environmental compatibility<br>•Versatility<br>•Energy efficiency<br>•Selectivity<br>•Amenability to automation and cost-effectiveness | •High requirement of manual labor<br>•Requires a high level of maintenance | [73–75] |

| | | | |
|---|---|---|---|
| Bioremediation | •Lower costs and less disruption of the contaminated environment when compared to other cleanup methods | •If the process is not controlled there is a possibility that the organic contaminants may not be broken down fully resulting in toxic by-products that could be more mobile than the initial contamination | [76, 77] |

### 2.4.1. Chemical precipitation

Chemical precipitation is a widely used method for the removal of heavy metals from water and wastewater. By definition, chemical precipitation is the creation of a solid from the solution [78]. In chemical precipitation processes, the addition of reagents is involved then followed by the separation of formed solids [79], for instance, magnesium and phosphate are required for chemical precipitation [80]. This technique is usually used to treat AMD, neutral drainage, and pit lake water [81]. Chemical precipitation can also be used in combination with other technologies. The sequencing batch reactor (SBR) process is one of the technologies used in combination with chemical precipitation [82].

### 2.4.2. Coagulation and flocculation

Coagulation and flocculation are used in the removal of heavy metals, color, turbidity, algae, and other micro-organisms from wastewater and surface waters [83, 84]. The processes involved in this method are sedimentation, precipitation, and filtration. The floc forms when a chemical coagulant is added to aqueous solutions and wastewater. The commonly used coagulants are aluminum sulfate and ferric chloride [85]. Various coagulants such as aluminum potash, Polyaluminum Chloride (PAC), ferric sulfate, iron salts, etc., are used in coagulation and flocculation for removing heavy metals from wastewater [86, 87]. Those coagulants do not completely remove heavy metals from water and wastewaters, therefore, the other techniques are further employed for the completion of heavy metals removal [88].

#### *2.4.2.1. Coagulation and flocculation mechanism*

Coagulation is the destabilization of colloidal particles formed after the addition of coagulants. The flocculation happens when the destabilized colloidal particles come together, agglomeration, into fine lumps and bulky lumps settle down [89]. The mechanism of coagulation and flocculation is grounded on zeta potential (ζ) measurement which entails the electrostatic interaction between the pollutants and coagulants [90, 91]. The chelating ability of coagulant and flocculant (polyelectrolytes)

helps in the optimization of the removal of different types of pollutants [91]. Figure 2.2 below shows the coagulation and flocculation mechanism.

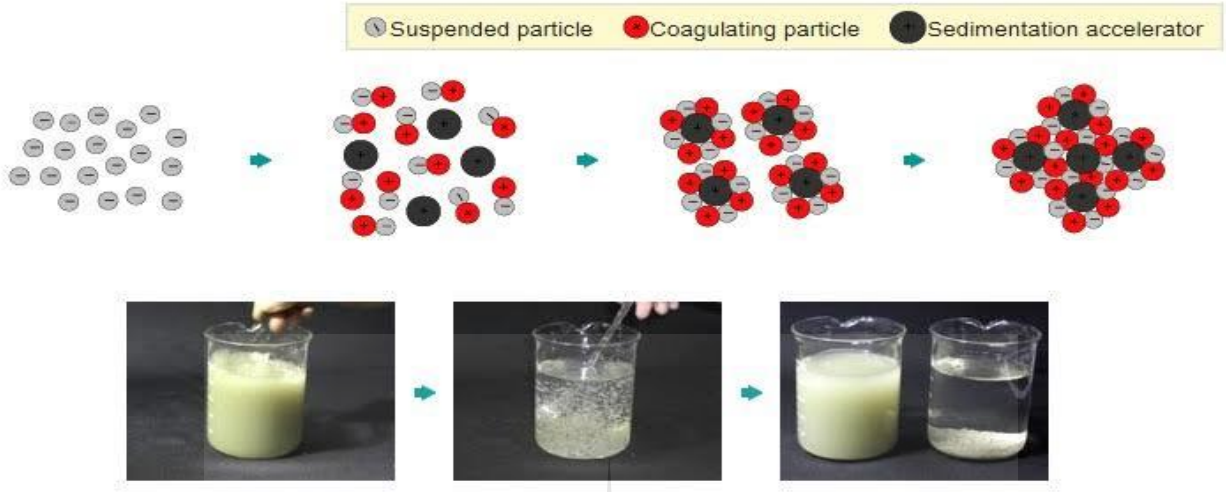


Figure 2.2: Coagulation and flocculation mechanism [92].

### 2.4.3. Flotation

The flotation technique is used for separating heavy metals from water and wastewater using bubble attachment [93]. The involved processes of this technique in the removal of heavy metals from wastewater are dissolved air flotation (DAF) [94], induced air flotation (IAF) [95], precipitation flotation [96], and ion flotation [97]. This method is mostly used to treat wastewater with a very low concentration of metals and it is normally employed in dams or simple treatment [98]. The flotation technique was found to be flexible by the researchers, the removal of Zn(II), Pb(II), and Cu(II) ions from simulated wastewater by (DAF) was reported [99, 100].

### 2.4.4. Ion-exchange

Ion exchange is another technology used for the removal of heavy metals. This technology involves the use of electrodes, synthetic and natural resins for the exchange of cations with heavy metals in water and wastewater [101, 102]. An example of the synthesized inorganic ion exchanger is sodium iron titanate (NaFeTiO) [103]. The reported fabricated electrodes used in ion exchange are ion-exchange polymer and modified carbonization bacterial cellulose (CBC) [104]. These electrodes are used by

varying amounts of cation-exchange polymers (glutaric acid (GA) and sulfosuccinic acid (SSA)) [105].

### 2.4.5. Membrane filtration

Membrane filtration is a conventional technique used for the removal of suspended solids, microorganisms, bacteria, particles, natural organic material and inorganic pollutants, heavy metals [106]. Generally, the membrane filtration technique makes use of a semi-permeable membrane that allows water to pass through obviating pollutants [107]. The membrane pores could be blocked and form lumps on the membrane surface causing membrane fouling which leads to a fast reduction of liquid flow in the early stage of the filtration process resulting in the reduction of membrane service life [108]. There are different types of membrane filtration processes divided into two general classes that are pressure-driven and electric-driven processes [109, 110]. The pressure-driven process comprises of ultrafiltration, nanofiltration, reverse osmosis and microfiltration, and the electric-driven process comprises of electrodialysis and electrodialysis reversal [111, 112]. The membrane used in microfiltration has the pore size ranging from 0.1 to 10.0 µm [113]. These pores allow water to pass while preventing the dissolved contaminants with bigger sizes. The membrane filtration technique has various applications, for instance, ultrafiltration (UF) is applied in oil emulsion waste treatment [114], production of ultra-pure water for electronics industry [109], reduction of high COD level in corn starch plants [115], wine or fruit juice clarification [116], treatment of whey in dairy industries and selective removal of dissolved toxic metals from groundwater consolidated with chemical treatment [117].



### 2.4.6. Electrochemical treatment

Electrochemical technology has been widely used for the extraction of metals such as Au, Mn Zn, Ni, Cu, etc., from water and wastewater, and to also recycle these metals [118, 119]. The mechanism of the electrochemical method for metal recovery is based on depositing a metal onto the cathode is shown in equation (1):

$$M^{+n} + ne^{-} \rightarrow M \quad (1)$$

This technology has been applied in the mining industry for metal electrorefining [120]. The metals are removed from the water in the cathode chamber of the electrochemical cell, whereas water is getting oxidized in the anode chamber of the electrochemical cell [121, 122].

### 2.4.7. Bioremediation

Bioremediation is used for water purification by removing heavy metals from water and wastewater. Bioremediation utilizes living organisms to break down the inorganic materials into compounds that are not harmful to the environment and aquatic organisms [123]. The types of bioremediation are phytoremediation and mycoremediation [124]. The bacteria used in bioremediation include *pseudomonas putida, dechloromonas aromatica* [125], *deinococcus radiodurans* [126]**,** *methylibium petroleiphilum* [127]**,** *alcanivorax borkumensis* and *phanerochaete chrysosporium* [128].

## 2.5. ADSORPTION

The adsorption method is used to remove a variety of heavy metals from wastewater, manganese and chromium are among those heavy metals. The advantages of the adsorption method are mentioned in Table 2.3. This method purifies water by removing a broad range of compounds from wastewater coming from the industries [129]. Adsorption occurs when molecules or ions in a solution bind themselves to the surface of the adsorbent, while adsorbate is the constituent to be adsorbed. The two main types of adsorption are physisorption and chemisorption. The mechanism of physisorption is that the Van der Waals forces hold the adsorbate molecules and the adsorbent together, and the process is always exothermic [130, 131]. The mechanism of chemisorption is that the chemical forces binding the molecules are attached to the adsorbent, therefore it is hard for this process to be reversed [132].

### 2.5.1. Adsorption equilibrium

The adsorption equilibrium is established when the adsorption rate of the adsorbate ions or molecules on the surface of the adsorbent is equal to the rate of the desorption rate of the adsorbate ions or molecules on the surface of the adsorbent. The capacity of the adsorbent to take up the adsorbate depends on adsorbent dosage, temperature, and the concentration of the adsorbate [133]. The isotherm of adsorption capacity vs the equilibrium concentration could be plotted when the temperature is kept fixed [134]. The adsorption isotherms supply more details about adsorption mechanisms. The common isotherm models are Langmuir, Freundlich, Temkin and Dubinin-Radushkevich [135].

#### *2.5.1.1. Langmuir isotherm model*

In 1932, Irving Langmuir developed a Langmuir adsorption isotherm model, it is described by equation (2) below.

$$q_e = \frac{q_m K_L C_e}{1+K_L C_e} \quad (2)$$

where: $q_m$ is the maximum adsorption capacity (mg/g); $q_e$ is the amount of adsorbate adsorbed per gram of adsorbent at equilibrium (mg/g) [136]; $K_L$ is the Langmuir isotherm constant (L/mg) [137] and $C_e$ is the equilibrium concentration of adsorbate (mg/L) [138]. The assumptions of the Langmuir model's derivation are:

(1) Monolayer adsorption

(2) Localized adsorption (occur on specific sites)

(3) The heat of adsorption is constant (independent of the amount of material adsorbed)

(4) Based on the kinetic model of the adsorption-desorption process

The linearization of equation (2) gives the equation below:

$$C_e / q_e = C_e / q_m + 1 / q_m K_L \quad (3)$$

Plotting $C_e$ / $q_e$ against $C_e$ gives a straight line with slope 1/ $q_m$ and intercept 1/ $q_m$ $K_L$ [139] if the adsorption data are described by the Langmuir model [140].

*2.5.1.2. Freundlich isotherm model*

The Freundlich isotherm model was developed in 1909 by Herbert Freundlich and it represents an empirical model [141]. The Freundlich isotherm can also be used for a mixture of compounds, no assumption is made for the Freundlich isotherm [142]. It is expressed by equation (4):

$$q_e = K_F (C_e)^{1/n} \quad (4)$$

where: $K_F$ is the Freundlich indicative of relative adsorption capacity of adsorbent and n is the Freundlich indicative of the intensity of adsorption [143]. $K_F$ and $n$ are constants which can be determined experimentally. The unit of $K_F$ depends on n. When taking the logarithms of equation (4), it becomes equation (5):

$$\log q_e = \log K_F + 1/n \log C_e \quad (5)$$

The plotting of Log $q_e$ versus log $C_e$ gives a straight line with slope 1/n and intercept log $K_F$ that means the data can be represented by the Freundlich model [144].

*2.5.1.3. Temkin isotherm model*

The Temkin isotherm was developed and grounded on the assumption that the heat of adsorption is decreasing linearly when the solid surface increases [145]. Temkin isotherm is expressed in equation (6):

$$q_e = (RT/b_T) \ln A_T C_e \quad (6)$$

The linearization of equation (6) makes it equation (7):

$$q_e = (RT/b_T) \ln A_T + (RT/b_T) \ln C_e \quad (7)$$

where: $b_T$ is the Temkin isotherm constant; $A_T$ is the Temkin isotherm equilibrium binding constant (L/g); T is the temperature (°K); R is the universal gas constant (8.314J/mol/K); $C_e$ is the equilibrium concentration of adsorbate (mg/L) and $q_e$ is the amount of adsorbate adsorbed at equilibrium (mg/g) [146].

*2.5.1.4. Dubinin-Radushkevich isotherm model*

The Dubinin-Radushkevich isotherm model is another model that is used to describe adsorption data, it has two parameters. The nonlinear equation of the Dubinin-Radushkevich isotherm model is shown in equation (8) :

$$q_e = q_s \exp [-K_{DR} \epsilon^2] \quad (8)$$

The linearization of equation (8) yields equation (9) below:

$$\ln q_e = \ln q_s - K_{DR} \epsilon^2 \quad (9)$$

$$\epsilon = RT \ln [1 + 1/C_e] \quad (10)$$

where: $q_e$ is the amount of adsorbate in the adsorbent at equilibrium (mg/g); $q_s$ is the theoretical isotherm saturation capacity (mg/g); $K_{DR}$ is the Dubinin–Radushkevich isotherm constant (mol²/ kJ²), R is the universal gas constant (8.314 J/mol.°K); T is the absolute temperature (°K) and $C_e$ is the adsorbate equilibrium concentration (mg/L) [147, 148].

## 2.6. ADSORBENTS

There are various adsorbents found in different forms. The most known adsorbents that are in use are silica gel, activated alumina, molecular sieve zeolite, molecular sieve carbon, and AC [149, 150]. The synthesized adsorbents are AC and nanoparticles [151]. There are also biomass, by-products from industries, and agricultural waste adsorbents [152, 153]. These adsorbents have interesting properties and characteristics include high pore volume, large surface area, and regeneration of the adsorbent [154].



The AC is frequently used as an adsorbent in wastewater treatment facilities. The raw materials such as banana peels, orange peels, wood, and vegetable shells are calcined with a temperature ranging from 700–1000 ºC to generate ACs with the desired pores [155,156]. The AC can also be generated by treating the raw materials with chemical reagents like sodium hydroxide, potassium hydroxide, zinc chloride, phosphoric acid or sulfuric acid [157]. The treated raw materials possess sufficient surface area and large pores enough to remove more heavy metals.

The AC is expensive and efficient, it makes the adsorption process costly. Consequently, low-cost and easily available materials are in need for application in

the removal of heavy metals from water and wastewater. The researchers have discovered various natural adsorbents that were applied to remove heavy metals from wastewater [158]. The natural adsorbents deployed are rice husk, pecan shells, and hazelnut shells [159–161]. The Fly ash and iron slags are industrial by-products that have been utilized as new adsorbents and they have similar properties as AC [162]. The generation of AC, the application of AC, and surface area modification will be explained in the following sections.

### 2.6.1. Generation of AC

AC is a carbonaceous material that is broadly used as an adsorbent and catalyst, it is also used as the catalyst support in industries [163]. Moreover, the functional groups, surface area, and micropore volume make the AC to be a suitable adsorbent for different environmental applications [164, 165]. The AC is mostly produced by chemical and thermal activation. A variety of raw and nonraw materials are used to synthesize AC, for example, AC nanoparticles (ACNPs) made from the biowaste [166]. The methods available to synthesize ACNPs are solution combustion, chemical vapor deposition, and hydrothermal synthesis [167]. In the hydrothermal process, the two steps involved are: (1) carbonization of carbon precursor material at high temperatures under inert conditions; (2) activated by using gas activating agents which are steam, air, and $CO_2$ [168, 169]. The chemical activation process involves only one step that is the chemical reaction on carbon precursor material with the addition of reagents such as salts, acids, and bases [170, 171]. The AC generated from the heating process has a large surface area compared to an AC produced from the chemical process [172]. The AC used for this study was generated by the heating method.

### 2.6.2. Application and modification of AC

The unique properties and characteristics of AC make it more deployed in various applications. Examples of AC applications are environmental, supercapacitors, and electronic applications [173, 174]. The materials used as electrodes in supercapacitors are mostly conductive polymers and metal compounds [175]. There is electrical double

layer capacitance (EDLC) and pseudocapacitance mechanism taking place in supercapacitors, in the EDLC mechanism the charges are accumulated and compensate lesser to the ions attached to the electrode interfaces through electrostatic interactions [176]. The pseudocapacitance mechanism is from the redox reactions on the pseudocapacitor surface that gives zero phase transitions due to fast ion insertion and extrusion [177, 178].

Although AC works efficiently, one of its difficulties is that it agglomerates in solutions due to chemical interactions, Van Der Waals forces, that occur [179]. This difficulty can be minimized by AC modification. Surface modification lessens the agglomeration on the AC and exposes the large surface area. This also increases adsorption capacity and the interactions of AC with pollutants [180]. Surface modification is mainly done chemically whereby the desired functional groups are permanently introduced to the AC [181]. The common reagents used in the surface modification process include potassium hydroxide (KOH) and Ethylenediaminetetraacetic acid (EDTA) [182]. Depending on the desired surface area, the other chemical reagents could be used. Scientific reports showed the biomass activation using KOH combined with $K_2CO_3$ and the AC obtained the greatest surface area of 2417 $m^2\ g^{-1}$ [183, 184]. The drawback of the chemical activation method is that a large number of chemicals are used and could cause a threat to the environment since some chemicals are not environmentally friendly [185]. The other influential method utilized is non-covalent whereby the functional groups are thermally leaped to the surface of the AC without demolishing the AC properties and structure [186]. The main advantages of the thermal activation process are low cost in the production of ACs, and AC shape is retained [187]. This process occurs under the air, $CO_2$, and steam conditions [188].

## 2.7. THE APPLICATION OF AC IN THE REMOVAL OF HEAVY METALS FROM WATER AND WASTEWATER

The AC has been used for the removal of heavy metals from wastewater due to its attractive properties. AC has hydroxyl, lactone, and carboxylic functional groups that have a greater affinity for metal ions [189]. These functional groups and their effect on the adsorption behavior were studied. The effect of parameters such as pH,

adsorbent dose, temperature, initial metal ion concentration, and contact time were determined [190]. The reports showed the successful adsorption of Cu(II), Cr(III), Cd(II), and Pb(II) ions from wastewater at pH 5 when the marine macroalga Ulva lactuca and its AC were applied [191]. The AC collected from exhausted home filtration systems was also used to remove Cu(II) from aqueous solution at the optimal solution pH 5.5 [192]. The previous adsorption studies have revealed that the optimal solution pH ranges from 5 to 7 and the contact time ranges from 5 to 120 minutes [193, 194]. The by-products from the industries are also used to generate efficient adsorbents, sewage sludge from wastewater treatment plants (WWTPs) converted into AC through pyrolysis and activated with $ZnCl_2$ [195]. The metal removal efficiency was investigated using AC generated from sewage sludge and the results suggested 98.9%, 34.6%, and 42.6% removal of Cu, Al, and Zn from the simulated solutions [196]. An AC was found to be working excellently in removing various heavy metals. The greatest adsorption capacities of As(III), Pb(II), and Cd(II) were 151.5, 147.1, and 119.00 $mg.g^{-1}$ when the AC synthesized from pistachio shell was used to remove these metal ions from wastewater [197]. In this study, the hydrochar produced from eucalyptus wood chips would be used as an adsorbent. This material was chosen due to the interesting properties it possesses. The eucalyptus wood hydrochar is suitable for adsorption, it has a surface area ranging from 460 to 1,490 $m^2/g$ respectively [198]. The surface area of the hydrochar can further be increased when it is heated at high temperatures to generate the AC.



Table 2.4: Summary of studies on heavy metals removal using AC

| Heavy Metal | Adsorption Capacity (mg/g) & Removal% | Contact time (min) | pH | References |
|---|---|---|---|---|
| Cr | 99 | 90 | 5.5 | [199] |
| Pb | 96.1 | 60 | 2.0–5.5 | [200] |
| Cd | 93.8 | | | |
| Cu | 83.3 | | | |

| | | | | |
|---|---|---|---|---|
| Zn | 69.6 | | | |
| Ni | 50.0 | | | |
| Pb | 95 | 60 | 2.6–8.7 | [201] |
| Cd | 86 | | | |

## 2.8. FACTORS AFFECTING THE ADSORPTION OF METAL IONS

In the adsorption process, AC removes heavy metals magnificently from water and wastewater. An AC is industrially utilized due to its versatility. The factors affecting the adsorption process are very important because they can impact the heavy metal ions binding to the adsorbent's surface [202, 203]. The factors are explained in detail in the following sections.

### 2.8.1. Effect of pH on adsorption efficiency

During the adsorption process, pH is one of the most important factors. It affects the active sites of the adsorbent that binds with heavy metal ions [204]. In general, pH affects the surface properties of the adsorbent. The adsorption of heavy metal ions is mainly successful at pH 6 and less, and the heavy metal ions begin to precipitate and form metallic hydroxides in the solution when the pH is above pH 8 [205, 206]. When the pH is low, hydronium ions compete with heavy metal ions for binding to the active sites of the adsorbent [207]. This results from the high concentration of protons which would decrease the heavy metal adsorption [208]. The hydronium ions get reduced when the pH is high and that reduces the competition with metal ions [209].

### 2.8.2. Effect of initial metal ion concentration on adsorption efficiency

Another crucial factor that influences the adsorption is the initial metal ion concentration. The increase in initial metal ion concentration contributes more to the adsorption capacity, the saturation point is reached since the driving forces in the solid-liquid bond get enhanced [210]. The available adsorption sites of the adsorbent become unfettered

by initial concentration at lower concentrations and there is a small number of free adsorption sites on the adsorbent at higher initial metal ion concentrations [211].

### 2.8.3. Effect of contact time on adsorption efficiency

The contact time is a vital parameter between the adsorbent and adsorbate in the adsorption. When contact time is investigated, the removal order of almost all metal ions sharply increases at initial points and then decreases slowly until the maximum equilibrium is achieved as the time is prolonged [212, 213]. The adsorption of Cr (VI) was reported and the maximum equilibrium occurred at 60 minutes, adsorption capacity increased as the time was increasing [214]. This is ascribed to the physicochemical properties of the adsorbent, countless available active sites are easily exposed and interact with metal ions through ion exchange and electrostatic interaction [215].

### 2.8.4. Effect of adsorbent dosage on adsorption efficiency

The adsorbent dosage also influences the adsorption process. An AC generated from cola nutshells showed a greater effect on the uptake of metal ions, the removal efficiency increased as the adsorbent dosage increased [216–218]. When the adsorbent dose increases results in excess in the solution and the surface area accessible for adsorption of metal ions gets reduced due to the aggregation of adsorption active sites [219].



### 2.8.5. Effect of temperature on adsorption efficiency

Apart from the factors mentioned above, temperature is also another parameter with a greater effect on the adsorption process. The adsorption capacity increases with increasing temperature as the reaction rate increases at higher temperatures [220]. When the temperatures get extremely higher, the adsorption capacity decreases [221, 222]. This is because when the temperature is increasing, the attractive forces involved between the adsorbent's surface and metal ions become weaker thus decreasing adsorption [223]. The adsorption process is endothermic at high temperatures, and the electrostatic interaction between adsorbent and metal ions becoming stronger [224].

## 2.9. REFERENCES


[1] Z. Li, Q. Zhang, and H. Liao, “Efficient-equiTable-ecological evaluation of regional water resource coordination considering both visible and virtual water,” *Omega (United Kingdom)*, vol. 83, pp. 223–235, 2019.

[2] C. Felgueiras, L. Kuski, P. Moura, and N. Caetano, “Water consumption monitoring system for public bathing facilities,” *Energy Procedia*, vol. 153. pp. 408–413, 2018.

[3] “The importance and impact of process water,” *Filtr. + Sep.*, vol. 54, no. 6, pp. 32–35, 2018.

[4] Tadepalli, S., Murthy, K. S. R., & Rakesh, N. N. (2016). Removal of Cu (II) and Fe (II) from Industrial waste water using orange peel as adsorbent in batch mode operation. *Int J Chem Tech Res*, *9*(5), 290-9.

[5] Jain, M., Garg, V. K., & Kadirvelu, K. (2009). Chromium (VI) removal from aqueous system using Helianthus annuus (sunflower) stem waste. *Journal of Hazardous Materials*, *162*(1), 365-372.

[6] Bhattacharya, A. K., Mandal, S. N., & Das, S. K. (2006). Adsorption of Zn (II) from aqueous solution by using different adsorbents. *Chemical Engineering Journal*, *123*(1-2), 43-51.

[7] Guyo, U., Mhonyera, J., & Moyo, M. (2015). Pb (II) adsorption from aqueous solutions by raw and treated biomass of maize stover–a comparative study. *Process Safety and Environmental Protection*, *93*, 192-200.

[8] Mohan, D., Pittman Jr, C. U., & Steele, P. H. (2006). Single, binary and multi-component adsorption of copper and cadmium from aqueous solutions on Kraft lignin—a biosorbent. *Journal of colloid and interface science*, *297*(2), 489-504.

[9] Amarasinghe, B. M. W. P. K., & Williams, R. A. (2007). Tea waste as a low cost adsorbent for the removal of Cu and Pb from wastewater. *Chemical Engineering Journal*, *132*(1-3), 299-309.

[10] Schweitzer, L., & Noblet, J. (2017). Water Contamination and Pollution. In *Green Chemistry* (pp. 261-290).

[11] Belayutham, S., González, V. A., & Yiu, T. W. (2016). The dynamics of proximal and distal factors in construction site water pollution. *Journal of Cleaner Production*, *113*, 54-65.

[12] Smith, L., Inman, A., Lai, X., Zhang, H., Fanqiao, M., Jianbin, Z., ... & Bellarby, J. (2017). Mitigation of diffuse water pollution from agriculture in England and China, and the scope for policy transfer. *Land use policy*, *61*, 208-219.

[13] Pacheco, F. A. L., & Fernandes, L. S. (2016). Environmental land use conflicts in catchments: a major cause of amplified nitrate in river water. *Science of the Total Environment*, *548*, 173-188.

[14] Dwivedi, S., Mishra, S., & Tripathi, R. D. (2018). Ganga water pollution: a potential health threat to inhabitants of Ganga basin. *Environment international*, *117*, 327-338.

[15] Sierra-Alvarez, R. (2009). Removal of copper, chromium and arsenic from preservative-treated wood by chemical extraction-fungal bioleaching. *Waste management*, *29*(6), 1885-1891.

[16] Kakitani, T., Hata, T., Kajimoto, T., Koyanaka, H., & Imamura, Y. (2009). Characteristics of a bioxalate chelating extraction process for removal of chromium, copper and arsenic from treated wood. *Journal of environmental management*, *90*(5), 1918-1923.

[17] White, K. D., Vaddey, S. V., Hamlet, A. F., Cohen, S., Neilsen, D., & Taylor, W. (2006). Integrating climate impacts in water resource planning and management. In *Current Practices in Cold Regions Engineering* (pp. 1-11).

[18] Perley, C., Moller, H., Hutcheson, J., & Hamilton, W. (2001). Towards safeguarding New Zealand's agricultural biodiversity: research gaps, priorities and potential case studies. *Ecosystems Consultants Report*, *23*, 230.

[19] Meissner, R., Steyn, M., Moyo, E., Shadung, J., Masangane, W., Nohayi, N., & Jacobs-Mata, I. (2018). South African local government perceptions of the state of water security. *Environmental Science & Policy*, *87*, 112-127.

[20] Nadeem, M., Mahmood, A., Shahid, S. A., Shah, S. S., Khalid, A. M., & McKay, G. (2006). Sorption of lead from aqueous solution by chemically modified carbon adsorbents. *Journal of Hazardous materials, 138*(3), 604-613.

[21] Hegazi, H. A. (2013). Removal of heavy metals from wastewater using agricultural and industrial wastes as adsorbents. *HBRC journal*, *9*(3), 276-282.

[22] Aschale, M., Sileshi, Y., Kelly-Quinn, M., & Hailu, D. (2016). Evaluation of potentially toxic element pollution in the benthic sediments of the water bodies of the city of Addis Ababa, Ethiopia. *Journal of Environmental Chemical Engineering*, *4*(4), 4173-4183.

[23] Wang, L., Dai, L., Li, L., & Liang, T. (2018). Multivariable cokriging prediction and source analysis of potentially toxic elements (Cr, Cu, Cd, Pb, and Zn) in surface sediments from Dongting Lake, China. *Ecological Indicators*, *94*, 312-319.

[24] Wang, X., Shi, Z., Shi, Y., Ni, S., Wang, R., Xu, W., & Xu, J. (2018). Distribution of potentially toxic elements in sediment of the Anning River near the REE and V-Ti magnetite mines in the Panxi Rift, SW China. *Journal of Geochemical Exploration*, *184*, 110-118.

[25] Brion-Roby, R., Gagnon, J., Deschênes, J. S., & Chabot, B. (2018). Investigation of fixed bed adsorption column operation parameters using a chitosan material for treatment of arsenate contaminated water. *Journal of environmental chemical engineering*, *6*(1), 505-511.

[26] Hegazi, H. A. (2013). Removal of heavy metals from wastewater using agricultural

and industrial wastes as adsorbents. *HBRC journal*, *9*(3), 276-282.

[27] Li, Y. J., Wang, Z. K., Qin, F. X., Fang, Z. Q., Li, X. L., & Li, G. (2018). Potentially Toxic Elements and Health Risk Assessment in Farmland Systems around High-Concentrated Arsenic Coal Mining in Xingren, China. *Journal of Chemistry*, *2018*.

[28] Yang, H., Yan, Z., Du, X., Bai, L., Yu, H., Ding, A., ... & Aminabhavi, T. M. (2019). Removal of manganese from groundwater in the ripened sand filtration: Biological oxidation versus chemical auto-catalytic oxidation. *Chemical Engineering Journal*, 123033.

[29] Tian, X., Zhang, R., Huang, T., & Wen, G. (2019). The simultaneous removal of ammonium and manganese from surface water by MeOx: Side effect of ammonium presence on manganese removal. *Journal of Environmental Sciences*, *77*, 346-353.

[30] Tekerlekopoulou, A. G., Vasiliadou, I. A., & Vayenas, D. V. (2008). Biological manganese removal from poTable water using trickling filters. *Biochemical Engineering Journal*, *38*(3), 292-301.

[31] Abalaka, S. E. (2015). Heavy metals bioaccumulation and histopathological changes in Auchenoglanis occidentalis fish from Tiga dam, Nigeria. *Journal of Environmental Health Science and Engineering*, *13*(1), 67.

[32] Rimayi, C., Odusanya, D., Weiss, J. M., de Boer, J., & Chimuka, L. (2018). Contaminants of emerging concern in the Hartbeespoort Dam catchment and the uMngeni River estuary 2016 pollution incident, South Africa. *Science of the Total Environment*, *627*, 1008-1017.

[33] Verlicchi, P., & Grillini, V. (2020). Surface water and groundwater quality in South Africa and mozambique—Analysis of the Most critical pollutants for drinking purposes and challenges in water treatment selection. *Water*, *12*(1), 305.

[34] Ghasemi, M., & Moazed, H. (2014). Determination of heavy metal in water and sediment of Dez River, Dezful, Khusestan Province, Iran. *International Journal of Biosciences*, *4*(2), 232-238.

[35] Abagale, F. K., Amoah, A. K., Abagale, S. A., & Osei, R. A. (2013). POLLUTION LEVEL ASSESSMENT OF DAM WATER USED FOR DOMESTIC ACTIVITIES, IN BUILPELA OF THE TAMALE METROPOLIS, GHANA.

[36] Anim-Gyampo, M., Kumi, M., & Zango, M. S. (2013). Heavy metals concentrations in some selected fish species in Tono Irrigation reservoir in Navrongo, Ghana. *Journal of Environment and Earth Science*, *3*(1), 109-119.

[37] Subari, F., Kamaruzzaman, M. A., Abdullah, S. R. S., Hasan, H. A., & Othman, A. R. (2018). Simultaneous removal of ammonium and manganese in slow sand biofilter (SSB) by naturally grown bacteria from lake water and its diverse microbial community. *Journal of environmental chemical engineering*, *6*(5), 6351-6358.

[38] Kouzbour, S., El Azher, N., Gourich, B., Gros, F., Vial, C., & Stiriba, Y. (2017).

Removal of manganese (II) from drinking water by aeration process using an airlift reactor. *Journal of water process engineering*, *16*, 233-239.

[39] Williams, M., Todd, G. D., Roney, N., Crawford, J., Coles, C., McClure, P. R., ... & Citra, M. (2012). Toxicological profile for manganese.

[40] Zeglam, A., Abugrara, A., & Kabuka, M. (2019). Autosomal-recessive iron deficiency anemia, dystonia and hypermanganesemia caused by new variant mutation of the manganese transporter gene SLC39A14. *Acta Neurologica Belgica*, *119*(3), 379-384.

[41] Hanson, B. R., Šimůnek, J., & Hopmans, J. W. (2006). Evaluation of urea–ammonium–nitrate fertigation with drip irrigation using numerical modeling. *Agricultural water management*, *86*(1-2), 102-113.

[42] Divya, J., & Belagali, S. L. (2012). Impact of chemical fertilizers on water quality in selected agricultural areas of Mysore district, Karnataka, India. *International journal of environmental sciences*, *2*(3), 1449-1458.

[43] Marsidi, N., Hasan, H. A., & Abdullah, S. R. S. (2018). A review of biological aerated filters for iron and manganese ions removal in water treatment. *Journal of Water Process Engineering*, *23*, 1-12.

[44] Alvarez-Bastida, C., Martínez-Miranda, V., Solache-Ríos, M., Linares-Hernández, I., Teutli-Sequeira, A., & Vázquez-Mejía, G. (2018). Drinking water characterization and removal of manganese. Removal of manganese from water. *Journal of Environmental Chemical Engineering*, *6*(2), 2119-2125.

[45] Biela, R., & Kučera, T. (2016). Efficacy of sorption materials for nickel, iron and manganese removal from water. *Procedia engineering*, *162*, 56-63.

[46] Vo, A. T., Nguyen, V. P., Ouakouak, A., Nieva, A., Doma, B. T., Tran, H. N., & Chao, H. P. (2019). Efficient Removal of Cr (VI) from Water by Biochar and Activated Carbon Prepared through Hydrothermal Carbonization and Pyrolysis: Adsorption-Coupled Reduction Mechanism. *Water*, *11*(6), 1164.

[47] Wu, J., Chen, K., Tan, X., Fang, M., Hu, X., Tang, Z., & Wang, X. (2018). Core-shell CMNP@ PDAP nanocomposites for simultaneous removal of chromium and arsenic. *Chemical Engineering Journal*, *349*, 481-490.

[48] Kartal, S. N. (2003). Removal of copper, chromium, and arsenic from CCA-C treated wood by EDTA extraction. *Waste management*, *23*(6), 537-546.

[49] Kartal, S. N., & Imamura, Y. (2005). Removal of copper, chromium, and arsenic from CCA-treated wood onto chitin and chitosan. *Bioresource technology*, *96*(3), 389-392.

[50] Gottipati, R. (2012). *Preparation and characterization of microporous activated carbon from biomass and its application in the removal of chromium (VI) from aqueous phase* (Doctoral dissertation).

[51] Adamczuk, A., & Kołodyńska, D. (2015). Equilibrium, thermodynamic and kinetic studies on removal of chromium, copper, zinc and arsenic from aqueous solutions

onto fly ash coated by chitosan. *Chemical Engineering Journal*, *274*, 200-212.

[52] Asere, T. G., Stevens, C. V., & Du Laing, G. (2019). Use of (modified) natural adsorbents for arsenic remediation: A review. *Science of the total environment*.

[53] Bilal, M., Shah, J. A., Ashfaq, T., Gardazi, S. M. H., Tahir, A. A., Pervez, A., ... & Mahmood, Q. (2013). Waste biomass adsorbents for copper removal from industrial wastewater—a review. *Journal of Hazardous Materials*, *263*, 322-333.

[54] Bakhat, H. F., Zia, Z., Abbas, S., Hammad, H. M., Shah, G. M., Khalid, S., ... & Fahad, S. (2019). Factors controlling arsenic contamination and potential remediation measures in soil-plant systems. *Groundwater for Sustainable Development*, 100263.

[55] Sodhi, K. K., Kumar, M., Agrawal, P. K., & Singh, D. K. (2019). Perspectives on arsenic toxicity, carcinogenicity and its systemic remediation strategies. *Environmental Technology & Innovation*, 100462.

[56] Kumar, C. P. (2015). Status and mitigation of arsenic contamination in groundwater in India. *Int J Earth Environ Sci*, *1*(1), 1-10.

[57] Abdullah, N., Yusof, N., Lau, W. J., Jaafar, J., & Ismail, A. F. (2019). Recent trends of heavy metal removal from water/wastewater by membrane technologies. *Journal of Industrial and Engineering Chemistry*, *76*, 17-38.

[58] Kumar, M., Goswami, L., Singh, A. K., & Sikandar, M. (2019). Valorization of coal fired-fly ash for potential heavy metal removal from the single and multi-contaminated system. *Heliyon*, *5*(10), e02562.

[59] del Alba Pacheco-Blas, M., & Vicente, L. (2019). Molecular Dynamics Simulation of Removal of heavy metals with sodium dodecyl sulfate micelle in water. *Colloids and Surfaces A: Physicochemical and Engineering Aspects*, 123613.

[60] Bai, S., Wang, L., Ma, F., Zhu, S., Xiao, T., Yu, T., & Wang, Y. (2020). Self-assembly biochar colloids mycelial pellet for heavy metal removal from aqueous solution. *Chemosphere*, *242*, 125182.

[61] Es-sahbany, H., Berradi, M., Nkhili, S., Hsissou, R., Allaoui, M., Loutfi, M., ... & El Youbi, M. S. (2019). Removal of heavy metals (nickel) contained in wastewater-models by the adsorption technique on natural clay. *Materials Today: Proceedings*, *13*, 866-875.

[62] Fan, J. P., Luo, J. J., Zhang, X. H., Zhen, B., Dong, C. Y., Li, Y. C., ... & Chen, H. P. (2019). A novel electrospun β-CD/CS/PVA nanofiber membrane for simultaneous and rapid removal of organic micropollutants and heavy metal ions from water. *Chemical Engineering Journal*, *378*, 122232.

[63] Gupta, V. K., Ali, I., Saleh, T. A., Nayak, A., & Agarwal, S. (2012). Chemical treatment technologies for waste-water recycling—an overview. *Rsc Advances*, *2*(16), 6380-6388.

[64] Foo, K. Y., & Hameed, B. H. (2009). An overview of landfill leachate treatment via activated carbon adsorption process. *Journal of hazardous materials*, *171*(1-3), 54-60.

[65] Gupta, V. K., Mittal, A., Jhare, D., & Mittal, J. (2012). Batch and bulk removal of hazardous colouring agent Rose Bengal by adsorption techniques using bottom ash as adsorbent. *RSC advances*, *2*(22), 8381-8389.

[66] Wilhelm, M., Soltmann, C., Koch, D., & Grathwohl, G. (2005). Ceramers—functional materials for adsorption techniques. *Journal of the European Ceramic Society*, *25*(2-3), 271-276.

[67] Mittal, A., Mittal, J., Malviya, A., & Gupta, V. K. (2009). Adsorptive removal of hazardous anionic dye "Congo red" from wastewater using waste materials and recovery by desorption. *Journal of Colloid and Interface Science*, *340*(1), 16-26.

[68] Guibal, E., & Roussy, J. (2007). Coagulation and flocculation of dye-containing solutions using a biopolymer (Chitosan). *Reactive and functional polymers*, *67*(1), 33-42.

[69] Amuda, O. S., & Amoo, I. A. (2007). Coagulation/flocculation process and sludge conditioning in beverage industrial wastewater treatment. *Journal of Hazardous Materials*, *141*(3), 778-783.

[70] Aziz, H. A., Alias, S., Adlan, M. N., Asaari, A. H., & Zahari, M. S. (2007). Colour removal from landfill leachate by coagulation and flocculation processes. *Bioresource technology*, *98*(1), 218-220.

[71] Roussy, J., Van Vooren, M., Dempsey, B. A., & Guibal, E. (2005). Influence of chitosan characteristics on the coagulation and the flocculation of bentonite suspensions. *Water Research*, *39*(14), 3247-3258.

[72] Hiraide, M., Ito, T., Baba, M., Kawaguchi, H., & Mizuike, A. (1980). Multielement preconcentration of trace heavy metals in water by coprecipitation and flotation with indium hydroxide for inductively coupled plasma-atomic emission spectrometry. *Analytical Chemistry*, *52*(6), 804-807.

[73] Hiraide, M., Yoshida, Y., & Mizuike, A. (1976). Flotation of traces of heavy metals coprecipitated with aluminum hydroxide from water and sea water. *Analytica Chimica Acta*, *81*(1), 185-189.

[74] Mavrov, V., Erwe, T., Blöcher, C., & Chmiel, H. (2003). Study of new integrated processes combining adsorption, membrane separation and flotation for heavy metal removal from wastewater. *Desalination*, *157*(1-3), 97-104.

[75] Kim, J., & Benjamin, M. M. (2004). Modeling a novel ion exchange process for arsenic and nitrate removal. *Water research*, *38*(8), 2053-2062.

[76] Clifford, D., Subramonian, S., & Sorg, T. J. (1986). Water treatment processes. III. Removing dissolved inorganic contaminants from water. *Environmental science & technology*, *20*(11), 1072-1080.

[77] Kurniawan, T. A., Chan, G. Y., Lo, W. H., & Babel, S. (2006). Physico–chemical

treatment techniques for wastewater laden with heavy metals. *Chemical engineering journal*, *118*(1-2), 83-98.

[78] Feng, D., Aldrich, C., & Tan, H. (2000). Treatment of acid mine water by use of heavy metal precipitation and ion exchange. *Minerals Engineering*, *13*(6), 623-642.

[79] Al-Enezi, G., Hamoda, M. F., & Fawzi, N. (2004). Ion exchange extraction of heavy metals from wastewater sludges. *Journal of Environmental Science and Health, Part A*, *39*(2), 455-464.

[80] Yeom, I. T., Nah, Y. M., & Ahn, K. H. (1999). Treatment of household wastewater using an intermittently aerated membrane bioreactor. *Desalination*, *124*(1-3), 193-203.

[81] Shams Ashaghi, K., Ebrahimi, M., & Czermak, P. (2007). Ceramic ultra-and nanofiltration membranes for oilfield produced water treatment: a mini review. *Open Environmental Sciences*, *1*(1).

[82] Blöcher, C., Dorda, J., Mavrov, V., Chmiel, H., Lazaridis, N. K., & Matis, K. A. (2003). Hybrid flotation—membrane filtration process for the removal of heavy metal ions from wastewater. *Water Research*, *37*(16), 4018-4026.

[83] Leiknes, T. (2009). The effect of coupling coagulation and flocculation with membrane filtration in water treatment: A review. *Journal of Environmental Sciences*, *21*(1), 8-12.

[84] Rajkumar, D., & Palanivelu, K. (2004). Electrochemical treatment of industrial wastewater. *Journal of hazardous materials*, *113*(1-3), 123-129.

[85] Tröster, I., Fryda, M., Herrmann, D., Schäfer, L., Hänni, W., Perret, A., ... & Stadelmann, M. (2002). Electrochemical advanced oxidation process for water treatment using DiaChem® electrodes. *Diamond and Related Materials*, *11*(3-6), 640-645.

[86] Lin, S. H., & Peng, C. F. (1996). Continuous treatment of textile wastewater by combined coagulation, electrochemical oxidation and activated sludge. *Water research*, *30*(3), 587-592.

[87] Martin, J. W., Barri, T., Han, X., Fedorak, P. M., El-Din, M. G., Perez, L., ... & Jiang, J. T. (2010). Ozonation of oil sands process-affected water accelerates microbial bioremediation. *Environmental science & technology*, *44*(21), 8350-8356.

[88] Ramos-Cormenzana, A., Monteoliva-Sanchez, M., & Lopez, M. J. (1995). Bioremediation of alpechin. *International biodeterioration & biodegradation*, *35*(1-3), 249-268.

[89] Vences-Alvarez, E., Flores-Arciniega, J. L., Flores-Zuñiga, H., & Rangel-Mendez, J. R. (2019). Fluoride removal from water by ceramic oxides from cerium and manganese solutions. *Journal of Molecular Liquids*, *286*, 110880.

[90] Wang, Z., Tan, K., Cai, J., Hou, S., Wang, Y., Jiang, P., & Liang, M. (2019). Silica

oxide encapsulated natural zeolite for high efficiency removal of low concentration heavy metals in water. *Colloids and Surfaces A: Physicochemical and Engineering Aspects*, *561*, 388-394.

[91] Huang, H., Song, Q., Wang, W., Wu, S., & Dai, J. (2012). Treatment of anaerobic digester effluents of nylon wastewater through chemical precipitation and a sequencing batch reactor process. *Journal of environmental management*, *101*, 68-74.

[92] Kalavathy, M. H., & Miranda, L. R. (2010). Moringa oleifera—A solid phase extractant for the removal of copper, nickel and zinc from aqueous solutions. *Chemical Engineering Journal*, *158*(2), 188-199.

[93] Huzir, N. M., Aziz, M. M. A., Ismail, S. B., Mahmood, N. A. N., Umor, N. A., & Muhammad, S. A. F. A. S. (2019). Optimization of coagulation-flocculation process for the palm oil mill effluent treatment by using rice husk ash. *Industrial Crops and Products*, *139*, 111482.

[94] Huang, X., Wan, Y., Shi, B., & Shi, J. (2020). Effects of powdered activated carbon on the coagulation-flocculation process in humic acid and humic acid-kaolin water treatment. *Chemosphere*, *238*, 124637.

[95] Rodrigues, R. T., & Rubio, J. (2007). DAF–dissolved air flotation: Potential applications in the mining and mineral processing industry. *International Journal of Mineral Processing*, *82*(1), 1-13.

[96] Painmanakul, P., Sastaravet, P., Lersjintanakarn, S., & Khaodhiar, S. (2010). Effect of bubble hydrodynamic and chemical dosage on treatment of oily wastewater by Induced Air Flotation (IAF) process. *Chemical Engineering Research and Design*, *88*(5-6), 693-702.

[97] Liu, J. C., & Chang, C. J. (2009). Precipitation flotation of phosphate from water. *Colloids and Surfaces A: Physicochemical and Engineering Aspects*, *347*(1-3), 215-219.

[98] Kumari, M., & Gupta, S. K. (2019). A novel process of adsorption cum enhanced coagulation-flocculation spiked with magnetic nanoadsorbents for the removal of aromatic and hydrophobic fraction of natural organic matter along with turbidity from drinking water. *Journal of Cleaner Production*, 118899.

[99] López-Maldonado, E. A., Oropeza-Guzman, M. T., Jurado-Baizaval, J. L., & Ochoa-Terán, A. (2014). Coagulation–flocculation mechanisms in wastewater treatment plants through zeta potential measurements. *Journal of hazardous materials*, *279*, 1-10.

[100] Ozun, S., & Ulus, D. A. (2019). Coagulation and flocculation behavior of fines in foid-bearing rock processing plant (FRPP) wastewater at alkaline environment. *Powder technology*, *344*, 335-342.

[101] Zahrim, A. Y., Dexter, Z. D., Joseph, C. G., & Hilal, N. (2017). Effective coagulation-flocculation treatment of highly polluted palm oil mill biogas plant

wastewater using dual coagulants: Decolourisation, kinetics and phytotoxicity studies. *Journal of water process engineering*, *16*, 258-269.

[102] Vandamme, D., Foubert, I., Fraeye, I., & Muylaert, K. (2012). Influence of organic matter generated by Chlorella vulgaris on five different modes of flocculation. *Bioresource technology*, *124*, 508-511.

[103] Fu, F., & Wang, Q. (2011). Removal of heavy metal ions from wastewaters: a review. *Journal of environmental management*, *92*(3), 407-418.

[104] de Souza Leite, L., Hoffmann, M. T., & Daniel, L. A. (2019). Coagulation and dissolved air flotation as a harvesting method for microalgae cultivated in wastewater. *Journal of Water Process Engineering*, *32*, 100947.

[105] Kang, J., Fan, R., Hu, Y., Sun, W., Liu, R., Zhang, Q., ... & Meng, X. (2018). Silicate removal from recycled wastewater for the improvement of scheelite flotation performance. *Journal of cleaner production*, *195*, 280-288.

[106] Azevedo, A., Oliveira, H. A., & Rubio, J. (2018). Treatment and water reuse of lead-zinc sulphide ore mill wastewaters by high rate dissolved air flotation. *Minerals Engineering*, *127*, 114-121.

[107] Hoseinian, F. S., Rezai, B., Safari, M., Deglon, D., & Kowsari, E. (2019). Effect of hydrodynamic parameters on nickel removal rate from wastewater by ion flotation. *Journal of environmental management*, *244*, 408-414.

[108] Yamamoto, S., Kanai, S., Takeyama, M., Nishiyama, Y., Imura, H., & Nagatani, H. (2020). Ion transfer and adsorption of water-soluble metal complexes of 8-hydroxyquinoline derivatives at the water| 1, 2-dichloroethane interface. *Journal of Electroanalytical Chemistry*, *856*, 113566.

[109] Song, Z., Chen, X., Gong, X., Gao, X., Dai, Q., Nguyen, T. T., & Guo, M. (2020). Luminescent carbon quantum dots/nanofibrillated cellulose composite aerogel for monitoring adsorption of heavy metal ions in water. *Optical Materials*, *100*, 109642.

[110] Shen, C., Zhao, Y., Li, W., Yang, Y., Liu, R., & Morgen, D. (2019). Global profile of heavy metals and semimetals adsorption using drinking water treatment residual. *Chemical Engineering Journal*.

[111] Cortes-Arriagada, D., & Mella, A. (2019). Performance of doped graphene nanoadsorbents with first-row transition metals (ScZn) for the adsorption of water-soluble trivalent arsenicals: A DFT study. *Journal of Molecular Liquids*, *294*, 111665.

[112] Liu, C., Wang, Q., Jia, F., & Song, S. (2019). Adsorption of heavy metals on molybdenum disulfide in water: A critical review. *Journal of Molecular Liquids*, 111390.

[113] Wöllner, M., Klein, N., & Kaskel, S. (2019). Measuring water adsorption processes of metal-organic frameworks for heat pump applications via optical calorimetry. *Microporous and Mesoporous Materials*, *278*, 206-211.

[114] Huang, Y., Fu, C., Li, Z., Fang, F., Ouyang, W., & Guo, J. (2019). Effect of dissolved organic matters on adsorption and desorption behavior of heavy metals in a water-level-fluctuation zone of the Three Gorges Reservoir, China. *Ecotoxicology and Environmental Safety*, *185*, 109695.

[115] Palash, M. L., Jahan, I., Rupam, T. H., Harish, S., & Saha, B. B. (2020). Novel technique for improving the water adsorption isotherms of metal-organic frameworks for performance enhancement of adsorption driven chillers. *Inorganica Chimica Acta*, *501*, 119313.

[116] Zhang, L., & Xu, K. (2020). Aggregation-enhanced adsorption and optoelectronic performance of metal-free organic dye on anatase (1 0 1) toward water-splitting purpose: A first-principles investigation. *Applied Surface Science*, *502*, 144139.

[117] An, H. J., Sarker, M., Yoo, D. K., & Jhung, S. H. (2019). Water adsorption/desorption over metal-organic frameworks with ammonium group for possible application in adsorption heat transformation. *Chemical Engineering Journal*, *373*, 1064-1071.

[118] Yao, N., Li, C., Yu, J., Xu, Q., Wei, S., Tian, Z., ... & Shen, J. (2020). Insight into adsorption of combined antibiotic-heavy metal contaminants on graphene oxide in water. *Separation and Purification Technology*, *236*, 116278.

[119] Siddiqui, S. H., & Ahmad, R. (2017). Pistachio Shell Carbon (PSC)–an agricultural adsorbent for the removal of Pb (II) from aqueous solution. *Groundwater for Sustainable Development*, *4*, 42-48.

[120] Shah, S. M., Makhdoom, A. R., Su, X., Faheem, M., Irfan, M., Irfan, M., ... & Gao, Y. (2019). Synthesis of sulphonic acid functionalized magnetic mesoporous silica for Cu (II) and Co (II) adsorption. *Microchemical Journal*, *151*, 104194.

[121] Khound, N. J., & Bharali, R. K. (2018). Biosorption of fluoride from aqueous medium by Indian sandalwood (Santalum album) leaf powder. *Journal of Environmental Chemical Engineering*, *6*(2), 1726-1735.

[122] Lam, S. T., Ballinger, R., & Forsberg, C. (2018). Modeling and predicting total hydrogen adsorption in nanoporous carbon materials for advanced nuclear systems. *Journal of Nuclear Materials*, *511*, 328-340.

[123] Piri, M., Sepehr, E., & Rengel, Z. (2019). Citric acid decreased and humic acid increased Zn sorption in soils. *Geoderma*, *341*, 39-45.

[124] Joshi, N. C., & Singh, A. (2019). Adsorptive performances and characterisations of biologically synthesised zinc oxide based nanosorbent (ZOBN). *Groundwater for Sustainable Development*, 100325.

[125] Ungureanu, G., Santos, S., Boaventura, R., & Botelho, C. (2015). Arsenic and antimony in water and wastewater: overview of removal techniques with

special reference to latest advances in adsorption. *Journal of Environmental Management*, *151*, 326-342.

[126] Ishtiaq, F., Bhatti, H. N., Khan, A., Iqbal, M., & Kausar, A. (2020). Polypyrole, polyaniline and sodium alginate biocomposites and adsorption-desorption efficiency for imidacloprid insecticide. *International Journal of Biological Macromolecules*.

[127] Yakout, S. M., Hassan, M. R., Abdeltawab, A. A., & Aly, M. I. (2019). Sono-sorption efficiencies and equilibrium removal of triphenylmethane (crystal violet) dye from aqueous solution by activated charcoal. *Journal of Cleaner Production*, *234*, 124-131.

[128] Araújo, C. S., Almeida, I. L., Rezende, H. C., Marcionilio, S. M., Léon, J. J., & de Matos, T. N. (2018). Elucidation of mechanism involved in adsorption of Pb (II) onto lobeira fruit (Solanum lycocarpum) using Langmuir, Freundlich and Temkin isotherms. *Microchemical Journal*, *137*, 348-354.

[129] Hao, J., Ji, L., Li, C., Hu, C., & Wu, K. (2018). Rapid, efficient and economic removal of organic dyes and heavy metals from wastewater by zinc-induced in-situ reduction and precipitation of graphene oxide. *Journal of the Taiwan Institute of Chemical Engineers*, *88*, 137-145.

[130] Du, C. M., Gao, X., Ueda, S., & Kitamura, S. Y. (2019). Separation and recovery of phosphorus from steelmaking slag via a selective leaching–chemical precipitation process. *Hydrometallurgy*, *189*, 105109.

[131] Du, C. M., Gao, X., Ueda, S., & Kitamura, S. Y. (2018). Recovery of phosphorus from modified steelmaking slag with high P2O5 content via leaching and precipitation. *ISIJ International*, *58*(5), 833-841.

[132] Rupa, M. J., Pal, A., & Saha, B. B. (2020). Activated carbon-graphene nanoplatelets based green cooling system: Adsorption kinetics, heat of adsorption, and thermodynamic performance. *Energy*, *193*, 116774.

[133] Wang, G., Li, N., Xing, X., Sun, Y., Zhang, Z., & Hao, Z. (2020). Gaseous adsorption of hexamethyldisiloxane on carbons: Isotherms, isosteric heats and kinetics. *Chemosphere*, 125862.

[134] Regazzoni, A. E. (2020). Adsorption kinetics at solid/aqueous solution interfaces: On the boundaries of the pseudo-second order rate equation. *Colloids and Surfaces A: Physicochemical and Engineering Aspects*, *585*, 124093.

[135] Dang, W., Zhang, J., Nie, H., Wang, F., Tang, X., Wu, N., ... & Wang, R. (2020). Isotherms, thermodynamics and kinetics of methane-shale adsorption pair under supercritical condition: Implications for understanding the nature of shale gas adsorption process. *Chemical Engineering Journal*, *383*, 123191.

[136] Bai, C., Wang, L., & Zhu, Z. (2019). Adsorption of Cr (III) and Pb (II) by graphene oxide/alginate hydrogel membrane: Characterization, adsorption

kinetics, isotherm and thermodynamics studies. *International journal of biological macromolecules*.

[137] Cao, R., Guo, J., Hua, X., & Xu, Y. (2020). Investigation on decolorization kinetics and thermodynamics of lignocellulosic xylooligosaccharides by highly selective adsorption with Amberlite XAD-16N. *Food Chemistry*, *310*, 125934.

[138] Dada, A. O., Olalekan, A. P., Olatunya, A. M., & Dada, O. J. I. J. C. (2012). Langmuir, Freundlich, Temkin and Dubinin–Radushkevich isotherms studies of equilibrium sorption of Zn2+ unto phosphoric acid modified rice husk. *IOSR Journal of Applied Chemistry*, *3*(1), 38-45.

[139] Vaz, M. G., Pereira, A. G., Fajardo, A. R., Azevedo, A. C., & Rodrigues, F. H. (2017). Methylene blue adsorption on chitosan-g-poly (acrylic acid)/rice husk ash superabsorbent composite: Kinetics, equilibrium, and thermodynamics. *Water, Air, & Soil Pollution*, *228*(1), 14.

[140] Mukhtar, A., Mellon, N., Saqib, S., Khawar, A., Rafiq, S., Ullah, S., ... & Tahir, M. S. (2020). CO2/CH4 adsorption over functionalized multi-walled carbon nanotubes; an experimental study, isotherms analysis, mechanism, and thermodynamics. *Microporous and Mesoporous Materials*, *294*, 109883.

[141] Azizian, S., Eris, S., & Wilson, L. D. (2018). Re-evaluation of the century-old Langmuir isotherm for modeling adsorption phenomena in solution. *Chemical Physics*, *513*, 99-104.

[142] Bai, C., Wang, L., & Zhu, Z. (2019). Adsorption of Cr (III) and Pb (II) by graphene oxide/alginate hydrogel membrane: Characterization, adsorption kinetics,isotherm and thermodynamics studies. *International journal of biological macromolecules*.

[143] Shalaby, N. H., Ewais, E. M., Elsaadany, R. M., & Ahmed, A. (2017). Rice husk templated water treatment sludge as low cost dye and metal adsorbent. *Egyptian journal of petroleum*, *26*(3), 661-668.

[144] Diagboya, P. N., & Dikio, E. D. (2018). Silica-based mesoporous materials; emerging designer adsorbents for aqueous pollutants removal and water treatment. *Microporous and Mesoporous Materials*, *266*, 252-267.

[145] Palza, H., Delgado, K., & Govan, J. (2019). Novel magnetic CoFe2O4/layered double hydroxide nanocomposites for recoverable anionic adsorbents for water treatment. *Applied Clay Science*, *183*, 105350.

[146] Siswoyo, E., Qoniah, I., Lestari, P., Fajri, J. A., Sani, R. A., Sari, D. G., & Boving, T. (2019). Development of a floating adsorbent for cadmium derived from modified drinking water treatment plant sludge. *Environmental technology & innovation*.

[147] Kumari, P., Alam, M., & Siddiqi, W. A. (2019). Usage of nanoparticles as adsorbents for waste water treatment: An emerging trend. *Sustainable Materials and Technologies*, e00128.

[148] Zeng, H., Yu, Y., Wang, F., Zhang, J., & Li, D. (2020). Arsenic (V) removal by granular adsorbents made from water treatment residuals materials and chitosan. *Colloids and Surfaces A: Physicochemical and Engineering Aspects*, *585*, 124036.

[149] Rasapoor, M., Young, B., Asadov, A., Brar, R., Sarmah, A. K., Zhuang, W. Q., & Baroutian, S. (2020). Effects of biochar and activated carbon on biogas generation: A thermogravimetric and chemical analysis approach. *Energy Conversion and Management*, *203*, 112221.

[150] Zhang, X., Li, C., Qu, J., Guo, Q., & Huang, K. (2019). Cotton stalk activated carbon-supported Co–Ce–B nanoparticles as efficient catalysts for hydrogen generation through hydrolysis of sodium borohydride. *Carbon Resources Conversion*, *2*(3), 225-232.

[151] Rambabu, K., Hai, A., Bharath, G., & Banat, F. (2019). Molybdenum disulfide decorated palm oil waste activated carbon as an efficient catalyst for hydrogen generation by sodium borohydride hydrolysis. *International Journal of Hydrogen Energy*, *44*(28), 14406-14415.

[152] Akbayrak, S., Özçifçi, Z., & Tabak, A. (2019). Noble metal nanoparticles supported on activated carbon: Highly recyclable catalysts in hydrogen generation from the hydrolysis of ammonia borane. *Journal of colloid and interface science*, *546*, 324-332.

[153] Newcombe, G., Drikas, M., & Hayes, R. (1997). Influence of characterised natural organic material on activated carbon adsorption: II. Effect on pore volume distribution and adsorption of 2-methylisoborneol. *Water Research*, *31*(5), 1065-1073.

[154] Lakshmi, S. D., Avti, P. K., & Hegde, G. (2018). Activated carbon nanoparticles from biowaste as new generation antimicrobial agents: a review. *Nano-Structures & Nano-Objects*, *16*, 306-321.

[155] Ros, A., Lillo-Ródenas, M. A., Fuente, E., Montes-Morán, M. A., Martín, M. J., & Linares-Solano, A. (2006). High surface area materials prepared from sewage sludge-based precursors. *Chemosphere*, *65*(1), 132-140.

[156] Herde, Z. D., Dharmasena, R., Sumanasekera, G., Tumuluru, J. S., & Satyavolu, J. (2020). Impact of hydrolysis on surface area and energy storage applications of activated carbons produced from corn fiber and soy hulls. *Carbon Resources Conversion*, *3*, 19-28.

[157] Cossutta, M., Vretenar, V., Centeno, T. A., Kotrusz, P., McKechnie, J., & Pickering, S. J. (2020). A comparative life cycle assessment of graphene and activated carbon in a supercapacitor application. *Journal of Cleaner Production*, *242*, 118468.

[158] Ahmed, S., Ahmed, A., & Rafat, M. (2019). Investigation on activated carbon derived from biomass Butnea monosperma and its application as a high performance supercapacitor electrode. *Journal of Energy Storage*, *26*, 100988.
[159] Guo, F., Jiang, X., Jia, X., Liang, S., Qian, L., & Rao, Z. (2019). Synthesis of biomass carbon electrode materials by bimetallic activation for the application in supercapacitors. *Journal of Electroanalytical Chemistry*, *844*, 105-115.
[160] Elaiyappillai, E., Srinivasan, R., Johnbosco, Y., Devakumar, P., Murugesan, K., Kesavan, K., & Johnson, P. M. (2019). Low cost activated carbon derived from Cucumis melo fruit peel for electrochemical supercapacitor application. *Applied Surface Science*, *486*, 527-538.
[161] Ahmed, S., Ahmed, A., & Rafat, M. (2019). Investigation on activated carbon derived from biomass Butnea monosperma and its application as a high performance supercapacitor electrode. *Journal of Energy Storage*, *26*, 100988.
[162] Guo, F., Jiang, X., Jia, X., Liang, S., Qian, L., & Rao, Z. (2019). Synthesis of biomass carbon electrode materials by bimetallic activation for the application in supercapacitors. *Journal of Electroanalytical Chemistry*, *844*, 105-115.
[163] Samantray, R., & Mishra, S. C. (2020). Saccharum spontaneum, a precursor of sustainable activated carbon: Synthesis, characterization and optimization of process parameters and its suitability for supercapacitor applications. *Diamond and Related Materials*, *101*, 107598.
[164] Kim, M. H., Tang, J., Jang, S. J., Pol, V. G., & Roh, K. C. (2019). Porous graphitic activated carbon sheets upcycled from starch-based packing peanuts for applications in ultracapacitors. *Journal of Alloys and Compounds*, *805*, 1282-1287.
[165] Khalifa, A. M., Abdulateef, S. A., Kabaa, E. A., Ahmed, N. M., & Sabah, F. A. (2020). Study of acidosis, neutral and alkalosis media effects on the behaviour of activated carbon threads decorated by zinc oxide using extended gate FET for glucose sensor application. *Materials Science in Semiconductor Processing*, *108*, 104911.
[166] Sreńscek-Nazzal, J., & Kiełbasa, K. (2019). Advances in modification of commercial activated carbon for enhancement of CO2 capture. *Applied Surface Science*, *494*, 137-151.
[167] Kopac, T., & Kırca, Y. (2019). Effect of ammonia and boron modifications on the surface and hydrogen sorption characteristics of activated carbons from coal. *International Journal of Hydrogen Energy*.
[168] Lv, S., Li, C., Mi, J., & Meng, H. (2020). A functional activated carbon for efficient adsorption of phenol derived from pyrolysis of rice husk, KOH-activation and EDTA-4Na-modification. *Applied Surface Science*, 145425.
[169] Lee, W., Yoon, S., Choe, J. K., Lee, M., & Choi, Y. (2018). Anionic surfactant modification of activated carbon for enhancing adsorption of ammonium ion from

aqueous solution. *Science of The Total Environment*, *639*, 1432-1439.

[170] Li, K., Chen, W., Yang, H., Chen, Y., Xia, S., Xia, M., ... & Chen, H. (2019). Mechanism of biomass activation and ammonia modification for nitrogen-doped porous carbon materials. *Bioresource technology*, *280*, 260-268.

[171] Abdulrasheed, A. A., Jalil, A. A., Triwahyono, S., Zaini, M. A. A., Gambo, Y., & Ibrahim, M. (2018). Surface modification of activated carbon for adsorption of SO2 and NOX: A review of existing and emerging technologies. *Renewable and Sustainable Energy Reviews*, *94*, 1067-1085.

[172] Xiao, C. Y., Zhang, W. L., Lin, H. B., Tian, Y. X., Li, X. X., Tian, Y. Y., & Lu, H. Y. (2019). Modification of a rice husk-based activated carbon by thermal treatment and its effect on its electrochemical performance as a supercapacitor electrode. *New Carbon Materials*, *34*(4), 341-348.

[173] Wang, C., Chen, S., Chen, Y., Zi, F., Hu, X., Qin, X., ... & Lin, Y. (2020). Modification of activated carbon by chemical vapour deposition through thermal decomposition of thiourea for enhanced adsorption of gold thiosulfate complex. *Separation and Purification Technology*, 116632.

[174] Cukierman, A. L. (2013). Development and environmental applications of activated carbon cloths. *ISRN Chemical Engineering*, *2013*.

[175] Li, Y., Fan, X., Zhang, M., Cui, L., & Jiao, T. (2019). Enhanced electrochemical performance of the activated carbon electrodes with a facile and in-situ phosphoric acid modification. *Journal of Energy Storage*, *24*, 100744.

[176] Lesaoana, M., Mlaba, R. P. V., Mtunzi, F. M., Klink, M. J., Edijike, P., & Pakade, V. E. (2019). Influence of inorganic acid modification on Cr (VI) adsorption performance and the physicochemical properties of activated carbon. *South African Journal of Chemical Engineering*.

[177] Contescu, C. I., Adhikari, S. P., Gallego, N. C., Evans, N. D., & Biss, B. E. (2018). Activated carbons derived from high-temperature pyrolysis of lignocellulosic biomass. *C—Journal of Carbon Research*, *4*(3), 51.

[178] Owlad, M., Aroua, M. K., & Daud, W. M. A. W. (2010). Hexavalent chromium adsorption on impregnated palm shell activated carbon with polyethyleneimine. *Bioresource technology*, *101*(14), 5098-5103.

[179] Pap, S., Knudsen, T. Š., Radonić, J., Maletić, S., Igić, S. M., & Sekulić, M. T. (2017). Utilization of fruit processing industry waste as green activated carbon for the treatment of heavy metals and chlorophenols contaminated water. *Journal of Cleaner Production*, *162*, 958-972.

[180] Ibrahim, W. M., Hassan, A. F., & Azab, Y. A. (2016). Biosorption of toxic heavy metals from aqueous solution by Ulva lactuca activated carbon. *Egyptian journal of basic and applied sciences*, *3*(3), 241-249.

[181] Da'na, E., & Awad, A. (2017). Regeneration of spent activated carbon obtained from home filtration system and applying it for heavy metals adsorption. *Journal of*

*environmental chemical engineering*, *5*(4), 3091-3099.

[182] Kim, D. W., Wee, J. H., Yang, C. M., & Yang, K. S. (2019). Efficient removals of Hg and Cd in aqueous solution through NaOH-modified activated carbon fiber. *Chemical Engineering Journal*, 123768.

[183] Yunus, Z. M., Al-Gheethi, A., Othman, N., Hamdan, R., & Ruslan, N. N. (2020). Removal of heavy metals from mining effluents in tile and electroplating industries using honeydew peel activated carbon: A microstructure and techno-economic analysis. *Journal of Cleaner Production*, *251*, 119738.

[184] Li, J., Xing, X., Li, J., Shi, M., Lin, A., Xu, C., ... & Li, R. (2018). Preparation of thiol-functionalized activated carbon from sewage sludge with coal blending for heavy metal removal from contaminated water. *Environmental pollution*, *234*, 677-683.

[185] Li, L. Y., Gong, X., & Abida, O. (2019). Waste-to-resources: Exploratory surface modification of sludge-based activated carbon by nitric acid for heavy metal adsorption. *Waste Management*, *87*, 375-386.

[186] Nejadshafiee, V., & Islami, M. R. (2019). Adsorption capacity of heavy metal ions using sultone-modified magnetic activated carbon as a bio-adsorbent. *Materials Science and Engineering: C*, *101*, 42-52.

[187] Lee, J., Sarmah, A. K., & Kwon, E. E. (2019). Production and formation of biochar. In *Biochar from Biomass and Waste* (pp. 3-18). Elsevier.

[188] Kamaraj, M., Srinivasan, N. R., Assefa, G., Adugna, A. T., & Kebede, M. (2020). Facile development of sunlit ZnO nanoparticles-activated carbon hybrid from pernicious weed as an operative nano-adsorbent for removal of methylene blue and chromium from aqueous solution: Extended application in tannery industrial wastewater. *Environmental Technology & Innovation*, *17*, 100540.

[189] Rahmani-Sani, A., Singh, P., Raizada, P., Lima, E. C., Anastopoulos, I., Giannakoudakis, D. A., ... & Hosseini-Bandegharaei, A. (2020). Use of chicken feather and eggshell to synthesize a novel magnetized activated carbon for sorption of heavy metal ions. *Bioresource Technology*, *297*, 122452.

[190] Dong, L., Hou, L. A., Wang, Z., Gu, P., Chen, G., & Jiang, R. (2018). A new function of spent activated carbon in BAC process: removing heavy metals by ion exchange mechanism. *Journal of hazardous materials*, *359*, 76-84.

[191] Ouyang, D., Zhuo, Y., Hu, L., Zeng, Q., Hu, Y., & He, Z. (2019). Research on the Adsorption Behavior of Heavy Metal Ions by Porous Material Prepared with Silicate Tailings. *Minerals*, *9*(5), 291.

[192] Que, W., Zhou, Y. H., Liu, Y. G., Wen, J., Tan, X. F., Liu, S. J., & Jiang, L. H. (2019). Appraising the effect of in-situ remediation of heavy metal contaminated sediment by biochar and activated carbon on Cu immobilization and microbial community. *Ecological engineering*, *127*, 519-526.

[193] Abdel-Halim, E. S., & Al-Deyab, S. S. (2011). Removal of heavy metals from their

aqueous solutions through adsorption onto natural polymers. *Carbohydrate Polymers*, *84*(1), 454-458.

[194] Abdullah, N. H., Shameli, K., Abdullah, E. C., & Abdullah, L. C. (2019). Solid matrices for fabrication of magnetic iron oxide nanocomposites: synthesis, properties, and application for the adsorption of heavy metal ions and dyes. *Composites Part B: Engineering*, *162*, 538-568.

[195] Farhan, S. N., & Khadom, A. A. (2015). Biosorption of heavy metals from aqueous solutions by Saccharomyces Cerevisiae. *International journal of industrial chemistry*, *6*(2), 119-130.

[196] Ndlovu, S., Simate, G. S., Seepe, L., Shemi, A., Sibanda, V., & Van Dyk, L. D. (2013). The removal of Co2+, V3+ and Cr3+ from waste effluents using cassava waste. *South African Journal of Chemical Engineering*, *18*(1), 51-69.

[197] Kumar, P. S., Ramakrishnan, K., Kirupha, S. D., & Sivanesan, S. (2010). Thermodynamic and kinetic studies of cadmium adsorption from aqueous solution onto rice husk. *Brazilian Journal of Chemical Engineering*, *27*(2), 347-355.

[198] Cozmuta, L. M., Cozmuta, A. M., Peter, A., Nicula, C., Nsimba, E. B., & Tutu, H. (2012). The influence of pH on the adsorption of lead by Na-clinoptilolite: Kinetic and equilibrium studies. *Water Sa*, *38*(2), 269-278.

[199] Farghali, A. A., Bahgat, M., Allah, A. E., & Khedr, M. H. (2013). Adsorption of Pb (II) ions from aqueous solutions using copper oxide nanostructures. *Beni-Suef University Journal of Basic and Applied Sciences*, *2*(2), 61-71.

[200] Bernal, V., Erto, A., Giraldo, L., & Moreno-Piraján, J. C. (2017). Effect of solution pH on the adsorption of paracetamol on chemically modified activated carbons. *Molecules*, *22*(7), 1032.

[201] Hegazi, H. A. (2013). Removal of heavy metals from wastewater using agricultural and industrial wastes as adsorbents. *HBRC journal*, *9*(3), 276-282.

[202] Liu, X., Guan, J., Lai, G., Xu, Q., Bai, X., Wang, Z., & Cui, S. (2020). Stimuli-responsive adsorption behavior toward heavy metal ions based on comb polymer functionalized magnetic nanoparticles. *Journal of Cleaner Production*, *253*, 119915.

[203] Asgari, P., Mousavi, S. H., Aghayan, H., Ghasemi, H., & Yousefi, T. (2019). Nd-BTC metal-organic framework (MOF); synthesis, characterization and investigation on its adsorption behavior toward cesium and strontium ions. *Microchemical Journal*, *150*, 104188.

[204] Wang, Z., Wang, Y., Cao, S., Liu, S., Chen, Z., Chen, J., ... & Fu, J. (2020). Fabrication of core@ shell structural Fe-Fe2O3@ PHCP nanochains with high saturation magnetization and abundant amino groups for hexavalent chromium adsorption and reduction. *Journal of hazardous materials*, *384*, 121483.

[205] Chen, X., Guo, Y., Ding, S., Zhang, H., Xia, F., Wang, J., & Zhou, M. (2019). Utilization of red mud in geopolymer-based pervious concrete with function of

adsorption of heavy metal ions. *Journal of cleaner production*, *207*, 789-800.

[206] Peng, W., Li, H., Liu, Y., & Song, S. (2017). A review on heavy metal ions adsorption from water by graphene oxide and its composites. *Journal of Molecular Liquids*, *230*, 496-504.

[207] Mahmoud, A. M., Ibrahim, F. A., Shaban, S. A., & Youssef, N. A. (2015). Adsorption of heavy metal ion from aqueous solution by nickel oxide nano catalyst prepared by different methods. *Egyptian Journal of Petroleum*, *24*(1), 27-35.

[208] Salam, O. E. A., Reiad, N. A., & ElShafei, M. M. (2011). A study of the removal characteristics of heavy metals from wastewater by low-cost adsorbents. *Journal of Advanced Research*, *2*(4), 297-303.

[209] Deng, J. H., Zhang, X. R., Zeng, G. M., Gong, J. L., Niu, Q. Y., & Liang, J. (2013). Simultaneous removal of Cd (II) and ionic dyes from aqueous solution using magnetic graphene oxide nanocomposite as an adsorbent. *Chemical Engineering Journal*, *226*, 189-200.

[210] Peng, X., Yan, Z., Hu, L., Zhang, R., Liu, S., Wang, A., ... & Chen, L. (2019). Adsorption behavior of hexavalent chromium in aqueous solution by polyvinylimidazole modified cellulose. *International journal of biological macromolecules*.

[211] Qi, X., Chen, M., Qian, Y., Liu, M., Li, Z., Shen, L., ... & Shen, J. (2019). Construction of macroporous salecan polysaccharide-based adsorbents for wastewater remediation. *International journal of biological macromolecules*, *132*, 429-438.

[212] Nsami, J. N., & Mbadcam, J. K. (2013). The Adsorption Efficiency of Chemically Prepared Activated Carbon from Cola Nut Shells by ZnCl 2 on Methylene Blue. *Journal of chemistry*.

[213] Kilic, M., Apaydin-Varol, E., & Pütün, A. E. (2011). Adsorptive removal of phenol from aqueous solutions on activated carbon prepared from tobacco residues: equilibrium, kinetics and thermodynamics. *Journal of Hazardous Materials*, *189*(1-2), 397-403.

[214] Newcombe, G., Drikas, M., & Hayes, R. (1997). Influence of characterised natural organic material on activated carbon adsorption: II. Effect on pore volume distribution and adsorption of 2-methylisoborneol. *Water Research*, *31*(5), 1065-1073.

[215] Das, B., & Mondal, N. K. (2011). Calcareous Soil as a New Adsorbent to Remove Lead from Aqueous Solution: Equilibrium, Kinetic and Thermodynamic Study. *Universal Journal of Environmental Research & Technology*, *1*(4).

[216] Panda, H., Tiadi, N., Mohanty, M., & Mohanty, C. R. (2017). Studies on adsorption behavior of an industrial waste for removal of chromium from aqueous solution. *south african journal of chemical engineering*, *23*, 132-138.

[217] Ogata, F., Nagai, N., Itami, R., Nakamura, T., & Kawasaki, N. (2020). Potential of virgin and calcined wheat bran biomass for the removal of chromium (VI) ion from a synthetic aqueous solution. *Journal of Environmental Chemical Engineering*, 103710.

[218] Razak, M. R., Yusof, N. A., Aris, A. Z., Nasir, H. M., Haron, M. J., Ibrahim, N. A., ... & Kamaruzaman, S. (2020). Phosphoric acid modified kenaf fiber (K-PA) as green adsorbent for the removal of copper (II) ions towards industrial waste water effluents. *Reactive and Functional Polymers*, 104466.

[219] Khosravi, R., Moussavi, G., Ghaneian, M. T., Ehrampoush, M. H., Barikbin, B., Ebrahimi, A. A., & Sharifzadeh, G. (2018). Chromium adsorption from aqueous solution using novel green nanocomposite: Adsorbent characterization, isotherm, kinetic and thermodynamic investigation. *Journal of Molecular Liquids*, *256*, 163-174.

[220] Sabri, N. A. M. (2012). *Surface Modification of Multiwalled Carbon Nanotubes by Chemical Oxidation and Immobilization of Tyrosinase* (Doctoral dissertation, Universiti Teknologi Malaysia).

[221] Zheng, Q., Farrauto, R., & Chau Nguyen, A. (2016). Adsorption and methanation of flue gas CO2 with dual functional catalytic materials: a parametric study. *Industrial & Engineering Chemistry Research*, *55*(24), 6768-6776.

[222] Khan, G., Basirun, W. J., Kazi, S. N., Ahmed, P., Magaji, L., Ahmed, S. M., ... & Badry, A. B. B. M. (2017). Electrochemical investigation on the corrosion inhibition of mild steel by Quinazoline Schiff base compounds in hydrochloric acid solution. *Journal of colloid and interface science*, *502*, 134-145.

[223] Li, H., Fang, Z., Luo, J., & Yang, S. (2017). Direct conversion of biomass components to the biofuel methyl levulinate catalyzed by acid-base bifunctional zirconia-zeolites. *Applied Catalysis B: Environmental*, *200*, 182-191.

[224] Rani, S., & Sud, D. (2015). Effect of temperature on adsorption-desorption behaviour of triazophos in Indian soils. *Plant, soil and environment*, *61*(1), 36-42.

# CHAPTER THREE: EXPERIMENTAL PROCEDURES

The hydrochar and AC used as adsorbents in this study were prepared from eucalyptus wood chips. The characterization of these adsorbents using different analytical instruments is also described. The experimental procedures used in this study are well elaborated in this section with all the apparatus and instruments.

## 3.1. CHEMICAL REAGENTS USED IN PREPARATION OF STOCK SOLUTIONS

All the chemical reagents used in this work were received from Sigma-Aldrich, Germany. The stock solution of manganese was prepared by dissolving the mass of 7.205 g of manganese(II) chloride tetrahydrate ($Cl_2Mn.4H_2O$), which is 99.0% pure, in a 500 mL volumetric flask and filled to the mark with deionized water (Milli-Q® Direct 8/16 System, Merck, Germany) to get the stock solution of a concentration of 4000 mg/L Mn(II). The stock solution of chromium was prepared by dissolving the mass of 3.846 g of chromium trioxide ($CrO_3$), which is 99.0% pure, in a 500 mL volumetric flask and filled to the mark with deionized water to generate the stock solution of a concentration of 4000 mg/L Cr(VI). A 1 M of sodium hydroxide (NaOH) and 1% nitric acid ($HNO_3$) were used to adjust the pH ranging from 3 to 8.5 of aqueous solutions.



## 3.2. APPARATUS AND INSTRUMENTS

All the glassware used in this work were washed with deionized water (Milli-Q® Direct 8/16 System, Merck, Germany) and soap, wiped with jumbo tissue paper roll then dried in a 310-glassware drier (LABOTEC, South Africa) for 24 hours to remove the moisture. The hydrochar and AC were grinded using an agate mortar and pestle. The process of generating AC from the hydrochar was carried out by using a tube furnace (Carbolite, USA). The mass measurements of the adsorbents were performed by using a PA423C analytical balance. The thermal stability of the hydrochar was determined through thermogravimetric analysis by using DSC-TGA SDT Q600 (TA Instruments, France). The discovery of the functional groups that are present in the adsorbent materials was done by employing MIRacle-10 FTIR (Shimadzu, Japan). The average diameter, pore volume, and surface area of the hydrochar and AC were achieved by using BET (GAPP

Instruments, China). The particle sizes of the adsorbent materials were accomplished using the DLS (Malvern Panalytical, Germany). The internal structure of the hydrochar and AC was examined utilizing a Jeol JEM-2100F TEM (JEOL, Japan) equipped with a LaB6 source. The external morphology (texture) was analyzed using a TESCAN Vega 3 SEM (JSM-7800F, JEOL, Japan). The pH contents of Mn(II) and Cr(VI) were measured using the pH Meter (520A pH/mV/SE, Thermo Scientific Orion, USA). The analysis of the filtrates was carried out through the FAAS (AA-7000, Shimadzu, Japan). The crystallinity of the adsorbent materials was revealed by using XRD (D8 Advance, Bruker, Germany). The elements present in the hydrochar and AC were uncovered by employing the EDS (NORANTM System 7, Thermo Scientific, USA) coupled with an Oxford detector. The conductivity improvement of the samples was done by carbon-coating hydrochar and activated carbon using a coater (Q300T ES, Quorum, Japan). The samples were sonicated by using an ultrasonic bath.

### 3.3. PREPARATION OF HYDROCHAR AND AC FROM EUCALYPTUS WOOD CHIPS

The eucalyptus wood chips were collected from a timber processing company in North West Province, South Africa. Hydrochar was produced by hydrothermal carbonization (HTC) of eucalyptus wood chips in the presence of a catalyst, water as a solvent, under the temperature of 240 °C and pressure of 4 bars. The AC was generated by heating the hydrochar in a tube furnace under the temperature of 700 °C in an inert atmosphere supported by nitrogen gas. This process is called annealing. The process of hydrochar and its AC generation is summarized in Figure 3.1. The hydrochar and AC produced were pulverized by using an agate mortar and pestle supplied by Merck, South Africa.


*(a)* *(b)*

(c)

Figure 3.1: The steps of hydrochar and AC generation from eucalyptus wood chips (a) Eucalyptus wood chips, (b) hydrochar, (c) AC



## 3.4. CHARACTERIZATION OF HYDROCHAR AND AC

### 3.4.1. TEM studies

TEM studies were performed at an acceleration voltage of 200 kV by using a Jeol JEM-2100F transmission electron microscope instrument equipped with a LaB6 source. Small sample masses of hydrochar and AC were mixed with methanol and sonicated for

5 minutes at room temperature using an ultrasonic bath. The TEM samples were prepared by dropping small amount of hydrochar and AC onto a TEM grid (200 mesh size Cu-grid) coated with a lacy carbon film. The images of the hydrochar and AC were captured using a digital charge-coupled device (CCD) camera connected to the transmission electron microscope.

3.4.2. SEM and EDS studies

The hydrochar and AC were carbon-coated to improve conductivity using a Q300 TT Plus triple sputter coater instrument for specimens up to 200 mm diameter. The analysis of the coated specimens was executed through SEM and EDS coupled with an oxford detector. The images were captured in different magnifications and the elements in the materials were confirmed.

3.4.3. Particle size studies of adsorbent materials

The Zetasizer samples were prepared by using water as a dispersant and the samples were placed into disposable sizing cuvettes. The particle sizes of the adsorbent materials were measured by using a DLS at 25 °C with a count rate of 140.5 kcps for a duration of 70s and the measurement position was 1.25 mm.



3.4.4. BET and FTIR studies

The sample masses of 0.094 g were used in BET instrument for the determination of the average diameter, pore volume, and surface area of the hydrochar and AC. The discovery of the functional groups present on the surface of adsorbent materials was done through the MIRacle-10 FTIR.

3.4.5. Thermal and XRD studies

The thermal stability of the hydrochar was carried out by TGA. The hydrochar and AC were placed in the steel sample holders then put in the XRD instrument for the determination of the crystallinity of the adsorbent materials.

3.5. ADSORPTION OF Mn(II) and Cr(VI)

The effect of pH, contact time, adsorbent dose, temperature, and initial metal ion concentration on the adsorption capacity of the hydrochar and AC was investigated. The volumes of 1.25, 3.75, 7.5, 10, 15, 20, 25, and 37.5 mL of 4000 mg/L manganese and 4000 mg/L chromium stock solutions were taken into 100 mL volumetric flasks and topped up with deionized water to get the solution of 50, 150, 300, 400, 600, 800, 1000, and 1500 mg/L of Mn(II) and 50, 150, 300, 400, 600, 800, 1000, and 1500 mg/L of Cr(VI) . The contents were transferred into 250 mL Erlenmeyer flasks and the pH of each of these mixtures was recorded. A mass of 1.00 g of hydrochar was added to each Erlenmeyer flask. The mixtures were then placed into a water bath and continuously agitated with magnetic stirring bars to make particles move around more rapidly and collide with each other more often. The mixtures were removed from the water bath and filtered using the Buchner funnel set. Similar experiments were performed with a mass of 1.00 g of AC. All the parameter conditions used in these experiments are mentioned in Table 3.1 and 3.2. The standard solutions that were used for the analysis were prepared prior analysis. A volume of 1 mL of 1000 mg/L of manganese and chromium standard solutions were taken into two different 100 mL volumetric flask and topped up with deionized water to get the intermediate standard solutions of a concentration of 10 mg/L of manganese and chromium. The volumes of 2.5, 5, 7.5, 10, and 15 mL of the intermediate standard solutions of manganese and chromium were taken into 50 mL volumetric flasks and topped up with deionized water to get the standard solutions of 0.5, 1.0, 1.5, 2.0, and 3.0 mg/L. The filtrates were analyzed by utilizing the FAAS.



Table 3.1: Optimum parameter conditions for Mn(II) removal

| Adsorbent | Initial metal ion concentration (mg/L) | Adsorbent mass (g) | Contact time (min) | pH | Temperature (ºC) |
|---|---|---|---|---|---|
| Hydrochar | 600 | 0.25 | 180 | 8 | 25 |
| AC | 800 | 0.25 | 210 | 7 | 25 |

Table 3.2: Optimum parameter conditions for Cr(VI) removal

| Adsorbent | Initial metal ion concentration (mg/L) | Adsorbent mass (g) | Contact time (min) | pH | Temperature (ºC) |
|---|---|---|---|---|---|
| Hydrochar | 600 | 0.25 | 150 | 5 | 25 |
| AC | 400 | 0.25 | 120 | 7 | 25 |

## 4.1. CHARACTERIZATION OF HYDROCHAR AND AC

### 4.1.1. FT-IR analysis

The FT-IR spectrum of the hydrochar is shown in Figure 4.1(a). It reveals a strong broad peak at 3429 $cm^{-1}$ assigned to be O–H vibration [1], while the weak peak at 2938 $cm^{-1}$ is the C-H stretching vibration. The sharp peak at 1611 $cm^{-1}$ suggests being the carbonyl (C=O) functional group. The peak at 1217 $cm^{-1}$ allotted to be C–O corresponding to syringol ring. The FT-IR spectrum of the AC shown in Figure 4.1(b) discloses the absorption band 3366 $cm^{-1}$ assigned to be O–H vibration. The absorption bands at 2930 $cm^{-1}$ and 2846 $cm^{-1}$ suggest C–H stretching vibrations while the absorption band at 1695 $cm^{-1}$ suggests carbonyl (C=O) functional group [2]. The peak at 1407 $cm^{-1}$ is assigned to the aromatic ring [3], and the peak at 1035 $cm^{-1}$ suggests the hydroxyl (O–H) functional group respectively. The carbonyl (C=O) and hydroxyl (O–H) functional groups are common to hydrochars derived from plant biomass [4]. The peak at 3366 $cm^{-1}$ assigned to O–H, on the FT-IR spectrum of the AC in Figure 4.1(b), got reduced and that means water was reduced due to the heating process when the hydrochar was transformed into the AC. The peak at 1035 $cm^{-1}$ has a transmittance of approximately 30% on the FT-IR spectrum of the AC in Figure 4.1(b), therefore, AC absorbed more radiation compared to hydrochar. The hydrochar started absorbing the radiation at approximately 77% as displayed on the FT-IR spectrum of the hydrochar in Figure 4.1(a).

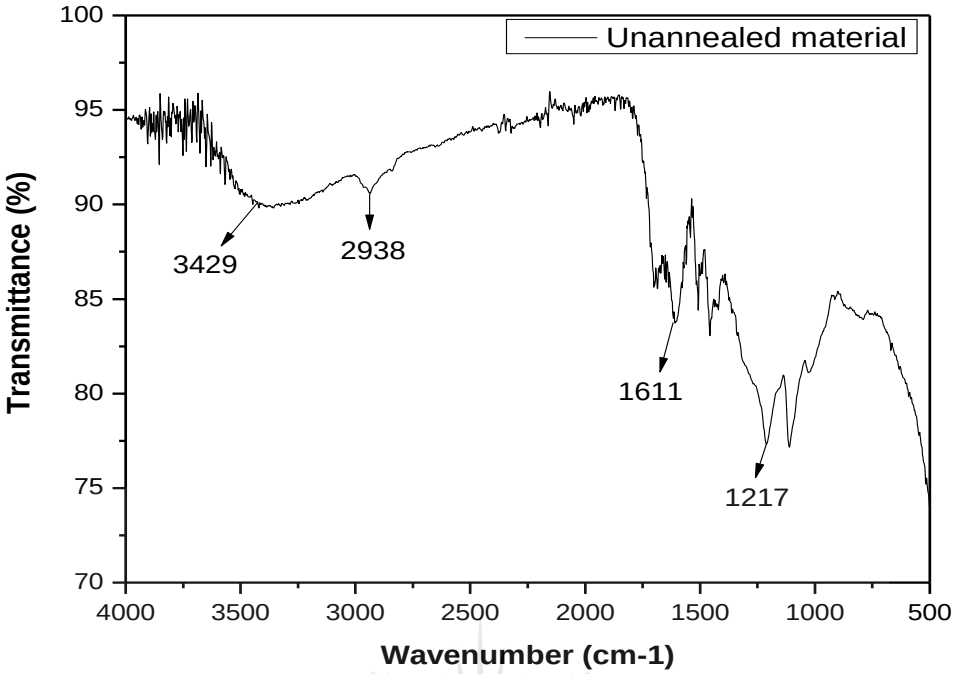


(a)

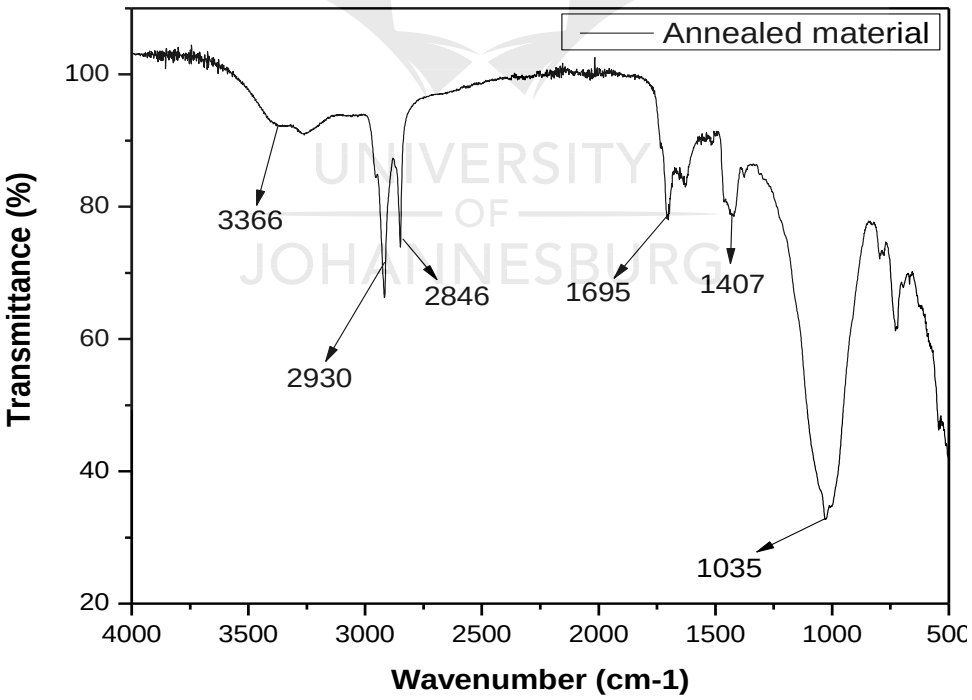


(b)

Figure 4.1: FT-IR spectra of (a) hydrochar and (b) AC

4.1.2. SEM analysis

The results of the surface morphologies of the hydrochar and AC analyzed by SEM displayed the aggregate texture on the hydrochar as depicted in different magnifications in Figure 4.2. As shown in Figure 4.2(a) and (c),hydrochar particles are thin with a small surface area. In Figure 4.2(b) and (d), it was observed that the particles were roughly packed together and well-distributed. This could be due to the activation method like heating the hydrochar in a tube furnace, leading to the removal of impurities such as organic compounds [5]. The surface of the hydrochar was relatively rough, while that of AC was spongelike. The similar surface properties of other types of hydrochars produced by HTCs have been reported before [6, 7].

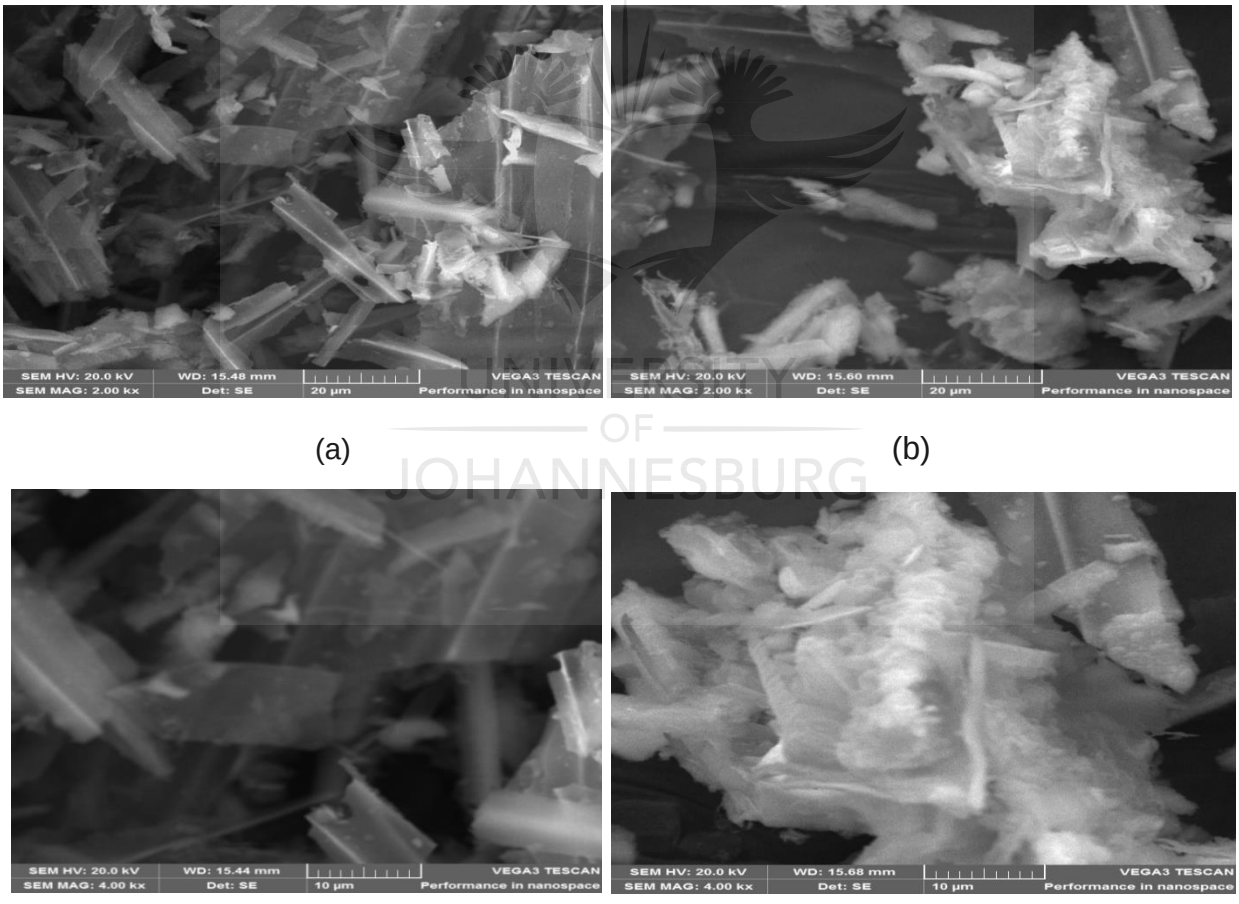


(a) (b)

(c) (d)

Figure 4.2: SEM images of hydrochar at (a) 2.00k×, (c) 4.00k× and AC at (b) 2.00k× (d) 4.00k× magnifications

4.1.3. TEM analysis

To identify the presence of nanopores, TEM analysis has been done. In Figure 4.3(a) and (c), the hydrochar had a small number of pores while the AC revealed a large number of pores as shown in Figure 4.3(b) and (d). In Figure 4.3(b), there are little dark spots that appear which are the small amounts of impurities representing traces of $SiO_2$ [8], and that is consistent with the particle distribution of the hydrochars and their AC [9].

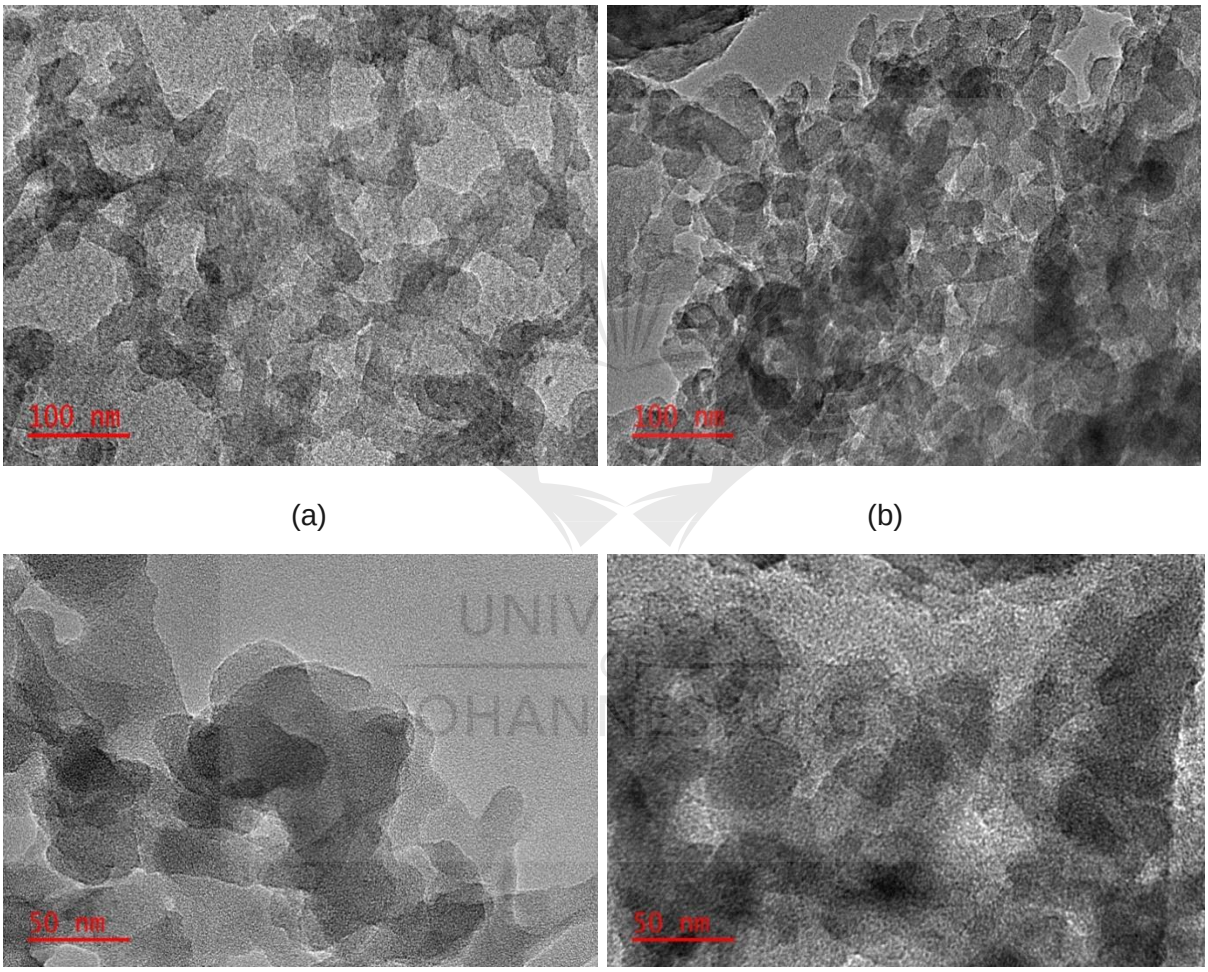


(a) (b)

(c) (d)

Figure 4.3: TEM images of hydrochar at 1.00k× (a) 5.00 k× (c) and AC at 1.00k× (b) 5.00k× (d) magnifications

4.1.4. EDX analysis

The EDX analysis was done to identify the elements present in the hydrochar and AC. The results of the hydrochar in Figure 4.4(a) are as follows (%): C, 38.9; O, 18.8; Si, 9.5; Al, 32.8 and the results of the AC shown in Figure 4.4(b) are as follows (%): C, 85.1; O, 13.1; P, 1.9. The high percentage of O element after activation in Figure 4.4(b) proved that the chemical properties of AC have been improved. The hydrochars that contain Al element have less porous structures [10], therefore, the AC has more porous structures since there is no Al element present in the AC as it is seen in Figure 4.4(a).

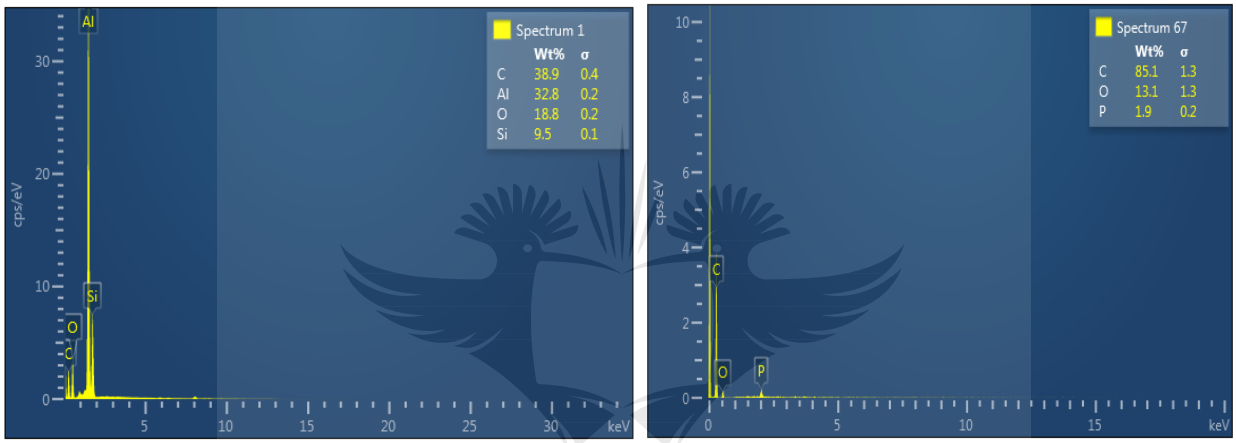


(a) (b)

Figure 4.4: EDX spectra of (a) hydrochar and (b) AC



4.1.5. BET analysis

The $N_2$ adsorption-desorption studies were carried out to measure the average diameter, pore volume, surface area, and isotherm of the hydrochar and AC. Figure 4.5(a) and 4.5(b) show type-IV isotherm, producing an easy capillary condensation step at P/P0 of 0.6–0.1, which was due to the mesoporosity present [11]. The average diameter, pore volume, and surface area of the hydrochar shown in Figure 4.5(a) were found to be 305.7 Å, 0.223 $cm^3/g$, and 29.16 $m^2/g$. The average diameter, pore volume, and surface area of the AC depicted in Figure 4.5(b) were found to be 515.00 Å, 0.767 $cm^3/g$, and 63.35 $m^2/g$. It was revealed that the surface parameters like average diameter, pore volume, and surface area had increased after the hydrochar was

activated by heating it in a tube furnace to generate AC, therefore, the surface parameters of AC had been improved.

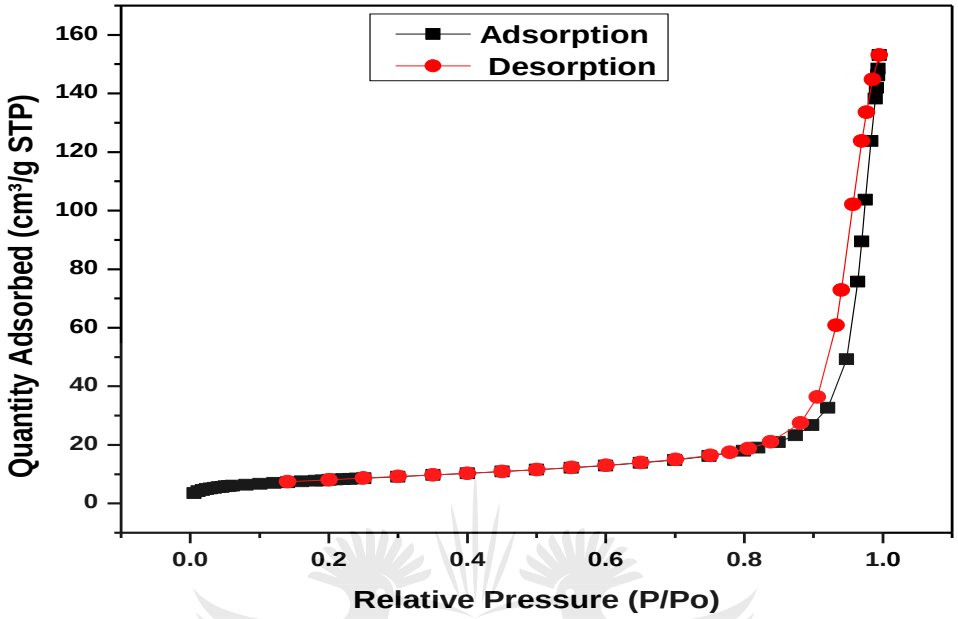


(a)

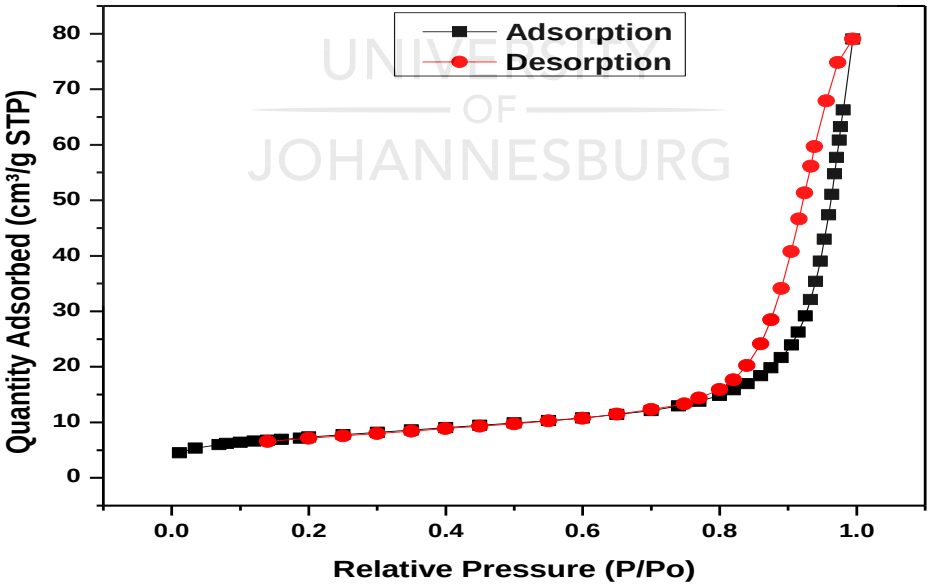


(b)

Figure 4.5: $N_2$ adsorption-desorption isotherm for (a) hydrochar and (b) AC

4.1.6. XRD analysis

The diffraction patterns of the hydrochar and AC are depicted in Figure 4.6(a) and 4.6(b), respectively. The peaks at around 2θ=23° of both hydrochar and AC in Figure 4.6(a) and 4.6(b) corresponding to the position of (002) and (100) crystal plane [12]. It suggested that the hydrochar prepared by hydrothermal carbonization (HTC) and the AC appear as porous and crystalline. The Si element was present in both the hydrochar and AC, it was confirmed in Figure 4.4(a) and 4.4(b). Consequently, the characteristic peak appearing in the 2θ angle at 45° in Figure 4.6(b) is the result of the $SiO_2$ impurities in the AC [13], and that peak originates from (111) plane of silicon and due to broad and medium-intensity signal [14].

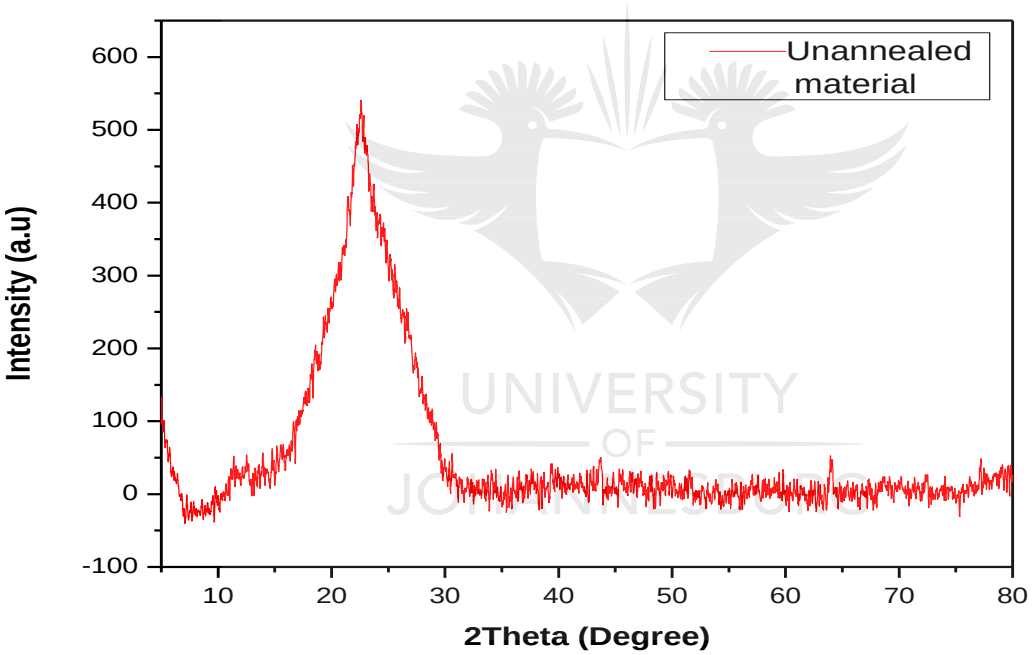

(a)

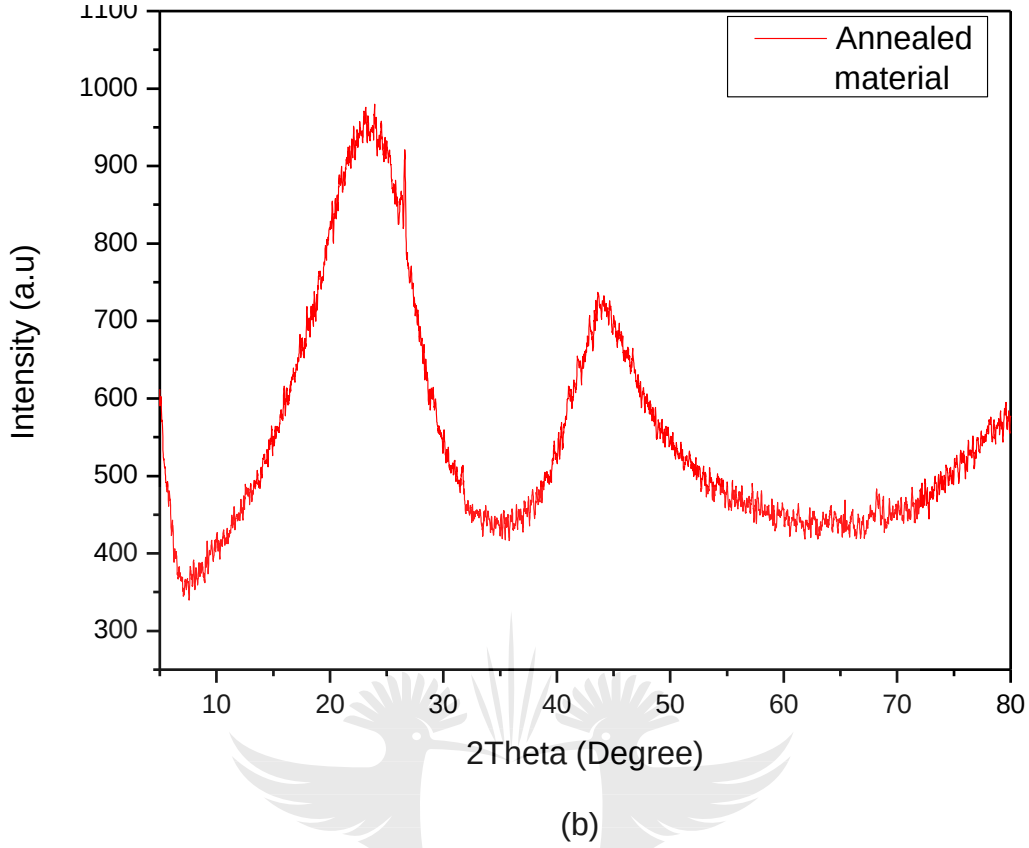


(b)

Figure 4.6: XRD patterns of (a) hydrochar and (b) AC

4.1.7. Particle size analysis

The Particle size studies were carried out to measure the particle size of the hydrochar and AC. As shown in Figure 4.7(a) and 4.7(b), the achieved average particle size values hydrochar and AC were 2084 and 3543 d.nm, respectively. The particle size of the AC was bigger than that of hydrochar, AC's chemical properties have been enhanced [15]. The particles of the AC were well dispersed in Figure 4.7(b), the annealing process removed the impurities and made AC particles to move freely without any disturbance [16]. Consequently, the AC particles increased in size.

| | | | Size (d.n... | % Intensity: | St Dev (d.n... |
|---|---|---|---|---|---|
| Z-Average (d.nm): | 2084 | Peak 1: | 753.0 | 92.8 | 118.2 |
| PdI: | 0.869 | Peak 2: | 205.0 | 7.2 | 22.39 |
| Intercept: | 1.04 | Peak 3: | 0.000 | 0.0 | 0.000 |
| Result quality | Refer to quality report | | | | |

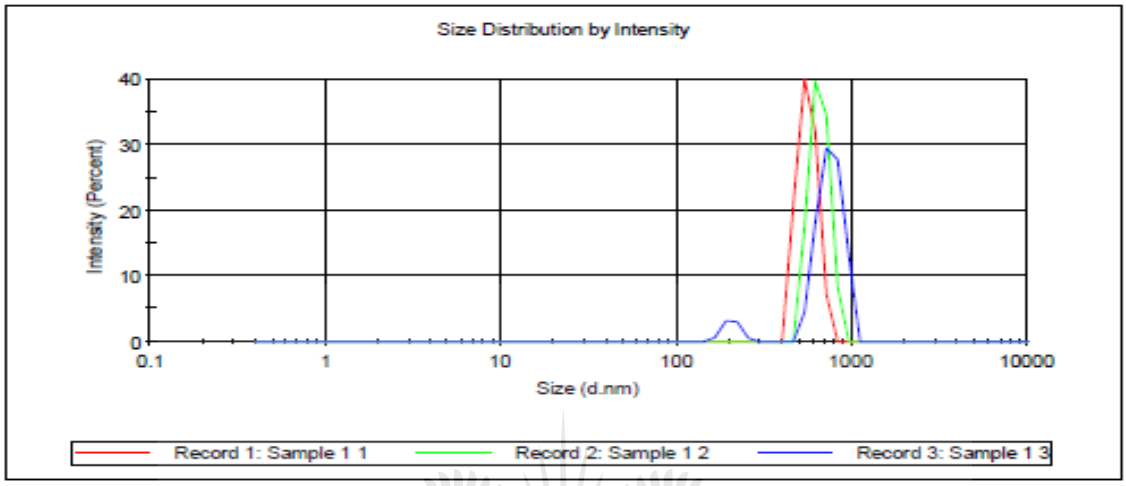


(a)

| | | | Size (d.n... | % Intensity: | St Dev (d.n... |
|---|---|---|---|---|---|
| Z-Average (d.nm): | 3543 | Peak 1: | 691.8 | 92.7 | 54.24 |
| PdI: | 1.000 | Peak 2: | 35.64 | 7.3 | 2.553 |
| Intercept: | 1.05 | Peak 3: | 0.000 | 0.0 | 0.000 |
| Result quality | Refer to quality report | | | | |

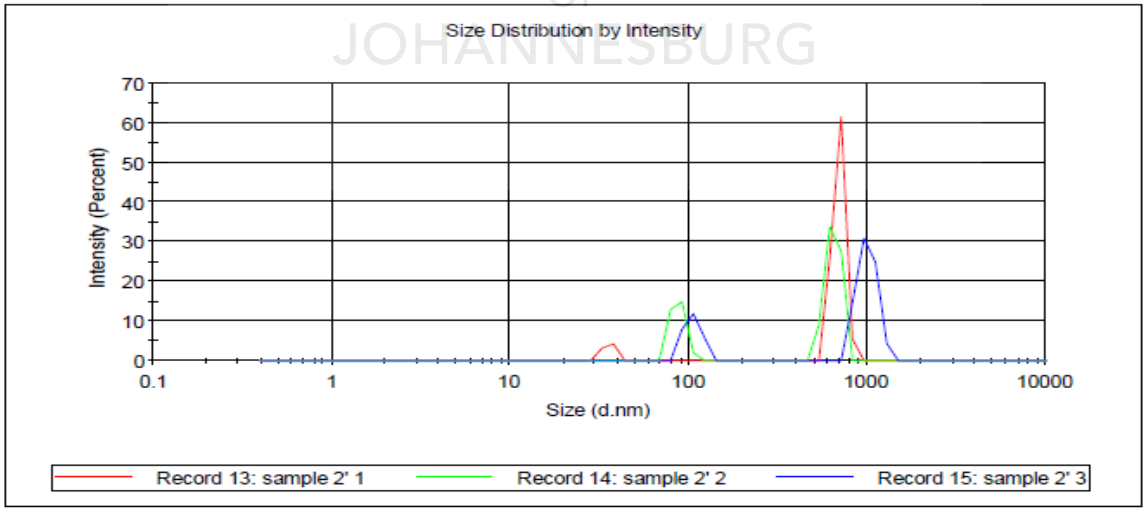


(b)

Figure 4.7: Particle size of (a) hydrochar and (b) AC

4.1.8. TGA analysis

The TGA thermograms of hydrochar and AC are shown in Figure 4.8(a) and 4.8(b). It showed that both the hydrochar and AC were not stable, they had decreased in mass with an increase in temperature. In Figure 4.8(a), there were three stages in the thermal decomposition of hydrochar during the pyrolysis: (1) the first stage occurred below 200 °C, including the removal of moisture; (2) the second stage occurred within the temperature range of 200–515 °C in which the decomposition of hemicelluloses and cellulose occurred [17]; and (3) the third stage occurred above 515 °C in which the decomposition reaction was starting to slow down. In Figure 4.8(b), there were two stages in the thermal decomposition of hydrochar during the pyrolysis: (1) the first stage occurred below 400 °C, moisture was also removed; and (2) the second stage occurred above 400 °C whereby decomposition reaction was occurring very slow. During the pyrolysis of hydrochars, the decomposition of lignin is possible within the temperature range of 455–1170 °C [18].

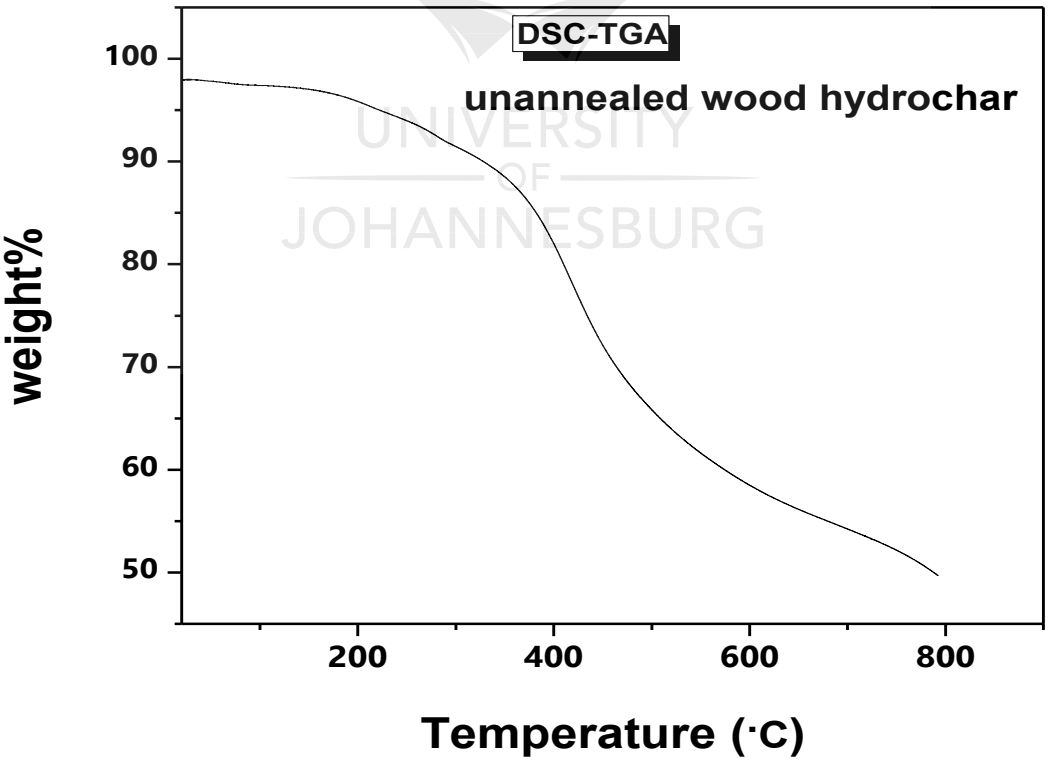


(a)

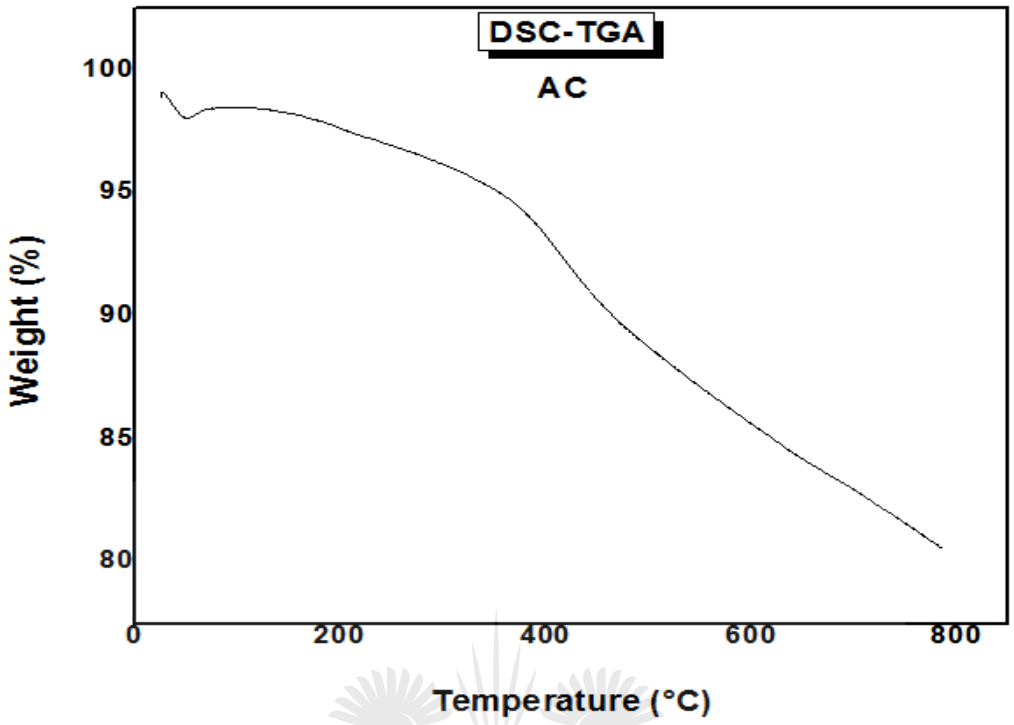


(b)

Figure 4.8: TGA thermogram of hydrochar and AC

## 4.2. ADSORPTION OF Mn(II)

### 4.2.1. Effect of initial metal ion concentration

The effect of initial metal ion concentration on the Mn(II) ions removal is shown in Tables 4.1 and 4.2. The results displayed that the adsorption capacity was increasing with the increase in initial metal ion concentration. That could be due to the utilization of more available active sites of the adsorbent [19]. The equilibrium was achieved and the increase in initial metal ion concentration did not bring about a positive change towards adsorption after the saturation point. This phenomenon appeared since there were no more available adsorption sites on the adsorbent materials [20]. It was evident from the listed data in Table 4.1 and 4.2 that the highest adsorption capacity was found to be 44.03 mg/g at an optimum initial metal ion concentration of 600 mg/L when hydrochar was applied while 56.31 mg/g adsorption capacity was obtained at an initial metal ion concentration of 800 mg/L when AC was used as an adsorbent.

Table 4.1: Effect of initial metal ion concentration using hydrochar in the removal of Mn(II)

| Initial conc. (mg/L) | Final conc. (mg/L) | Adsorption capacity (mg/g) | Metal removal efficiency (%) | Adsorbent mass (g) | Contact time (min) | pH |
|---|---|---|---|---|---|---|
| 50.00 | 16.33 | 3.361 | 67.3 | 1.001 | 60 | 5.48 |
| 150.00 | 49.26 | 10.08 | 67.2 | 1.002 | 60 | 6.18 |
| 300.00 | 122.5 | 17.75 | 59.2 | 1.001 | 60 | 5.60 |
| 400.00 | 130.6 | 26.95 | 67.4 | 1.001 | 60 | 5.45 |
| 600.00 | 159.7 | 44.03 | 73.4 | 1.002 | 60 | 5.30 |
| 800.00 | 366.5 | 43.35 | 54.2 | 1.007 | 60 | 5.67 |
| 1000.00 | 561.5 | 43.85 | 43.9 | 1.002 | 60 | 5.10 |
| 1500.00 | 1060.00 | 44.00 | 29.3 | 1.002 | 60 | 5.81 |

Table 4.2: Effect of initial metal ion concentration using AC in the removal of Mn(II)

| Initial conc. (mg/L) | Final conc. (mg/L) | Adsorption capacity (mg/g) | Metal removal efficiency (%) | Adsorbent mass (g) | Contact time (min) | pH |
|---|---|---|---|---|---|---|
| 50.00 | 3.213 | 4.679 | 93.5 | 1.001 | 60 | 7.01 |
| 150.00 | 4.235 | 14.58 | 97.2 | 1.007 | 60 | 7.03 |
| 300.00 | 5.999 | 29.40 | 98.0 | 1.008 | 60 | 7.02 |
| 400.00 | 5.000 | 39.50 | 98.7 | 1.008 | 60 | 7.04 |
| 600.00 | 229.00 | 37.10 | 61.8 | 1.007 | 60 | 7.01 |
| 800.00 | 8.879 | 56.31 | 98.9 | 1.001 | 60 | 6.98 |
| 1000.00 | 397.6 | 60.25 | 60.2 | 1.007 | 60 | 6.92 |
| 1500.00 | 1023.00 | 47.68 | 31.8 | 1.007 | 60 | 7.04 |

4.2.2. Effect of adsorbent dose

The effect of adsorbent dose on the Mn(II) ion removal was studied to attain the optimum value of adsorbent dose as shown in Table 4.3 and 4.4. It was perceived that the adsorption capacity of Mn(II) decreased as the adsorbent dose was increased when the hydrochar and AC were used as adsorbents. The highest Mn(II) adsorption capacities of 172.2 and 280.2 mg/g were achieved when hydrochar and AC were applied with the optimum adsorbent dosage of 0.25 g/L. Table 4.3 and 4.4 show the specific conditions at which the adsorption occurred. The decreasing of adsorption capacity when the adsorbent dose is increasing is attributed to the fact that the particles of the adsorbents are clustered [21, 22], as a result, the available active adsorption sites might get reduced [23]. Thus, the increasing of adsorbent dose did not improve the removal of Mn(II) ions. After the hydrochar was thermally activated, the higher removal percentage was improved from 63.2% to 88.7% as it appears in Table 4.3 and 4.4.

Table 4.3: Effect of adsorbent dose using hydrochar in the removal of Mn(II)

| Adsorbent mass (g) | Initial conc. (mg/L) | Final conc. (mg/L) | Adsorption capacity (mg/g) | Metal removal efficiency (%) | Contact time (min) | pH |
|---|---|---|---|---|---|---|
| 0.251 | 600.00 | 169.6 | 172.2 | 71.7 | 60 | 5.31 |
| 0.502 | 600.00 | 180.5 | 83.92 | 69.9 | 60 | 5.31 |
| 0.750 | 600.00 | 189.3 | 54.80 | 68.5 | 60 | 5.28 |
| 1.002 | 600.00 | 191.3 | 40.87 | 68.1 | 60 | 5.26 |
| 1.251 | 600.00 | 191.8 | 32.66 | 68.0 | 60 | 5.25 |
| 1.502 | 600.00 | 184.3 | 27.71 | 69.3 | 60 | 5.22 |

Table 4.4: Effect of adsorbent dose using AC in the removal of Mn(II)

| Adsorbent mass (g) | Initial conc. (mg/L) | Final conc. (mg/L) | Adsorption capacity (mg/g) | Metal removal efficiency (%) | Contact time (min) | pH |
|---|---|---|---|---|---|---|
| 0.2501 | 800.00 | 99.63 | 280.2 | 87.5 | 60 | 5.31 |

| | | | | | | |
|---|---|---|---|---|---|---|
| 0.5013 | 800.00 | 112.2 | 137.6 | 85.9 | 60 | 5.31 |
| 0.7506 | 800.00 | 121.4 | 90.49 | 84.8 | 60 | 5.28 |
| 1.0021 | 800.00 | 129.9 | 67.01 | 83.8 | 60 | 5.26 |
| 1.2514 | 800.00 | 133.6 | 53.31 | 83.3 | 60 | 5.25 |
| 1.5013 | 800.00 | 156.4 | 42.91 | 80.5 | 60 | 5.22 |

### 4.2.3. Effect of contact time

The effect of contact time was studied as shown Table 4.5 and 4.6. In general, the adsorption process incorporates the rapid adsorption phase in the first few minutes then followed by a slower reaction to reach the equilibrium stage at a certain point in time [24, 25]. Therefore, it was seen that for the removal of Mn(II), when the hydrochar was applied the metal removal efficiency (%) increased fast when contact time was increasing up to 180 minutes and decreased as the contact time increased. The percentage removal was 66.2% with an adsorption capacity of 159.00 mg/g as listed in Tabe 4.5. When AC was used, the metal removal efficiency (%) increased fast when contact time was increasing up to 210 minutes and gradually decreased as the contact time increased, this could be ascribed to the available number of adsorption sites [26]. From the data in Tabe 4.6, it had shown that the percentage removal was 77.7% with an adsorption capacity of 248.6 mg/g.



Table 4.5: Effect of contact time using hydrochar in the removal of Mn(II)

| Contact time (min) | Initial conc. (mg/L) | Final conc. (mg/L) | Adsorption capacity (mg/g) | Metal removal efficiency (%) | Adsorbent mass (g) | pH |
|---|---|---|---|---|---|---|
| 5 | 600.00 | 299.3 | 120.3 | 50.1 | 0.251 | 5.28 |
| 10 | 600.00 | 297.5 | 121.00 | 50.4 | 0.251 | 5.08 |
| 30 | 600.00 | 279.1 | 128.4 | 53.5 | 0.251 | 5.12 |
| 60 | 600.00 | 277.4 | 129.1 | 53.8 | 0.252 | 5.37 |
| 90 | 600.00 | 250.7 | 139.7 | 58.2 | 0.251 | 5.09 |

| | | | | | | |
|---|---|---|---|---|---|---|
| 120 | 600.00 | 218.3 | 152.7 | 63.6 | 0.251 | 5.24 |
| 150 | 600.00 | 208.00 | 156.9 | 65.3 | 0.250 | 5.80 |
| 180 | 600.00 | 202.6 | 159.00 | 66.2 | 0.250 | 4.68 |
| 210 | 600.00 | 249.3 | 140.3 | 58.5 | 0.251 | 4.41 |
| 240 | 600.00 | 248.00 | 140.9 | 58.7 | 0.251 | 5.53 |

Table 4.6: Effect of contact time using AC in the removal of Mn(II)

| Contact time (min) | Initial conc. (mg/L) | Final conc. (mg/L) | Adsorption capacity (mg/g) | Metal removal efficiency (%) | Adsorbent mass (g) | pH |
|---|---|---|---|---|---|---|
| 5 | 800.00 | 311.4 | 195.4 | 61.1 | 0.250 | 5.70 |
| 10 | 800.00 | 275.8 | 209.7 | 65.5 | 0.251 | 4.97 |
| 30 | 800.00 | 282.5 | 207.00 | 64.7 | 0.251 | 5.20 |
| 60 | 800.00 | 277.00 | 209.2 | 65.4 | 0.250 | 5.08 |
| 90 | 800.00 | 239.3 | 224.3 | 70.1 | 0.251 | 5.42 |
| 120 | 800.00 | 219.9 | 232.00 | 72.5 | 0.252 | 4.87 |
| 150 | 800.00 | 219.6 | 232.2 | 72.5 | 0.251 | 4.79 |
| 180 | 800.00 | 209.00 | 236.4 | 73.9 | 0.250 | 4.65 |
| 210 | 800.00 | 178.4 | 248.7 | 77.7 | 0.251 | 5.01 |
| 240 | 800.00 | 205.1 | 238.00 | 74.4 | 0.252 | 4.98 |



### 4.2.4. Effect of pH

One of the most important parameters studied is the effect of pH on the Mn(II) ions removal. Table 4.7 and 4.8 show the pH variation ranging from 3 to 8.5 on Mn(II) adsorption. A pH controls protons in the solution during the adsorption process [27]. When hydrochar was applied, the highest adsorption capacity of 28.32 mg/g was

obtained at pH 8, and there was a drastic drop of adsorption capacity to 9.876 mg/g at pH 8.5. When AC was applied, adsorption capacity increased as the pH was increasing. The adsorption capacity got to almost the same value from pH 4-6, the highest adsorption capacity of 254.4 mg/g was achieved at pH 7. A similar trend was reported, many metal ions precipitate in solution at pH>8 [28].

Table 4.7: Effect of pH using hydrochar in the removal of Mn(II)

| pH | Initial conc. (mg/L) | Final conc. (mg/L) | Adsorption capacity (mg/g) | Metal removal efficiency (%) | Adsorbent mass (g) | Temperature (ºC) | Contact time (min) |
|---|---|---|---|---|---|---|---|
| 3.03 | 600 | 598.8 | 0.484 | 0.2 | 0.251 | 25 | 180 |
| 4.04 | 600 | 598.5 | 0.508 | 0.2 | 0.250 | 25 | 180 |
| 5.06 | 600 | 595.2 | 1.908 | 0.8 | 0.251 | 25 | 180 |
| 6.02 | 600 | 530.1 | 27.98 | 11.7 | 0.251 | 25 | 180 |
| 7.07 | 600 | 529.9 | 28.03 | 11.7 | 0.251 | 25 | 180 |
| 8.03 | 600 | 529.2 | 28.32 | 11.8 | 0.250 | 25 | 180 |
| 8.56 | 600 | 575.3 | 9.876 | 4.1 | 0.250 | 25 | 180 |



Table 4.8: Effect of pH using AC in the removal of Mn(II)

| pH | Initial conc. (mg/L) | Final conc. (mg/L) | Adsorption capacity (mg/g) | Metal removal efficiency (%) | Adsorbent mass (g) | Temperature (ºC) | Contact time (min) |
|---|---|---|---|---|---|---|---|
| 3.00 | 800 | 194.4 | 242.2 | 75.7 | 0.250 | 25 | 210 |
| 4.02 | 800 | 179.9 | 248.1 | 77.5 | 0.250 | 25 | 210 |
| 5.04 | 800 | 178.3 | 248.7 | 77.7 | 0.250 | 25 | 210 |
| 6.03 | 800 | 181.4 | 247.5 | 77.3 | 0.251 | 25 | 150 |
| 7.04 | 800 | 164.1 | 254.4 | 79.5 | 0.250 | 25 | 150 |
| 8.02 | 800 | 191.4 | 243.5 | 76.1 | 0.250 | 25 | 150 |
| 8.51 | 800 | 180.4 | 247.8 | 77.5 | 0.252 | 25 | 210 |

4.2.5. Effect of temperature

The effect of temperature on the Mn(II) ions removal was assessed. The results showed that the adsorption capacity decreased with the increase in temperature as seen in Table 4.9 and 4.10. The data in Table 4.9 showed that when the hydrochar was used, the adsorption capacity decreased from 26.54 to 8.688 mg/g as the temperature was increasing from 25 to 45 ºC while adsorption capacity decreased from 72.10 to 68.20 mg/g when AC was applied as it was stated in Table 4.10. The decrease in adsorption capacity with an increase in temperature showed a linear pattern that had started from the higher to the lower point of adsorption capacity [29]. When the temperature was increased the boundary layer at the adsorbate surface might have become thinner and this reduction in the boundary layer would have made the adsorbate easily to move back into the solution from the hydrochar and AC surfaces [30]. Both the hydrochar and AC removed more Mn(II) ions at the temperature of 25 ºC.

Table 4.9: Effect of temperature using hydrochar in the removal of Mn(II)

| Temperature (ºC) | Initial conc. (mg/L) | Final conc. (mg/L) | Adsorption capacity (mg/g) | Metal removal efficiency (%) | pH | Adsorbent mass (g) | Contact time (min) |
|---|---|---|---|---|---|---|---|
| 25 | 600.00 | 533.6 | 26.54 | 11.1 | 8.06 | 0.251 | 180 |
| 35 | 600.00 | 552.8 | 18.89 | 07.9 | 8.04 | 0.251 | 180 |
| 45 | 600.00 | 578.3 | 8.688 | 03.6 | 8.02 | 0.251 | 180 |

Table 4.10: Effect of temperature using AC in the removal of Mn(II)

| Temperature (ºC) | Initial conc. (mg/L) | Final conc. (mg/L) | Adsorption capacity (mg/g) | Metal removal efficiency (%) | pH | Adsorbent mass (g) | Contact time (min) |
|---|---|---|---|---|---|---|---|
| 25 | 800.00 | 223.6 | 230.2 | 72.1 | 7.03 | 0.250 | 210 |
| 35 | 800.00 | 146.6 | 219.5 | 69.2 | 7.06 | 0.252 | 210 |
| 45 | 800.00 | 254.4 | 217.1 | 68.2 | 7.01 | 0.251 | 210 |

## 4.3. ADSORPTION OF Cr(VI)

### 4.3.1. Effect of initial metal ion concentration

The results of the effect of the initial metal ion concentration are shown in Table 4.11and 4.12. The adsorption of Cr(VI) was very rapid at the initial points as the initial metal ion concentration was increasing as seen in Table 4.11and 4.12. Generally, the metal ions removal is decreased as the concentration increased with increasing adsorption capacity [31]. This may be due to the utilization of more available active sites of the adsorbent at the higher initial metal ion concentration. From the data in Table 4.11, the maximum percentage removal was found to be 73.0% at an optimal initial metal ion concentration of 600 mg/L with an adsorption capacity of 43.81 mg/g when the hydrochar was used as an adsorbent. It was shown in Table 4.12 that when the AC was used as an adsorbent, the maximum percentage removal was found to be 98.8% at an optimal initial metal ion concentration of 400 mg/L with an adsorption capacity of 38.26 mg/g. As the concentration increases, the movement of metal ions in solution becomes more intense, increasing the chances of contacting with adsorption sites. Consequently, the available sites are occupied and saturated very quickly [32, 33]. Due to the limited number of adsorption sites in adsorbents, the surplus of Cr(VI) ions would remain in the solution, resulting in the lower percentage removal.

Table 4.11: Effect of initial metal ion concentration using hydrochar in the removal of Cr(VI)

| Initial conc. (mg/L) | Final conc. (mg/L) | Adsorption capacity (mg/g) | Metal removal efficiency (%) | Adsorbent mass (g) | Contact time (min) | pH |
|---|---|---|---|---|---|---|
| 50.00 | 15.99 | 3.401 | 68.0 | 1.003 | 60 | 6.68 |
| 150.00 | 50.41 | 9.959 | 66.4 | 1.005 | 60 | 6.55 |
| 300.00 | 120.1 | 17.99 | 60.0 | 1.004 | 60 | 6.39 |
| 400.00 | 128.1 | 27.19 | 68.0 | 1.005 | 60 | 6.30 |
| 600.00 | 162.00 | 43.81 | 73.0 | 1.001 | 60 | 6.29 |
| 800.00 | 365.6 | 43.79 | 54.3 | 1.007 | 60 | 6.29 |

| | | | | | | |
|---|---|---|---|---|---|---|
| 1000.00 | 562.1 | 43.79 | 43.8 | 1.009 | 60 | 6.25 |
| 1500.00 | 1062.00 | 43.73 | 29.2 | 1.008 | 60 | 6.27 |

Table 4.12: Effect of initial metal ion concentration using AC in the removal of Cr(VI)

| Initial conc. (mg/L) | Final conc. (mg/L) | Adsorption capacity (mg/g) | Metal removal efficiency (%) | Adsorbent mass (g) | Contact time (min) | pH |
|---|---|---|---|---|---|---|
| 50.00 | 3.333 | 4.667 | 93.3 | 1.001 | 60 | 6.39 |
| 150.00 | 4.840 | 14.52 | 96.8 | 1.007 | 60 | 6.04 |
| 300.00 | 6.336 | 29.37 | 97.9 | 1.008 | 60 | 6.11 |
| 400.00 | 4.800 | 38.26 | 98.8 | 1.008 | 60 | 6.10 |
| 600.00 | 229.7 | 37.04 | 61.7 | 1.007 | 60 | 5.97 |
| 800.00 | 443.3 | 35.67 | 44.6 | 1.004 | 60 | 5.94 |
| 1000.00 | 637.8 | 36.22 | 36.2 | 1.007 | 60 | 5.98 |
| 1500.00 | 1124.00 | 37.65 | 25.1 | 1.007 | 60 | 5.93 |



### 4.3.2. Effect of adsorbent dose

The effect of hydrochar and AC dose on the Cr(VI) ions removal was studied as shown in Table 4.13 and 4.14. Generally, the removal of contaminants increases as the adsorbent dose increases due to the increase of active adsorption sites [34, 35]. But from Table 4.13 and 4.14 it was revealed that the adsorption capacity was high at a smaller amount of 0.25 g of hydrochar and AC. The adsorption capacity decreased as the adsorbent dose was increasing. However, parts of the hydrochar and AC as adsorbents might have generated aggregates at high dose concentrations [36], which shielded the reactive sites and reduced the adsorption capacity [37]. As it was listed in Table 4.13 and 4.14, the optimal adsorbent dose, maximum percentage removal and

adsorption capacity of the hydrochar and AC are as follows: 0.25 g, 70.2%, and 168.6 mg/g; and 0.25 g, 80.3%, and 128.5 mg/g, respectively.

Table 4.13: Effect of adsorbent dose using hydrochar in the removal of Cr(VI)

| Adsorbent mass (g) | Initial conc. (mg/L) | Final conc. (mg/L) | Adsorption capacity (mg/g) | Metal removal efficiency (%) | Contact time (min) | pH |
|---|---|---|---|---|---|---|
| 0.251 | 600.00 | 178.6 | 168.6 | 70.2 | 60 | 5.31 |
| 0.502 | 600.00 | 183.5 | 83.31 | 69.4 | 60 | 5.31 |
| 0.750 | 600.00 | 192.4 | 54.34 | 67.9 | 60 | 5.28 |
| 1.002 | 600.00 | 193.00 | 40.70 | 67.8 | 60 | 5.26 |
| 1.251 | 600.00 | 193.9 | 32.49 | 67.7 | 60 | 5.25 |
| 1.502 | 600.00 | 181.00 | 27.93 | 69.8 | 60 | 5.22 |

Table 4.14: Effect of adsorbent dose using AC in the removal of Cr(VI)

| Adsorbent mass (g) | Initial conc. (mg/L) | Final conc. (mg/L) | Adsorption capacity (mg/g) | Metal removal efficiency (%) | Contact time (min) | pH |
|---|---|---|---|---|---|---|
| 0.250 | 400.00 | 78.83 | 128.5 | 80.3 | 60 | 5.31 |
| 0.501 | 400.00 | 85.21 | 62.96 | 78.7 | 60 | 5.31 |
| 0.751 | 400.00 | 102.5 | 39.67 | 74.4 | 60 | 5.28 |
| 1.002 | 400.00 | 115.2 | 28.48 | 71.2 | 60 | 5.26 |
| 1.251 | 400.00 | 122.9 | 22.17 | 69.3 | 60 | 5.25 |
| 1.501 | 400.00 | 131.3 | 17.92 | 67.2 | 60 | 5.22 |



### 4.3.3. Effect of contact time

The effect of contact time was evaluated. According to Table 4.15 and 16, when the hydrochar was used as an adsorbent, the process of Cr(VI) adsorption involved three distinct steps. In the first step (5–60 minutes), the adsorption process was rapid. In the

second step (60–150 minutes), the adsorption process increased and reached equilibrium at 150 minutes. Lastly, (150–240 minutes), the adsorption process decreased, and a similar trend was reported in Guerra et al. (2014). The decrease in the rate of adsorption could be attributed to the exchange of Cr(VI) ions with reactive adsorption sites [38]. The percentage removal was 65.0% with an adsorption capacity of 155.9 mg/g as presented in Table 4.15. When AC was applied, the process of Cr(VI) adsorption was very quick from the beginning of the experiment and reached equilibrium at 120 minutes. It was noticeable in Table 4.16 that the percentage removal was 76.7% with an adsorption capacity of 122.7 mg/g.

Table 4.15: Effect of contact time using hydrochar in the removal of Cr(VI)

| Contact time (min) | Initial conc. (mg/L) | Final conc. (mg/L) | Adsorption capacity (mg/g) | Metal removal efficiency (%) | Adsorbent mass (g) | pH |
|---|---|---|---|---|---|---|
| 5 | 600.00 | 300.6 | 119.8 | 49.9 | 0.252 | 5.38 |
| 10 | 600.00 | 295.4 | 121.8 | 50.8 | 0.251 | 4.97 |
| 30 | 600.00 | 280.5 | 127.8 | 53.3 | 0.252 | 5.22 |
| 60 | 600.00 | 280.00 | 128.00 | 53.3 | 0.252 | 5.32 |
| 90 | 600.00 | 245.2 | 141.9 | 59.1 | 0.250 | 5.01 |
| 120 | 600.00 | 220.3 | 151.9 | 63.3 | 0.252 | 5.34 |
| 150 | 600.00 | 210.3 | 155.9 | 65.0 | 0.252 | 4.80 |
| 180 | 600.00 | 219.4 | 152.2 | 63.4 | 0.250 | 4.78 |
| 210 | 600.00 | 248.2 | 140.7 | 58.6 | 0.251 | 4.79 |
| 240 | 600.00 | 251.8 | 139.3 | 58.0 | 0.252 | 5.04 |

Table 4.16: Effect of contact time using AC in the removal of Cr(VI)

| Contact time (min) | Initial conc. (mg/L) | Final conc. (mg/L) | Adsorption capacity (mg/g) | Metal removal efficiency (%) | Adsorbent mass (g) | pH |
|---|---|---|---|---|---|---|
| 5 | 400.00 | 191.7 | 83.32 | 52.1 | 0.250 | 5.38 |
| 10 | 400.00 | 176.00 | 89.60 | 56 | 0.252 | 4.97 |
| 30 | 400.00 | 146.9 | 101.3 | 63.3 | 0.251 | 5.22 |
| 60 | 400.00 | 124.5 | 110.2 | 68.9 | 0.251 | 5.32 |
| 90 | 400.00 | 101.6 | 119.3 | 74.6 | 0.251 | 5.01 |
| 120 | 400.00 | 93.30 | 122.7 | 76.7 | 0.251 | 5.34 |
| 150 | 400.00 | 101.6 | 119.4 | 74.6 | 0.251 | 4.80 |
| 180 | 400.00 | 98.44 | 120.6 | 75.4 | 0.250 | 4.78 |
| 210 | 400.00 | 95.21 | 121.9 | 76.2 | 0.251 | 4.79 |
| 240 | 400.00 | 96.49 | 121.4 | 75.9 | 0.251 | 5.04 |



### 4.3.4. Effect of pH

Another imperative parameter that was studied is the effect of pH on the Cr(VI) ions removal. The range of pH values evaluated in this work were from 3 to 8.5. The effect of pH on the Cr(VI) ions removal is shown in Table 4.17 and 4.18. The process of Cr(VI) adsorption included two steps when hydrochar was used as an adsorbent. In the first step, the adsorption rate was rapid from the beginning of the experiment up to pH 5. At lower pH, the electrostatic attraction between the hydroxyl (O–H) group of the hydrochar and Cr(VI) ions resulted in high adsorption capacity [39–41]. In the last step, pH (5-8.5), the rate of the adsorption process decreased. Table 4.17 showed that the highest adsorption capacity of 119.1 mg/g was reached at pH 5 with the percentage removal of 49.6% when hydrochar was used as an adsorbent. For AC, it was seen that the adsorption process was very fast from pH 3 and reached the equilibrium at pH 7, then at pH (7–8.5) the rate of adsorption decreased. From Table 4.18, it could be seen that

when AC was used, the highest adsorption capacity of 117.4 mg/g was reached at pH 7 with the percentage removal of 73.4%.

Table 4.17: Effect of pH using hydrochar in the removal of Cr(VI)

| pH | Initial conc. (mg/L) | Final conc. (mg/L) | Adsorption capacity (mg/g) | Metal removal efficiency (%) | Adsorbent mass (g) | Temperature (ºC) | Contact time (min) |
|---|---|---|---|---|---|---|---|
| 3.03 | 600 | 495.4 | 41.83 | 17.4 | 0.251 | 25 | 150 |
| 4.02 | 600 | 421.00 | 71.59 | 29.8 | 0.251 | 25 | 150 |
| 5.05 | 600 | 302.1 | 119.1 | 49.6 | 0.252 | 25 | 150 |
| 6.01 | 600 | 322.2 | 111.1 | 46.3 | 0.250 | 25 | 150 |
| 7.06 | 600 | 365.9 | 93.64 | 39.0 | 0.250 | 25 | 150 |
| 8.04 | 600 | 355.7 | 97.73 | 40.7 | 0.251 | 25 | 150 |
| 8.53 | 600 | 480.00 | 48.40 | 20.2 | 0.251 | 25 | 150 |

Table 4.18: Effect of pH using AC in the removal of Cr(VI)

| pH | Initial conc. (mg/L) | Final conc. (mg/L) | Adsorption capacity (mg/g) | Metal removal efficiency (%) | Adsorbent mass (g) | Temperature (ºC) | Contact time (min) |
|---|---|---|---|---|---|---|---|
| 3.01 | 400 | 268.00 | 52.80 | 33 | 0.251 | 25 | 120 |
| 4.02 | 400 | 242.9 | 62.84 | 39.3 | 0.251 | 25 | 120 |
| 5.03 | 400 | 186.7 | 85.32 | 53.3 | 0.251 | 25 | 120 |
| 6.02 | 400 | 149.7 | 100.1 | 62.6 | 0.250 | 25 | 120 |
| 7.05 | 400 | 106.4 | 117.4 | 73.4 | 0.251 | 25 | 120 |
| 8.03 | 400 | 115.2 | 113.9 | 71.2 | 0.251 | 25 | 120 |
| 8.51 | 400 | 121.00 | 111.6 | 69.8 | 0.251 | 25 | 120 |

4.3.5. Effect of temperature

The effect of the temperature on the adsorption was evaluated at 25, 35, and 45 ºC. The effect of temperature for the removal of Cr(VI) ions is shown in Figure 4.18. In most cases, the metal ions move very fast in solution at high temperatures and new reactive adsorption sites might be developed on the surface of the adsorbents, which would then result in higher adsorption capacity [42, 43]. According to Figure 4.18, when hydrochar was used as an adsorbent, the adsorption capacity decreased from 32.53 to 27.92 mg/g as the temperature was increased from 25 to 45 ºC as it was noticeable in Table 4.19. When the AC was used as an adsorbent for the Cr(VI) ions removal, the adsorption capacity decreased from 109.00 to 90.06 mg/g as the temperature was increased from 25 to 45 ºC. Table 4.20 presented all the adsorption conditions. The adsorption capacity decreased since high temperatures cause the desorption of Cr(VI) from the adsorbent surface [44].

Table 4.19: Effect of temperature using hydrochar in the removal of Cr(VI)

| Temperature (ºC) | Initial conc. (mg/L) | Final conc. (mg/L) | Adsorption capacity (mg/g) | Metal removal efficiency (%) | pH | Adsorbent mass (g) | Contact time (min) |
|---|---|---|---|---|---|---|---|
| 25 | 600.00 | 274.8 | 32.53 | 54.2 | 5.26 | 1.009 | 60 |
| 35 | 600.00 | 291.4 | 30.86 | 51.4 | 5.24 | 1.001 | 60 |
| 45 | 600.00 | 320.8 | 27.92 | 46.5 | 5.21 | 1.007 | 60 |

Table 4.20: Effect of temperature using AC in the removal of Cr(VI)

| Temperature (ºC) | Initial conc. (mg/L) | Final conc. (mg/L) | Adsorption capacity (mg/g) | Metal removal efficiency (%) | pH | Adsorbent mass (g) | Contact time (min) |
|---|---|---|---|---|---|---|---|
| 25 | 400.00 | 127.6 | 109.00 | 68.1 | 7.06 | 0.251 | 120 |
| 35 | 400.00 | 156.00 | 97.60 | 61.0 | 7.04 | 0.251 | 120 |
| 45 | 400.00 | 174.9 | 90.06 | 56.3 | 7.01 | 0.250 | 120 |

## 4.4. ADSORPTION ISOTHERM MODELS

### 4.4.1 Langmuir and Freundlich isotherms

Adsorption isotherms play a very important role in adsorption processes. Langmuir and Freundlich isotherm [45, 46] were used for modeling the experimental data. These isotherms are grounded on the type of interaction and the nature of the adsorbent materials. Table 4.21 and 4.22 listed Langmuir isotherm model parameters for the adsorption of Mn(II) and Cr(VI) onto hydrochar and AC. The $1/C_e$ vs $1/q_e$ were plotted and the trend-line was used to determine the equations and the coefficients of determination, in Figure 4.19, the obtained coefficients of determination of the Langmuir model for Mn(II) metal ions were $R^2$ =0.9915 for hydrochar and $R^2$ =0.9924 for AC. Similar $R^2$ values were reported for the adsorption of Pb(II) by banana peel [47]. The obtained coefficients of determination of the Langmuir model for Cr(VI) metal ions were $R^2$ =0.5326 for hydrochar and $R^2$ =0.5082 for AC Cr(VI) metal ions as it is displayed in Figure 4.20. The data was fitted well with the Langmuir model [48]. Therefore, there was only a monolayer on the on hydrochar and AC surface as it was assumed by the Langmuir model. The high value of the coefficients of determination indicates a better adsorption process [49].



Table 4.21: Langmuir isotherm x and y axes values for the adsorption of Mn(II) onto hydrochar and AC

| Hydrochar | | AC | |
|---|---|---|---|
| $1/C_e$ | $1/q_e$ | $1/C_e$ | $1/q_e$ |
| 0.061 | 0.298 | 0.312 | 0.214 |
| 0.020 | 0.099 | 0.236 | 0.069 |
| 0.008 | 0.056 | 0.167 | 0.034 |
| 0.008 | 0.037 | 0.200 | 0.025 |
| 0.007 | 0.023 | 0.004 | 0.027 |
| 0.003 | 0.023 | 0.113 | 0.018 |

| | | | |
|---|---|---|---|
| 0.002 | 0.023 | 0.003 | 0.017 |
| 0.001 | 0.023 | 0.001 | 0.021 |

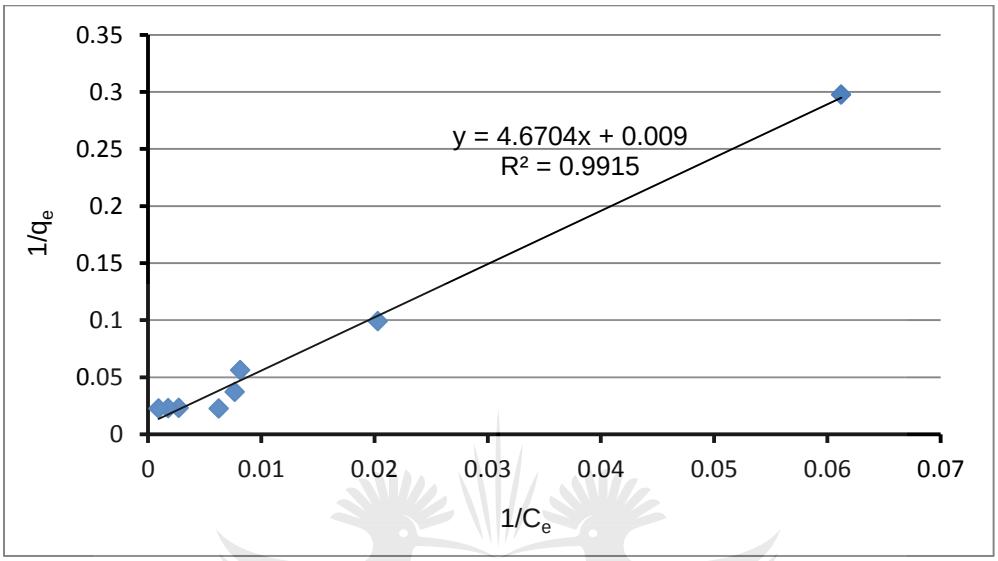


(a)

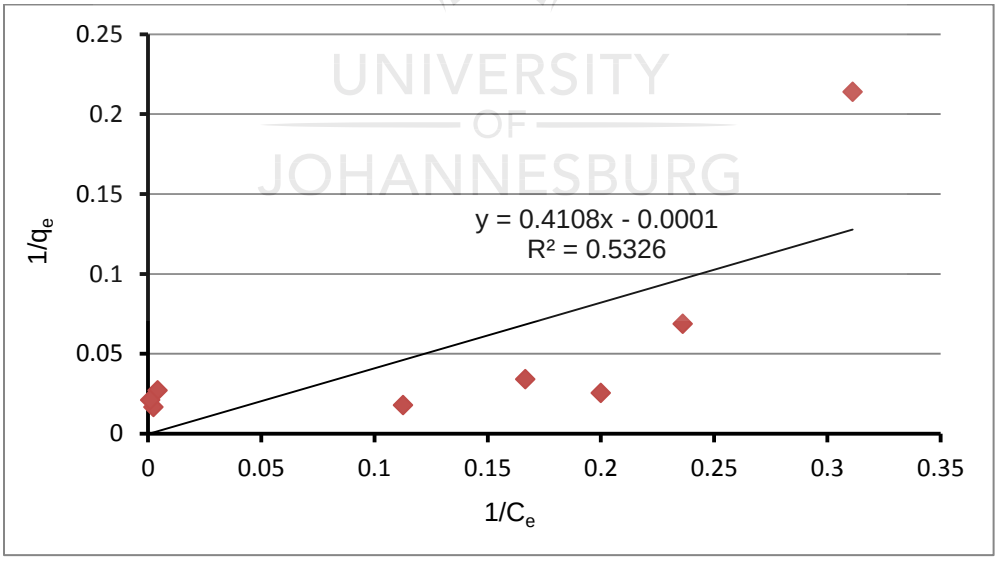


(b)

Figure 4.9: Plots of the for Langmuir isotherm for the adsorption of Mn(II) onto (a) Hydrochar, (b) AC

Table 4.22: Langmuir isotherm x and y axes values for the adsorption of Cr(VI) onto hydrochar and AC

| Hydrochar | | AC | |
|---|---|---|---|
| $1/C_e$ | $1/q_e$ | $1/C_e$ | $1/q_e$ |
| 0.063 | 0.294 | 0.300 | 0.214 |
| 0.020 | 0.100 | 0.207 | 0.069 |
| 0.008 | 0.056 | 0.158 | 0.034 |
| 0.008 | 0.037 | 0.208 | 0.026 |
| 0.006 | 0.023 | 0.004 | 0.027 |
| 0.003 | 0.023 | 0.002 | 0.028 |
| 0.002 | 0.023 | 0.003 | 0.027 |
| 0.001 | 0.023 | 0.001 | 0.027 |

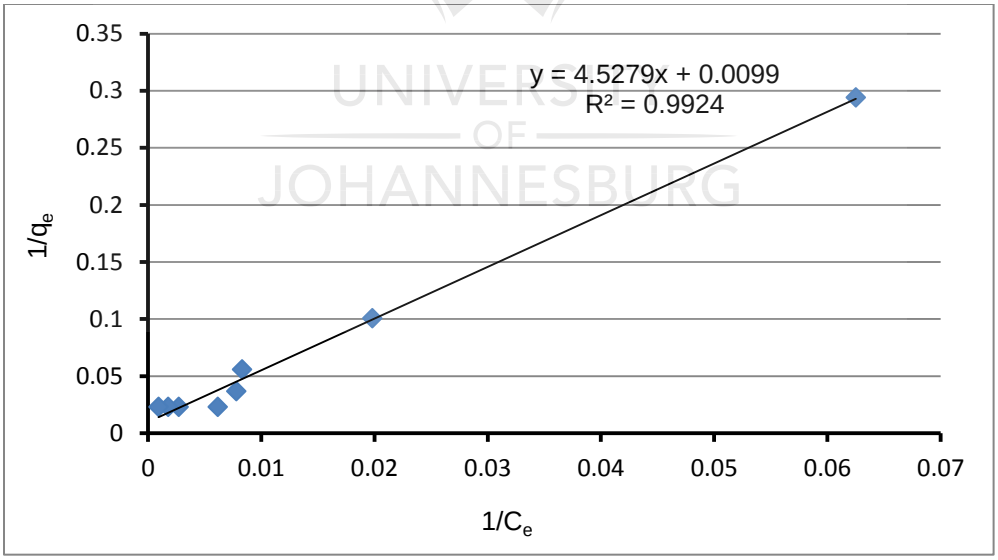


(a)

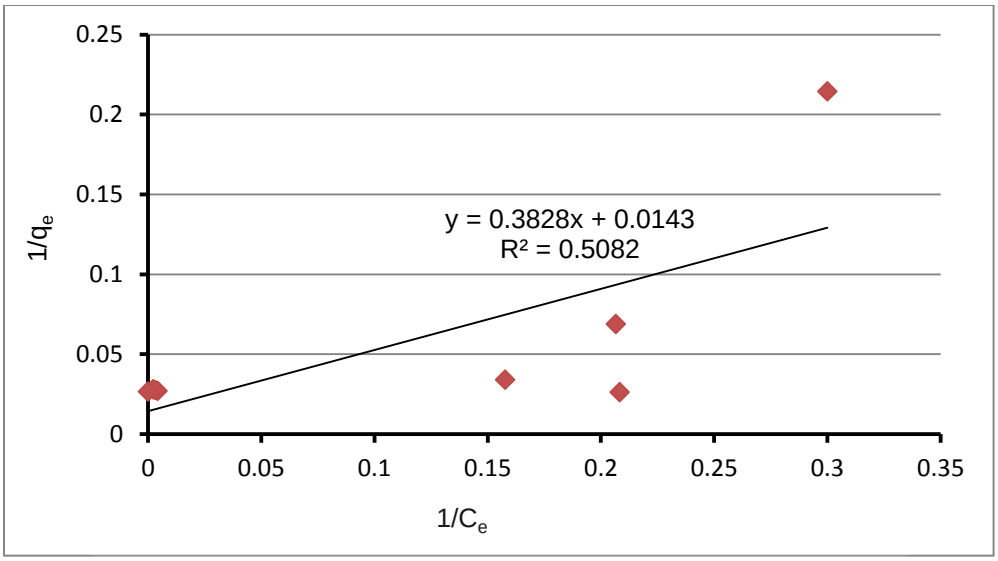


(b)

Figure 4.10: Langmuir isotherm plot for the adsorption of Cr(VI) onto (a) Hydrochar, (b) AC

As for the Freundlich model, the logarithm of $C_e$ (the amount of metal ion adsorbed in unit of adsorbent mass) was plotted against the logarithm of $q_e$ (the equilibrium concentration of the metal ion) a straight line was obtained. Table 4.23 and 4.24 listed Freundlich isotherm model parameters for the adsorption of Mn(II) and Cr(VI) onto hydrochar and AC. Figure 4.21 and 4.22 showed the obtained coefficients of determination of the Freundlich model for Mn(II) metal ions to be $R^2$ =0.8248 for hydrochars and $R^2$ =0.3285 for AC while the obtained coefficients of determination to be $R^2$ =0.8261for hydrochars and $R^2$ =0.3648 for AC of the Cr(VI) metal ions. Langmuir adsorption isotherm was the best model for the metal ions adsorption onto hydrochar and AC. The essential features of the Langmuir adsorption isotherm parameter can be used to predict the affinity between the sorbate and sorbent using a dimensionless constant called separation factor or equilibrium parameter, which is expressed by the following relationship [50–52].

Table 4.23: Freundlich isotherm x and y axes values for the adsorption of Mn(II) onto hydrochar and AC

| Hydrochar | | AC | |
|---|---|---|---|
| log $C_e$ | log $q_e$ | log $C_e$ | log $q_e$ |
| 1.213 | 0.527 | 0.507 | 0.670 |
| 1.692 | 1.003 | 0.627 | 1.164 |
| 2.088 | 1.249 | 0.778 | 1.468 |
| 2.116 | 1.430 | 0.699 | 1.597 |
| 2.203 | 1.644 | 2.360 | 1.569 |
| 2.564 | 1.637 | 0.948 | 1.751 |
| 2.749 | 1.642 | 2.599 | 1.770 |
| 3.025 | 1.643 | 3.001 | 1.678 |



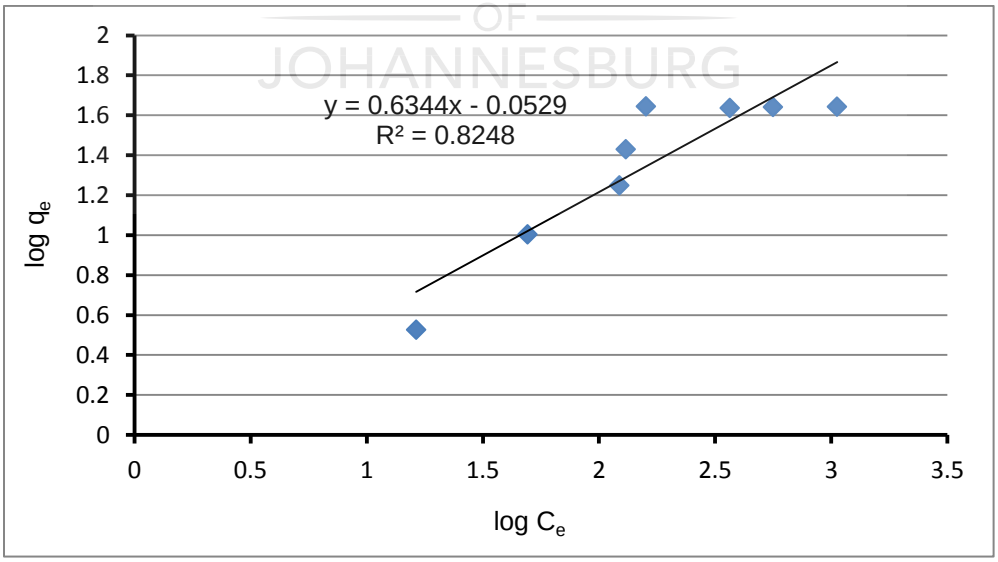


(a)

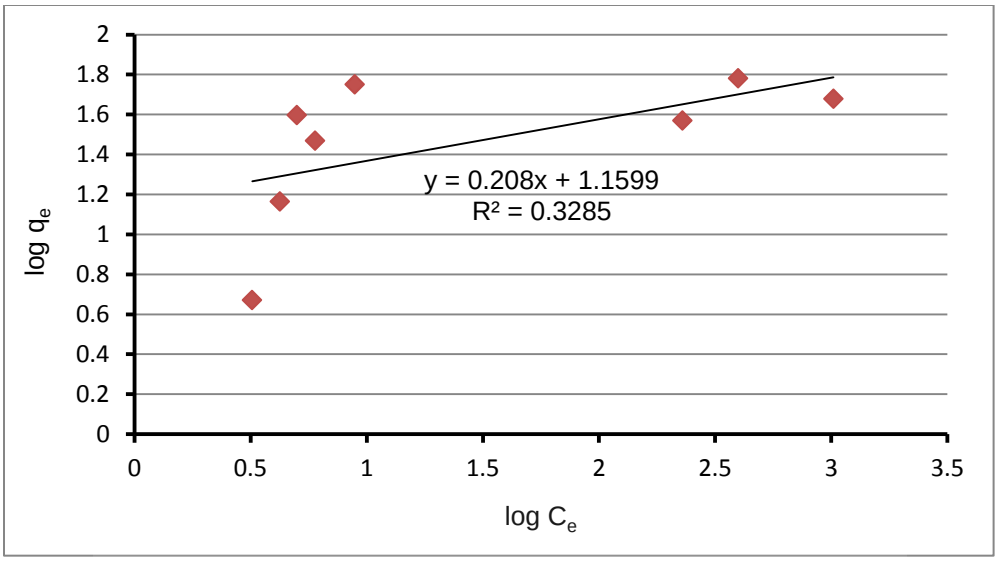


(b)

Figure 4.11: Plots of the Freundlich isotherm for the adsorption of Mn(II) onto (a) Hydrochar, (b) AC

Table 4.24: Freundlich isotherm x and y axes values for the adsorption of Cr(VI) onto hydrochar and AC

| Hydrochar | | AC | |
|---|---|---|---|
| log $C_e$ | log $q_e$ | log $C_e$ | log $q_e$ |
| 1.204 | 0.532 | 0.523 | 0.669 |
| 1.703 | 0.998 | 0.685 | 1.162 |
| 2.080 | 1.255 | 0.802 | 1.468 |
| 2.107 | 1.434 | 0.681 | 1.583 |
| 2.209 | 1.642 | 2.361 | 1.569 |
| 2.563 | 1.641 | 2.647 | 1.552 |
| 2.750 | 1.641 | 2.805 | 1.559 |
| 3.026 | 1.641 | 3.051 | 1.576 |

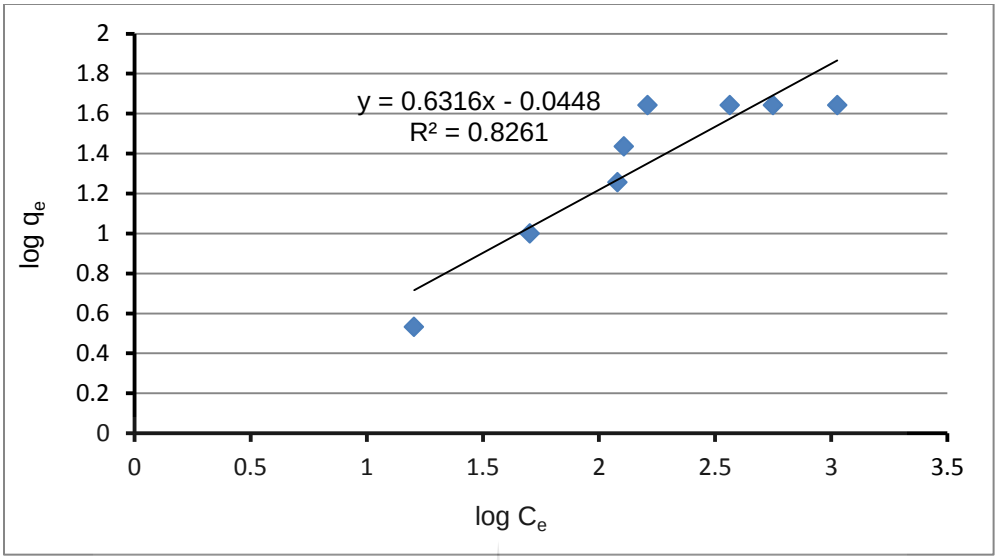


(a)

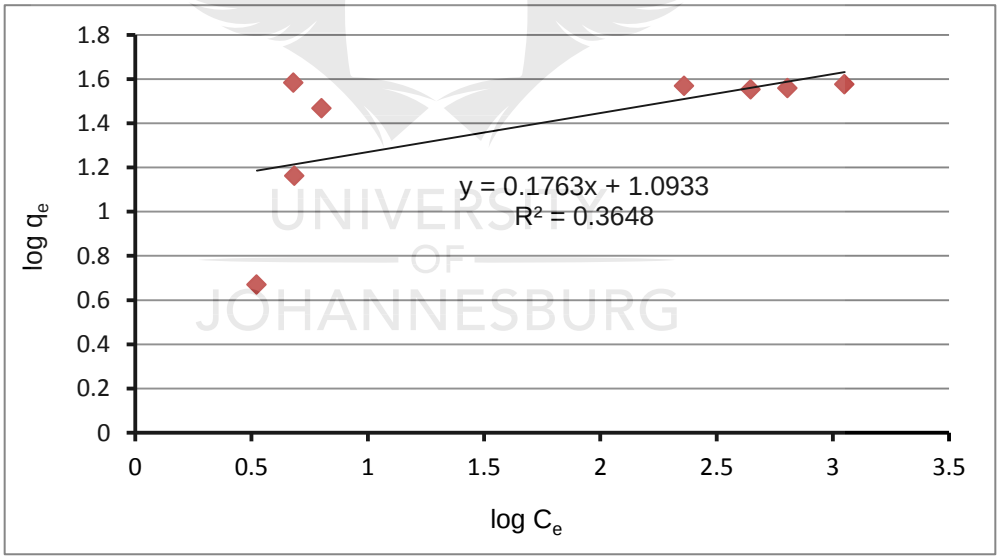


(b)

Figure 4.12: Plots of the Freundlich isotherm for the adsorption of Cr(VI) onto (a) Hydrochar, (b) AC

## 4.5. REFERENCES


[1] Asuquo, E. D., & Martin, A. D. (2016). Sorption of cadmium (II) ion from aqueous solution onto sweet potato (Ipomoea batatas L.) peel adsorbent: characterisation, kinetic and isotherm studies. *Journal of environmental chemical engineering*, *4*(4), 4207-4228.

[2] Li, B., Guo, J. Z., Liu, J. L., Fang, L., Lv, J. Q., & Lv, K. (2020). Removal of aqueous-phase lead ions by dithiocarbamate-modified hydrochar. *Science of The Total Environment*, *714*, 136897.

[3] Ramaiah, G. B., Chillal, P. S., & Ari, A. P. (2020). Thermal behaviour of waterproof coated fabrics and identification of chemical groups present in melt-blown polyester non-woven fabrics coated with waterproof acrylic polymer binder. *Materials Today: Proceedings*.[4]Renu, M. A., Singh, K., Upadhyaya, S., & Dohare, R. K. (2017). Removal of heavy metals from wastewater using modified agricultural adsorbents. *Materials Today: Proceedings*, *4*(9), 10534-10538.

[5] Feng, Y., Sun, H., Han, L., Xue, L., Chen, Y., Yang, L., & Xing, B. (2019). Fabrication of hydrochar based on food waste (FWHTC) and its application in aqueous solution rare earth ions adsorptive removal: process, mechanisms and disposal methodology. *Journal of Cleaner Production*, *212*, 1423-1433.

[6] Madduri, S., & Elsayed, I. (2020). Novel oxone treated hydrochar for the removal of Pb (II) and methylene blue (MB) dye from aqueous solutions. *Chemosphere*, *260*, 127683.

[7] Shafiq-ul-Hassan, M., Zhang, G. G., Latifi, K., Ullah, G., Hunt, D. C., Balagurunathan, Y., ... & Court, L. E. (2017). Intrinsic dependencies of CT radiomic features on voxel size and number of gray levels. *Medical physics*, *44*(3), 1050-1062.

[8] Hao, W., Liu, Y., Neagu, A., Bacsik, Z., Tai, C. W., Shen, Z., & Hedin, N. (2019). Core-Shell and Hollow Particles of Carbon and SiC Prepared from Hydrochar. *Materials*, *12*(11), 1835.

[9] Yusuf, I., Flagiello, F., Ward, N. I., Arellano-García, H., Avignone-Rossa, C., & Felipe-Sotelo, M. (2020). ; Valorisation of banana peels by hydrothermal carbonisation: Potential use of the hydrochar and liquid by-product for water purification and energy conversion. *Bioresource Technology Reports*, *12*, 100582.

[10] Li, F., Zimmerman, A. R., Hu, X., & Gao, B. (2020). Removal of aqueous Cr (VI) by Zn-and Al-modified hydrochar. *Chemosphere*, *260*, 127610.

[11] Zhang, S., Sheng, K., Yan, W., Liu, J., Shuang, E., Yang, M., & Zhang, X. Bamboo derived hydrochar microspheres fabricated by acid-assisted hydrothermal carbonization. *Chemosphere*, *263*, 128093.

[12] Fayazi, M., Shuai, G., Liu, B., Lei, L., Sameera, I., Odunmbaku, O., ... & Boi, F. S. (2020). Vacancy-induced interfacial ferromagnetic features in SmFeO 3-filled graphitic carbon foam. *RSC Advances*, *10*(17), 9878-9883.

[13] Liu, T., Li, Y., Peng, N., Lang, Q., Xia, Y., Gai, C., ... & Liu, Z. (2017). Heteroatoms doped porous carbon derived from hydrothermally treated sewage sludge: Structural characterization and environmental application. *Journal of environmental management*, *197*, 151-158.

[14] Liang, M., Liu, X., Wang, L., He, Y., Huang, F., Li, B., ... & Tian, H. (2020). Preparation and characterization of nano silver immobilized hydrochar derived from hydrothermal carbonization of tobacco stem. *Materials Research Express*, *7*(1), 015611.

[15] Azzaz, A. A., Khiari, B., Jellali, S., Ghimbeu, C. M., & Jeguirim, M. (2020). Hydrochars production, characterization and application for wastewater treatment: A review. *Renewable and Sustainable Energy Reviews*, *127*, 109882.

[16] Saçmacı, Ş., & Saçmacı, M. (2020). Application of a new functionalized magnetic graphane oxide for aluminum determination at trace levels in honey samples by the zetasizer system. *Microchemical Journal*, 104962.

[17] Ong, H. C., Chen, W. H., Singh, Y., Gan, Y. Y., Chen, C. Y., & Show, P. L. (2020). A state-of-the-art review on thermochemical conversion of biomass for biofuel production: A TG-FTIR approach. *Energy Conversion and Management*, *209*, 112634.

[18] Hassan H, Lim JK, Hameed BH. Recent progress on biomass co-pyrolysis conversion into high-quality bio-oil. Bioresour Technol 2016;221:645–55.

[19] Mahmoud, M. E., El-Kholy, A. E., Kassem, T. S., & Obada, M. K. (2012). Adsorptive removal of Mn (II)–Mn (VII) from various aqueous and nonaqueous solutions by using layer-by-layer chemical deposition technique. *Journal of Industrial and Engineering Chemistry*, *18*(6), 2191-2198.

[20] Queiroz, P. S., Barboza, N. R., Cordeiro, M. M., Leão, V. A., & Guerra-Sá, R. (2018). Rich growth medium promotes an increased on Mn (II) removal and manganese oxide production by Serratia marcescens strains isolates from wastewater. *Biochemical Engineering Journal*, *140*, 148-156.

[21] Esfandiar, N., Nasernejad, B., & Ebadi, T. (2014). Removal of Mn (II) from groundwater by sugarcane bagasse and activated carbon (a comparative study): Application of response surface methodology (RSM). *Journal of industrial and engineering chemistry*, *20*(5), 3726-3736.

[22] Rao, D., Sun, Y., Shao, B., Qiao, J., & Guan, X. (2019). Activation of oxygen with sulfite for enhanced Removal of Mn (II): The involvement of SO4•. *Water research*, *157*, 435-444.

[23] Indah, S., & Helard, D. (2017). Evaluation of iron and manganese-coated pumice from Sungai Pasak, West Sumatera, Indonesia for the removal of Fe (II) and Mn (II) from aqueous solutions. *Procedia Environmental Sciences*, *37*, 556-563.

[24] T. Ngulube, J.R. Gumbo, V. Masindi, A. Maity, An update on synthetic dyes adsorption onto clay based minerals: a state-of-art review, J. Environ. Manage. 191 (2017) 35–57.

[25] R.O. James, T.W. Healy, J. Colloid Interface Sci. 40 (1972) 65e79.

[26] Mehrali-Afjani, M., & Nezamzadeh-Ejhieh, A. (2020). Efficient solid amino acid–clinoptilolite nanoparticles adsorbent for Mn (II) removal: A comprehensive study on designing the experiments, thermodynamic and kinetic aspects. *Solid State Sciences*, *101*, 106124.

[27] Agrafioti, E., Kalderis, D., & Diamadopoulos, E. (2014). Arsenic and chromium removal from water using biochars derived from rice husk, organic solid wastes and sewage sludge. *Journal of environmental management*, *133*, 309-314.

[28] Langmuir, I. (1918). The adsorption of gases on plane surfaces of glass, mica and platinum. *Journal of the American Chemical society*, *40*(9), 1361-1403.

[29] Priya, S. S., & Radha, K. (2015). Equilibrium, isotherm, kinetic and thermodynamic adsorption studies of tetracycline hydrochloride onto commercial grade granular activated carbon. *Int. J. Pharm. Pharm. Sci*, *7*(1), 42-51.

[30] S. Wadhawan, A. Jain, J. Nayyar, S.K. Mehta, Role of nanomaterials as adsorbents in heavy metal ion removal from waste water: a review, J. Water Process Eng. 33 (2020), 101038.

[31] Michael Horsfall Jnr, Ayebaemi Spiff I. Effects of temperature on the sorption of Pb2+ and Cd2+ from aqueous solution by *Caladium bicolor* (Wild Cocoyam) biomass. Electron J Biotechnol 2005;8:162-9.

[32] Naiyaa, T. K., Bhattacharya, A. K., Mandalb, S., and Das S. K. (2009). The sorption of lead (II) ions on rice husk ash, Journal of Hazardous Materials, 163, 1254–1264.

[33] Shrestha, R. M., Varga, M., Varga, I., Yadav, A. P., Pokharel, B. P., & Pradhananga, R. R. (2013). Removal of Ni (II) from aqueous solution by adsorption onto activated carbon prepared from Lapsi (Choerospondias axillaris) seed stone. *Journal of the Institute of Engineering*, *9*(1), 166-174.

[34] G.K. Sarma, S. Sen Gupta, K.G. Bhattacharyya, Adsorption of Crystal violet on raw and acid-treated montmorillonite, K10, in aqueous suspension, J. Environ. Manag. 171 (2016) 1–10.

[35] H. Wu, Q. Wen, L. Hu, M. Gong, Effect of adsorbate concentration to adsorbent dosage ratio on the sorption of heavy metals on soils, J. Environ. Eng. (United States) 144 (2018).

[36] T. Chen, Y. Zhao, S. Song, Electrophoretic mobility study for heterocoagulation of montmorillonite with fluorite in aqueous solutions, Powder Technol. 309 (2017) 61–67.

[37] W. Peng, H. Li, Y. Liu, S. Song, A reviewon heavy metal ions adsorption fromwater by graphene oxide and its composites, J. Mol. Liq. 230 (2017) 496–504.

[38] Rouhaninezhad, A. A., Hojati, S., & Masir, M. N. (2020). Adsorption of Cr (VI) onto micro-and nanoparticles of palygorskite in aqueous solutions: Effects of pH and humic acid. *Ecotoxicology and Environmental Safety*, *206*, 111247.

[39] Enhancement of Cr(VI) removal efficiency via adsorption/photocatalysis synergy using electrospun chitosan/g-C3N4/TiO2 nanofibers.

[40] K. Garg, P. Rawat, B. Prasad, Removal of Cr (VI) and COD from electroplating wastewater by corncob based activated carbon, Int. J. Water and Wastewater Treatment 1 (2015).

[41] Haroon, H., Shah, J. A., Khan, M. S., Alam, T., Khan, R., Asad, S. A., ... & Bilal, M. (2020). Activated carbon from a specific plant precursor biomass for hazardous Cr (VI) adsorption and recovery studies in batch and column reactors: Isotherm and kinetic modeling. *Journal of Water Process Engineering*, *38*, 101577.

[42] Shi, X., Qiao, Y., An, X., Tian, Y., & Zhou, H. (2020). High-capacity adsorption of Cr (VI) by lignin-based composite: Characterization, performance and mechanism. *International Journal of Biological Macromolecules*.

[43] A.B. Albadarin, C. Mangwandi, A.a.H. Al-Muhtaseb, G.M. Walker, S.J. Allen, M.N.M. Ahmad, Kinetic and thermodynamics of chromium ions adsorption onto low-cost dolomite adsorbent, Chem. Eng. J. 179 (2012) 193–202.

[44] E. Alveroglu, N. ˙Ilker, M.T. Shah, K. Rajar, A.T. Gokceoren, K. Koc, Effects of gel morphology on the lysozyme adsorption and desorption kinetics of temperature sensitive magnetic gel composites, Colloids Surfaces B Biointerfaces 181 (2019) 981–988.

[45] Moreon-Pirajan, J.C.; Giraldo, L. Heavy metal ions adsorption from wastewater using activated carbon from Orange peel. *E-J*. *Chem*. 2012, *9*, 926-937.

[46] Aqeel, M.A.; Mahmood, K.; Wajid, A. Study of low cost biosorbent for biosorption of heavy metals. *Int*. *Conf*. *F*. *Eng*. *Biotechnol*. 2011, *9*, 60-68.

[47] Aqeel, M.A.; Mahmood, K.; Wajid, A. Study of low cost biosorbent for biosorption of heavy metals. *Int*. *Conf*. *F*. *Eng*. *Biotechnol*. 2011, *9*, 60-68.

[48] Ata, S., Imran Din, M., Rasool, A., Qasim, I., & Ul Mohsin, I. (2012). Equilibrium, thermodynamics, and kinetic sorption studies for the removal of coomassie brilliant blue on wheat bran as a low-cost adsorbent. *Journal of analytical methods in chemistry*, *2012*.

[49] Özacar, M. (2003). Equilibrium and kinetic modelling of adsorption of phosphorus on calcined alunite. *Adsorption*, *9*(2), 125-132.

[50] Hall, K. R., Eagleton, L. C., Acrivos, A., & Vermeulen, T. (1966). Pore-and solid-diffusion kinetics in fixed-bed adsorption under constant-pattern conditions. *Industrial & engineering chemistry fundamentals*, *5*(2), 212-223.

[51] Malik, P. K. (2004). Dye removal from wastewater using activated carbon developed from sawdust: adsorption equilibrium and kinetics. *Journal of Hazardous Materials*, *113*(1-3), 81-88.

[52] Desta, M. B. (2013). Batch sorption experiments: Langmuir and Freundlich isotherm studies for the adsorption of textile metal ions onto teff straw (Eragrostis tef) agricultural waste. *Journal of thermodynamics*, *2013*.

# CHAPTER FIVE: CONCLUSIONS AND RECOMMENDATIONS

## 5.1. CONCLUSIONS

The aim of this study was to produce PCS (hydrochar and AC) from the wood chips and evaluate their potential as adsorbents for toxic inorganic ions from aqueous systems. In the process of producing PCS, to ensure that the PCS would be suitable for inorganic ion adsorption, the reaction pressure, temperature, and time were successfully investigated. After the hydrochar was produced, then its AC was generated through annealing process shown (Figure 3.1) and explained in chapter 3. The hydrochar and AC were characterized by FTIR, XRD, BET, SEM, TGA, TEM, EDX, and DLS. The properties of AC were improved compared to hydrochar, the moisture was removed from the AC and that was confirmed by the first stage of TGA thermogram (Figure 4.8) that occurred below 200 °C and it was complemented by the reduced peak of a hydroxyl group from the FTIR (Figure 4.1(b)). The AC's surface area and particle sizes increased (Figure 4.5 and 4.7). Therefore, hydrochar and AC were used as adsorbents for the removal of Mn(II) and Cr(VI) from aqueous solutions. Based on the results of this study, the investigated adsorption capacity for Mn(II) was found to be 44.03 mg/g when hydrochar was applied while 56.31 mg/g adsorption capacity was obtained when AC was used. The investigated adsorption capacity for Cr(VI) was 43.81 mg/g when the hydrochar was applied and 38.26 mg/g was obtained when the AC was used as an adsorbent. The results showed that the AC removed more Mn(II) and less Cr(VI) ions than the hydrochar did, hydrochar removed 73.4% and AC 98.9% of Mn(II); and hydrochar removed 73.0% and AC removed 98.8% of Cr(VI). The optimum parameter conditions for the adsorption of Mn(II) were pH 8, adsorbent dose=0.25 g/L, contact time=180 mins, initial metal ions concentration=600 mg/g, and temperature= 25°C when the hydrochar was used as an adsorbent; and pH 7, adsorbent dose=0.25 g/L, contact time=210 mins, initial metal ions concentration=800 mg/g, and temperature=25°C when the AC was used as an adsorbent. Then the optimum parameter conditions for the adsorption of Cr(VI) were pH 5, adsorbent dose=0.25 g/L, contact time=150 mins, initial metal ions concentration=600 mg/g, and temperature= 25°C when the hydrochar was used as an adsorbent; and pH 7, adsorbent dose=0.25 g/L, contact time=120 mins,

initial metal ions concentration=400 mg/g, and temperature=25°C when the AC was used as an adsorbent. Langmuir and Freundlich isotherms were used to model the experimental data and the adsorption process favored the Langmuir model with coefficient of determination of $R^2$ =0.9915 for hydrochar and $R^2$ =0.9924 for AC for the removal of Mn(II) and $R^2$ =0.5326 for hydrochar and $R^2$ =0.5082 for AC for the removal of Cr(VI).

## 5.2. RECOMMENDATIONS

Although some works have already been done on the production of PCS through HTC and their application as adsorbents for potentially toxic elements in water and wastewater. For further studies, the following are recommended:

- Chemical activation of PCS and their application as adsorbents for potentially toxic elements in water and wastewater.
- The application of chemically and thermally activated PCS in environmental samples.